OAK RIDGE
NATIONAL LABORATORY
MANAGED BY UT-BATTELLE
FOR THE DEPARTMENT OF ENERGY

ORNL/TM-2010/326

Intermediate Ethanol Blends Infrastructure Materials Compatibility Study: Elastomers, Metals, and Sealants

March 2011

Prepared by

M. D. Kass
T. J. Theiss
C. J. Janke
S. J. Pawel
S. A. Lewis

UT-BATTELLE
ORNL-27 (4-00)

ORNL/TM-2010/326

Energy and Transportation Science Division

INTERMEDIATE ETHANOL BLENDS INFRASTRUCTURE MATERIALS COMPATIBILITY STUDY: ELASTOMERS, METALS, AND SEALANTS

Michael D. Kass
Timothy J. Theiss
Christopher J. Janke
Steven J. Pawel
Samuel A. Lewis

Date Published: March 2011

Prepared by
OAK RIDGE NATIONAL LABORATORY
Oak Ridge, Tennessee 37831-6283
managed by
UT-BATTELLE, LLC
for the
U.S. DEPARTMENT OF ENERGY
under contract DE-AC05-00OR22725

CONTENTS

Page

LIST OF FIGURES

LIST OF TABLES

ACRONYMS

ACN	Acrylonitrile
ASTM	American Society for Testing and Materials
API	American Petroleum Institute
CRC	Coordinating Research Council
DOE	Department of Energy
DMA	Dynamic Mechanical Analysis
E’	Storage modulus
E'_{25}	Storage modulus at 25^{o}C
E25	Gasoline containing 25% ethanol by volume
E85	Gasoline containing 85% ethanol by volume
EISA	Energy Independence and Security Act
EPA	U. S. Environmental Protection Agency
FFV	Flex-Fuel Vehicle
GC-MS	Gas chromatography–mass spectrometry
ISO	International Organization for Standardization
LG	Leaded gasoline
MTBE	Methyl tertiary butyl ether
NBR	Acrylonitrile (or nitrile) butadiene rubber
NREL	National Renewable Energy Laboratory
OBP	DOE Office of Biomass Program
Onset E'	Storage modulus associated with the onset of the glass to rubber transition
ORNL	Oak Ridge National Laboratory
PEI	Petroleum Equipment Institute
PTFE	polytetrafluoroethylene
RFS	Renewable Fuel Standard
SAE	Society of Automotive Engineers
SBR	Styrene butadiene rubber
T_g	Glass-to-rubber transition temperature
UG	Unleaded gasoline
UL	Underwriters Laboratories
UST	Underground Storage Tank
VTP	DOE Vehicle Technologies Program
XPS	x-ray photoelectron spectroscopy

FOREWORD

It is not the purpose of the ORNL-led materials compatibility studies to define the acceptable limits of material performance or to rate individual materials. Rather, the purpose of this study was to measure critical property changes (volume, hardness, mass, etc.) for representative classes of dispenser materials in ethanol-blended test fluids. The test results are intended to be used by material designers and users to identify potential issues and guide the selection and development of materials compatible for use in E15 dispensers.

ACKNOWLEDGMENTS

This report and the work described were sponsored by the Biomass, Clean Cities, and Vehicle Technologies Programs within the U.S. Department of Energy (DOE) Office of Energy Efficiency and Renewable Energy (EERE). The authors gratefully acknowledge the support and editorial guidance of Brian Duff, Shab Fardanesh, Joan Glickman, Steve Przesmitzki, Dennis Smith, and Kevin Stork at DOE.

This effort originated from a collaboration of Oak Ridge National Laboratory (ORNL), the National Renewable Energy Laboratory (NREL), and Underwriters Laboratories (UL). Our NREL collaborators were Kristi Moriarty and Wendy Clark. We also respectively acknowledge our UL collaborators Tom Chapin, Ken Boyce, Tom Fabian, and Edwin Yang, who provided substantial input, direction, and research assistance. This work also benefitted from discussions and suggestions provided by participants from the E10+ Research and Planning Meetings sponsored by the American Petroleum Institute (API). We are especially grateful for the technical exchanges with Prentiss Searles and Brian Knapp, from the API; Andrea Barbery and Mark Barolo, of the Environmental Protection Agency Office of Underground Storage Tanks (EPA-UST); and Bob Renkes, of the Petroleum Equipment Institute. Dennis Boyd from BP also provided much useful input. We also acknowledge and appreciate the thorough review and input provided by Marc Goodman from New West Technologies, LLC. The authors are indebted to many technical experts in industry and other government agencies. While these companies and their experts provided valuable guidance and information as noted above, this consultation does not constitute endorsement by their organizations. This study also benefitted greatly from the material contributions from Dupont and 3M and two gracious suppliers of nitrile rubbers. Their contributions and guidance on material selection were crucial to facilitating the experiments and subsequent analysis of the results.

Several ORNL staff made important contributions to this work; key support was provided by Michelle Kidder, Harry Meyer, Raynella Connatser, John M. Storey, Brian West, Eric Nafziger, Norberto Domingo, Steve Whitted, and Jeff Chambers.

The authors also wish to thank the staff of Publishing Services at ORNL for help with preparation of the final manuscript.

EXECUTIVE SUMMARY

E.1 BACKGROUND

The Energy Independence and Security Act (EISA) of 2007 was an omnibus energy policy law designed to move the United States toward greater energy security and independence. A key provision of EISA is the Renewable Fuel Standard (RFS) which requires the nation to use 36 billion gallons of renewable fuel in vehicles by 2022. Ethanol is the most widely used renewable fuel, and a significant portion of the 36 billion gallon goal can be achieved by increasing the ethanol in gasoline to 15%. In fact in March 2009, Growth Energy (a coalition of ethanol producers and supporters) requested a waiver from the Environmental Protection Agency to allow the use of 15% ethanol in gasoline. In anticipation of this waiver being granted, uncertainties arose as to whether additional fuel ethanol, such as E15 and E20, would be compatible with legacy and current materials used in standard gasoline fueling hardware. In the summer of 2008, the U.S. Department of Energy recognized the need to assess the impact of intermediate blends of ethanol on the fueling infrastructure, specifically located at the fueling station. This research effort was led by Oak Ridge National Laboratory and the National Renewable Energy Laboratory in collaboration with Underwriters Laboratories. The DOE program has been co-led and funded by the Office of the Biomass Program and Vehicle Technologies Program.

The infrastructure material compatibility work has been supported through strong collaborations between the DOE labs and UL. NREL led the effort to select and test a limited number of new and legacy fueling dispenser units using 17% ethanol; the actual testing was conducted at UL under subcontract to NREL. ORNL led the effort to evaluate the impact of intermediate blends of ethanol on a large number of materials (metals, elastomers, plastics and sealants) representing those typically used in dispenser infrastructure. The ORNL materials studies are reported herein, but additional work is under way at ORNL, and additional interpretation of the combined data from ORNL, NREL, and UL is expected in the near future.

E.2 EXPERIMENTAL OVERVIEW

Material selection was based on a thorough investigation of dispenser materials by the ORNL materials research team. Team members contacted dispenser component and elastomer/seal manufacturers and received input from stakeholders including UL, the Petroleum Equipment Institute (PEI), and the API members. Although the research team was able to identify typical dispenser materials (especially elastomers) according to class, specific grades and formulations could not be precisely identified. As a result the material selection does not necessarily include those specific grades or formulations used in legacy and current standard gasoline dispensers. The broad material classes that were identified for use in gasoline fuel dispensers include metals, elastomers, plastics, and sealants. Testing was accomplished for the metals, elastomers, and sealants only. During the time this report was being written, the plastic specimens were undergoing compatibility exposures. Therefore, only the metal, elastomer, and sealant results are discussed in this report. A follow-up report discussing the plastic results will be issued upon completion of that portion of the study.

In this study four test fuels based on the Fuel C composition, and aggressive ethanol were examined. These formulations are based on test fuels described in SAE J1681, "Gasoline, Alcohol, and Diesel Fuel Surrogates for Materials Testing."[1] The fuel types studied were Fuel C, CE10a, CE17a, and CE25a. Fuel C is a 50-50 mixture of toluene and isooctane and is representative of highly aromatic gasoline (>40% aromatics by volume). The other test fuels contain an aggressive ethanol solution added to Fuel C—hence, the CE nomenclature. The numbers that follow CE refer to the volume fraction of aggressive ethanol added to Fuel C, and the aggressive nature is represented by the "a" at the end. The ethanol-

bearing fuels contain an aggressive ethanol formulation containing NaCl, dilute acetic and sulfuric acids, and 0.9% water. All of these contaminants are found in ethanol-gasoline fuels and represent the bounds allowable for fuel-grade ethanol. They are also intended to minimize the length of exposure necessary to rigorously evaluate materials while providing a standard method of testing fuel system materials. In order to reflect the conditions associated with vapor recovery, selected elastomer and metal specimens were placed in the gaseous region above the liquid fuel line (headspace) to prevent contact with the moving fluid.

The metals and alloys that were evaluated in this study included single metal/alloy coupons of 1020 carbon steel, 304 stainless steel, 1100 aluminum, nickel 201, cartridge brass, phosphor bronze, and terne-plated steel. In addition, to better reflect dissimilar metal-to-metal contacts existing in the field, specimens composed of steel, brass, and aluminum were coupled with lead, zinc, chromium and nickel to create galvanic scenarios for evaluation. Corrosion was primarily assessed by measuring the mass loss for each exposed coupon and observing any discoloration that may have occurred. For each metal sample, one or more specimens were exposed to the liquid and one was exposed to the vapor region of the test chambers.

The elastomer classes that were selected for study were fluorocarbon, fluorosilicone, silicone, acrylonitrile butadiene rubber (also known as nitrile rubber or NBR), styrene butadiene rubber (SBR), polyurethane, and neoprene. The test matrix included eight types of fluorocarbons and six grades of NBR, while the remaining elastomer types consisted of one sample only. The elastomers placed in the liquid phase region were evaluated for volume, mass, and hardness changes for both wetted and dried conditions. Dynamic mechanic analysis (DMA) was performed on each specimen to assess elasticity over a wide temperature range. Three specimens were exposed to the liquid phase, while one specimen was exposed to the vapor-only regions. The metal and elastomer coupons were loaded into the stir chambers which were held at 60°C for 4 weeks while being subjected to a constant flow of 0.8 m/s.

Pipe thread sealants were introduced into the study matrix at different times; thus, they were not exposed to each test fluid, nor were the samples all exposed under the same test fuels. However, a standard sealant representative of those used in legacy equipment for gasoline and diesel use was evaluated in Fuel C, CE10a, and CE25a test fuels. An ethanol-resistant sealant (developed specifically for E10 and E85 use) and the standard sealant combined with Teflon tape were evaluated in CE10a and CE25a. A total of three specimens were exposed for each sealant test case, and the sealant performance was evaluated according to ASTM D 6396, “Standard Test Method for Testing of Pipe Thread Sealants on Pipe Tees.”[2]

E.3 METAL RESULTS

Very little corrosion of any of the metallic coupons was observed from exposure to Fuels C, CE10a, CE17a, or CE25a. Coupons exposed to the vapor phase above each solution exhibited slight discoloration in some cases (particularly the brass and bronze coupons), but no loss of mass was observed for any of the metals exposed in the vapor regions.

Among the coupons immersed in the different test solutions, 1020 mild steel, 1100 aluminum, 201 nickel, and 304 stainless steel were found to be essentially immune to corrosion for the exposure conditions evaluated. This result suggests that these materials are suitable for extended service in intermediate fuel blends of this type. Cartridge brass, phosphor bronze, zinc-plated (galvanized) steel, and lead-plated (terne) steel exhibited variable degrees of discoloration and minor corrosion product film formation. The highest corrosion rate observed among these very slightly susceptible materials was about 30 µm/year for the cartridge brass immersed in CE10a, and this result is still considered to be a low rate of corrosion. No significant corrosion was observed for the Fuel C immersions (<0.3 µm/year), and there was no apparent trend associated with the corrosion rate of any materials as a function of ethanol concentration in the fuel.

X-ray photoelectron spectroscopy (XPS) was performed on representative coupon surfaces following testing (to compare with results from unexposed coupons) to assess the corrosion film thickness and composition as a function of ethanol content in the exposure environment. The results showed that corrosion film composition and thickness were not dependent on fuel ethanol concentration. An example surface analysis of cartridge brass exposed to CE25a indicated that copper sulfide was the predominant corrosion product present in the surface films, and was likely responsible for the observed discoloration.

None of the plated coupons—Cr-, Ni-, Pb-, or Zn-plated steels, Cr-plated brass, or Ni-plated aluminum—revealed any readily observable discoloration/change or measurable corrosion (no weight loss, no pit/crevice initiation). Further, none of the partially plated coupons showed accelerated corrosion due to galvanic coupling between the plating material and substrate.

E.4 ELASTOMER RESULTS

All of the elastomer specimens that were exposed to the test fuels (including Fuel C) exhibited some level of volume swell. Ethanol was found to further increase the volume swell and produce softening. The level of swell is an indication of solubility, and for most elastomers tested, the highest level of swell occurred with either the CE10a or CE17a (not CE25a). This result suggests that the highest level of mutual solubility for elastomers occurs at relatively low levels of added ethanol. After drying for 20hr at 60^{o}C, all of the samples, except the fluorocarbons, exhibited some level of shrinkage and mass loss. Interestingly, the fluorocarbons retained a slight increase in dry mass and volume, indicating that residual test fluids were trapped in the microstructure (even after dry-out).

The dominant feature of the test results is that the compatibility properties were observed to group according to elastomer class. The fluoroelastomers (fluorocarbons and fluorosilicone) showed the best retention of baseline properties of the elastomers studied. These materials incurred the lowest decline in physical properties of the elastomers tested in this study. The addition of ethanol did not drastically affect the measured properties, and the eight fluorocarbons exhibited only modest swell (around 20%) and softening (wet hardness decrease) upon exposure to the test fuels. The properties for the fluorosilicone rubber sample were found to be close to those measured for the fluoroelastomer samples. Volume swell was somewhat higher than the fluorocarbon results but is still considered relatively low (~20%).

Of all the elastomers tested, silicone rubber underwent the highest level of volume expansion (>120%) when exposed to the test fuels. This swell was accompanied by a 20 point drop in hardness. However, following dry-out, the silicone sample returned to its original condition with only a slight level of shrinkage and mass loss. The excessive volume swell means that silicone is susceptible to fluid permeation and extrusion (between sealed surfaces), depending on the sealing application. As with the fluoroelastomers, silicone did not suffer any structural degradation from exposure to the test fluids.

The eight NBR samples (and polyurethane) showed a pronounced increase in volume swell and softening when exposed to fuels containing ethanol. Exposures to Fuel C resulted in volume expansion approaching 20% or more. When exposed to the ethanol-blended test fluids, the NBRs swelled by more than 30%. Likewise, the hardness values dropped an additional 10 points when ethanol was added to the test fluid. When all of the samples (including Fuel C exposures) were dried, 8% to 14% of the original mass was lost and the accompanying shrinkage was between 10% and 18%. The dried hardness was increased 5 to 16 points, indicating that embrittlement had occurred. NBR was one of only two elastomer types (the other being neoprene) that exhibited significant embrittlement in the dried state, indicating that plasticizer components were being removed by the test fuels. The results of the NBRs showed a high degree of variance, which is not surprising since different NBRs are designed for a wide variety of applications. NBRs showed a significant increase in the glass transition temperature (a measure of potential

embrittlement at low temperatures) with Fuel C exposure, but the addition of ethanol was observed to reduce this shift rather than extend it.

The polyurethane results essentially matched those of the NBRs, with one notable exception: Polyurethane became softer (not harder) when dried from the wetted state, but only for those specimens exposed to ethanol. The reduction in hardness (after drying) upon exposure to ethanol indicates that the aggressive ethanol reacted with the polyurethane, causing permanent degradation. The poor wetted properties combined with the high shrinkage and mass loss indicate that polyurethane may not be an acceptable elastomer in many sealing applications for use with fuels containing up to 25% ethanol.

The SBR sample experienced the highest combination of swell and softening. The volume expansion exceeded 90%, and the hardness dropped 50 points when wet. As a result, the sample evaluated in this study would not be considered compatible with many sealing applications with the test fluids. SBR is similar to NBR in that the properties are highly dependent on additives, processing, and copolymer concentrations. This flexibility of design means that there may be appropriate formulations of SBR that will, in fact, meet a given sealing specification.

The neoprene sample's decrease in wet hardness was relatively low and was comparable to the fluorocarbon results; however, the volume swell exceeded 60%, which may limit its use. Particularly disconcerting was the fact that neoprene exhibited the poorest dried properties of the elastomers in the study. Upon drying the mass and volume were reduced 15% and 20%, respectively. Neoprene also exhibited a high level of embrittlement as the hardness was increased by 14 points. The high mass loss and shrinkage, and the accompanying increase in hardness, suggest that neoprene (along with NBR) contained significant levels of plasticizers prior to the exposure runs. These plasticizer additives were removed by the test fuels, leaving the neoprene sample in a less durable condition.

The physical properties of the vapor-exposed specimens correlated with the results obtained for the wetted specimens for the elastomers tested. Embrittlement was observed for the NBRs and neoprene by vapor phase alone. The chemistry of the head space region will have higher concentrations of ethanol and isooctane (relative to toluene) due to the volatility of these fuel components. It is reasonable to assume that this scenario will also occur in the field as well.

E.5 SEALANT RESULTS

The results show that the standard sealant passed the ASTM D6396 criteria in Fuel C but did not pass following exposure to either CE10a or CE25a. However, when standard sealant was combined with Teflon tape, leaking did not occur. The results also show that the ethanol-resistant sealant product passed when tested with both CE10a and CE25a. Hence the standard sealants may not be compatible without the additional sealing provided by Teflon tape. The ethanol-resistant sealant product was successful at preventing leakage in CE25a according to the ASTM standard.

It is anticipated that the results of this study will be used to assist with the design and selection of materials to be used in future dispensers, possibly including retrofits. The upcoming experimental analysis of the plastic specimens will conclude this test series, and a final report summarizing these conclusions will be forthcoming. It is also our intention to present these results in several open forums during the year, and we will be collaborating with UL on assessing polymer chemistry and solubility.

1. INTRODUCTION

1.1 ETHANOL USE AS A TRANSPORTATION FUEL

In the United States oil dependence is driven by the transportation sector. In fact, transportation accounts for 69% of the total oil consumption in the United States, and the industry itself is around 90% oil dependent (and the remainder being natural gas, propane, electric and ethanol).[3] In 2008 the average daily consumption of the U.S. transportation sector was approximately 14 million barrels. This rate is projected to increase to around 16 million barrels per day by 2025.[4] Currently, the bulk of our oil usage is provided by other countries as foreign oil imports and makes up around 57% of the total oil usage.[5] This dependency impacts our nation's security, since our oil supply is determined partly by other countries, some of whom are not friendly to the United States. Foreign disruption has been shown to negatively impact the nation's economy and makes the United States more vulnerable during times of international crisis.

The Energy Independence and Security Act of 2007 is an omnibus energy policy law created for the purpose of moving the United States toward greater energy security and independence. A key provision of EISA is the renewable fuel standard which requires the nation to use 36 billion gallons of renewable fuels in vehicles by 2022. This mandate is structured to incrementally increase from 9 billion gallons in 2008 to 15 billion gallons in 2012 and, eventually 36 billion gallons in 2022.[6] The vast majority of this requirement has been met using ethanol derived from corn, but other ethanol feedstocks (especially cellulosic-based sources) are being looked at as a means of increasing total ethanol production toward achieving the 36 billion gallon requirement.[6]

However, the amount of ethanol that may be blended and sold as an additive to gasoline is restricted to 10% by volume (E10) by the EPA.[7] A small amount is sold as E85 (gasoline containing 85% by volume of ethanol) for use in flex fuel vehicles (FFVs), but most (approximately 90% of dispenser product) is sold as E10. In 2012, the RFS will require over 15 billion gallons of renewable fuel, but the renewable fuel mandate will continue to increase. Assuming that most of the RFS is met using ethanol, gasoline blenders are likely to hit a limit in the next few years, since 10% ethanol cannot likely exceed 14 billion gallons per year. This "blend-wall" is the maximum possible volume of ethanol that can be achieve with E10. Because of this limitation, there is interest in increasing the allowable concentration of ethanol in gasoline to meet the RFS 2022 mandate to "intermediate-level" blends, ranging from 15 to 50% ethanol by volume.[8]

A key concern is that as the ethanol level in gasoline is increased, the fuel becomes less compatible to the fueling infrastructure materials, which were originally designed for E0 use. These materials are considered adequate (by many) for E10, and there is no notable public record of a major leak or failure directly attributable to ethanol use, although accelerated corrosion has occurred in some instances. It is conceivable that many compatibility issues that do arise have been, and are, corrected onsite and unreported. However, there is some concern that higher ethanol concentrations, such as E15 or E25, may be incompatible with current materials used in standard gasoline fueling hardware. In the summer of 2008, DOE initiated a study to investigate the impact of intermediate blends of ethanol on the fueling infrastructure, specifically the dispenser hanging hardware and associated piping to the underground storage tank.

The DOE program has been co-led and funded by the Office of the Biomass Program and Vehicle Technologies Program with technical support from the ORNL and the NREL. The infrastructure material compatibility work has been supported through strong collaborations and testing at UL. NREL has been responsible for the selection and testing of a limited number of new and legacy fueling dispensers using

17% ethanol, with the testing being conducted at UL under subcontract to NREL. These results were reported separately.[9] ORNL and UL performed a postmortem analysis of rubberized cork gaskets used in several of these dispensers, and these results are summarized in Appendix A. A separate but corollary study was led by ORNL to evaluate the impact of intermediate blends of ethanol on a larger number of materials (elastomers, plastics, and metals) used in fuel dispensers. It was expected that many of the materials evaluated in the ORNL study were also used in the prototype dispensers that were tested in the NREL study. The ORNL results form the basis of this report, but additional research is underway at ORNL, and further interpretation of the combined data from ORNL, NREL, and UL is expected in the near future. The reader will note that the term fluid is used frequently throughout this manuscript. Here fluid refers to the liquid state of the test fuel.

Under ambient conditions, pure ethanol is not generally considered corrosive toward most metallic materials; however, as a polar molecule, ethanol will be more susceptible to having compatibility issues with both metals and polymers due to (1) increased polarity relative to gasoline, (2) adsorption of water, and (3) a high solubility parameter relative to gasoline. The first two factors are relevant to metals and alloys, while the latter primarily affects polymers. A detailed study measuring the electrical conductivity of gasoline as a function of ethanol and water concentration was performed by Kirk.[10] Kirk's study shows that the conductivity of ethanol-blended gasoline increases marginally with ethanol concentrations up to 20%. However, although the conductivity numbers are low, relatively speaking, E15 is 10 times more conductive than E10, as shown in Figs. 1 and 2. As the ethanol concentration increases from 20% to 50%, the corresponding conductivity increases by more than two orders of magnitude. As a result, metal corrosion becomes a significant concern for ethanol blends containing 50% or higher levels of ethanol. The results in Fig. 2 show that water also has a pronounced effect on conductivity. As the level of ethanol increases, the amount of water that can be dissolved also increases. In fact, the water solubility limit increases the conductivity by an order of magnitude when going from E10 to E15. In addition, water itself is a solvent for NaCl and acids, which can lead to even higher rates of corrosion.

Ethanol also affects the material-fluid mutual solubility associated with the fuel blend, which is an important parameter for gauging the compatibility of fuels with polymers. The influence of the solubility

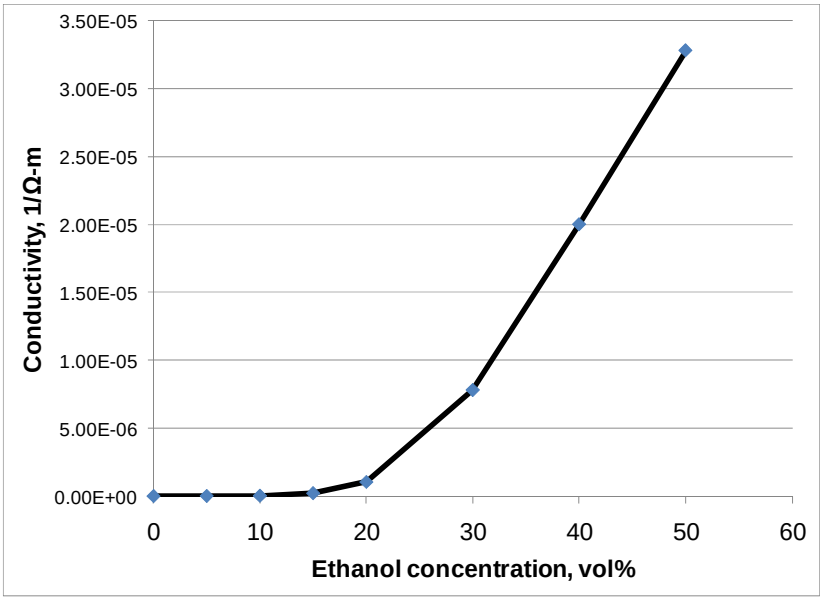

Fig. 1. Influence of conductivity with ethanol concentration of gasoline (reprinted with permission). *Source:* D. W. Kirk, Fuel 62, 1512–1513 (December 1983).

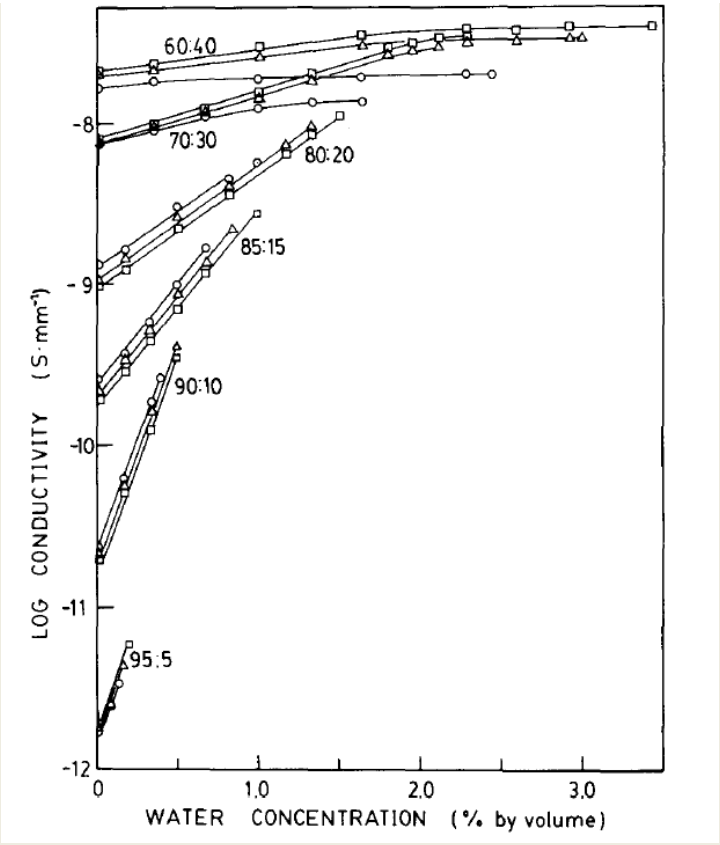

Fig. 2. Influence of conductivity as a function of ethanol and water content (reprinted with permission). *Source:* D. W. Kirk, Fuel 62, 1512–1513 (December 1983).

parameter is complex; however, solvents and solutes having similar solubility parameters will have a greater affinity for permeation and dissolution.[11] A simplified representation of solubility as a function of ethanol concentration in gasoline is shown in Fig. 3. The shaded zone in the chart represents the range of solubility parameters for many dispenser polymers. As the ethanol concentration increases from zero to 15%, it effectively raises the solubility parameter (measured as the total Hansen Solubility Parameter) so that it approaches the values of most dispenser polymers. Therefore, the propensity for the fuel to permeate into and dissolve polymeric components is enhanced. It is important to note that, in reality, solubility is determined from multiple thermodynamic factors, and that the highest level of mutual solubility for a given polymer does not necessarily match precisely with the theoretically-derived parameters which have been simplified in Fig. 3. Standard gasoline fuel delivery systems contain elastomeric materials having excellent compatibility and stability with hydrocarbon fuels. However, the ethanol molecule is relatively small and highly polar due to the –OH group. In addition, the tendency to introduce hydrogen bonding is high. These features enable its permeation into and interaction with the elastomer structure, which can result in swelling and softening of elastomers. Another negative feature associated with permeation is that soluble components, especially plasticizers added to impart flexibility and durability in the elastomer, may be leached out, thereby affecting the mechanical properties of the compounded elastomer component and degrading the ability of the component to perform its intended function. This affect is exacerbated under alternating wet/dry conditions.

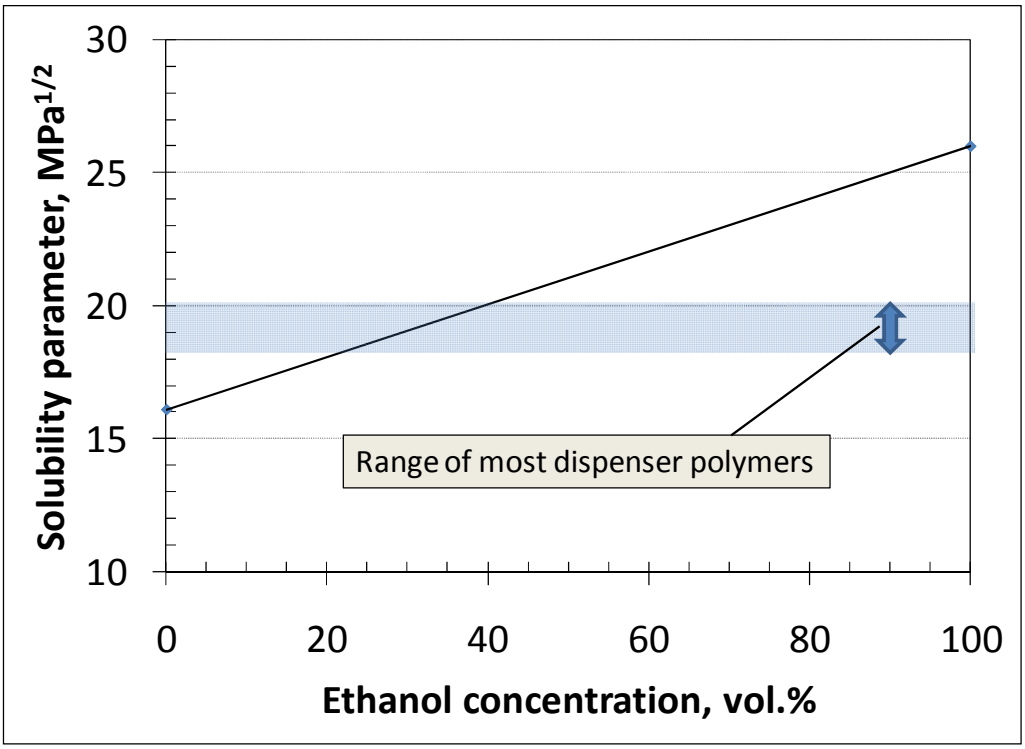

Fig. 3. Total Hansen Solubility Parameter as a function of ethanol concentration.
The blue horizontal band represents the solubility range of many dispenser polymers.

Several studies have been undertaken to evaluate the compatibility of ethanol with engine materials, especially those used in fuel system components such as pumps, and much of this work has recently focused on the intermediate E15, E20, and E25 blends.[12–18] However, little work has been reported on the compatibility of these fuels to standard fuel dispenser materials, including sealants. Additionally the ethanol compatibility of high-performance fluoroelastomers needs to be evaluated since these materials are considered potential alternatives to the current rubber materials used dispenser seals and o-rings.

Elastomers are a class of polymers used predominantly in most sealing applications. They are widely used in fuel dispenser systems and exist predominantly as o-rings and gasket-type seals. Modern elastomeric sealing compounds typically contain 50% to 60% base polymer and are often known as rubbers; the balance consists of various fillers, vulcanizing agents, accelerators, aging retardants, plasticizers, and other additives used to engineer physical properties to meet specific sealing requirements.[19-20] Synthetic rubbers are grouped according to their chemical structure, and several elastomers commonly used in fuel dispensers are listed in Table 1.

It is important to note that cork gaskets frequently used in petroleum sealing applications are typically impregnated with one of these rubber types and are commonly known as rubberized cork. The resulting performance is determined by both the properties of the rubber and cork components. In this study we evaluated the performance of cork impregnated with NBR. These specimens were placed alongside the plastics, and therefore, these results are not reported in this report.

Table 1. Rubber types used in this study[a]

Chemical name	ASTM D1418 abbreviation
M-Group (saturated carbon molecules in the main macromolecule group)	
Fluorocarbon rubber	FKM
R-Group (unsaturated hydrogen carbon chain)	
Neoprene rubber	CR
Nitrile butadiene rubber	NBR
Styrene butadiene rubber	SBR
Q-Group (silicone in the main chain)	
Silicone rubber	PVMQ
Fluorosilicone rubber	FVMQ
U-Group (carbon, oxygen, and nitrogen in the main chain)	
Polyurethane	AU

[a]Classifications obtained from *Parker O-Ring Handbook*, ORD 5700, Parker Hannifin Corp., Cleveland, Ohio.

2. LITERATURE REVIEW OF ELASTOMER COMPATIBILITY WITH ETHANOL-BLENDED GASOLINE

An extensive literature survey was performed which focused on the compatibility of elastomers and metals with ethanol-blended gasoline or standard test fuels. Most of the citations discussed in this report were provided by UL and several additional key articles were found in the trade journal *Sealing Technology*. Concerns regarding the compatibility of oxygenated gasoline with elastomers surfaced in the early 1980s in response to the introduction of gasohol (gasoline blended with 5 to 20% ethanol by volume) and methyl tertiary butyl ether (MTBE).[21] The o-ring and sealing manufacturers and suppliers were among the first to recognize that gasoline containing either MTBE or ethanol at levels between 10% and 25% may increase solubility with existing elastomer seals, leading to potential loss of durability. Unfortunately there has not been much research on elastomer compatibility with ethanol-blended gasoline. In fact, methanol-based compatibility studies were much more prevalent in the open literature than ethanol-based efforts. Also, the range of elastomers studied in the literature has also been quite limited. The majority of the work has focused on fluorocarbons and NBRs rather than other elastomer types.

The key properties used to assess seal performance in a test fluid are wet volume swell, hardness, and shrinkage during drying. Swell is usually accompanied by a decrease in hardness (softening), which also affects performance. Most o-ring manufacturers and suppliers use a common rating system to assess fluid compatibility.[20, 22–24] A sample rating system is shown in Table 2 and is based on a combination of published literature, laboratory tests, field experience, and informed judgments. It is important to note that this system is based on volume swell alone, which is only one indicator of elastomer–fluid compatibility.

O-ring suppliers are careful to mention, however, that the above rating system does not indicate accuracy or suitability for all applications. In fact, the *Dichtomatik O-Ring Handbook*[22] clearly states that users of

Table 2. Standard compatibility rating system

Rating	Description	Volume change, %
1	Little or no effect	<10
2	Possible loss of physical properties	10–20
3	Noticeable change	20–40
4	Excessive change	>40

their products must conduct their own evaluations to determine suitability. The particular application will dictate material specifications. For instance, for static o-ring applications (where the o-ring is not compressed against a moving surface), volume swells up to 30% (and sometimes 50%) can usually be tolerated. In contrast, for dynamic applications involving rotational or directional surface movement (such as those used in valves), the acceptable swell limit is often less than 20%. These limitations are considered general rules, and exceptions to these rules exist depending on the application. Shrinkage caused by dry-out is also a prime cause of failure. For most o-ring applications, the maximum allowable shrinkage is around 3–4% of the original volume for either static or dynamic applications. Hardness change is another critical property that needs to be measured. Excessive softening will lead to extrusion and extraction, which can result in a loss of mechanical integrity (such as compressibility, compliance and tensile and impact strength), while hardening may cause embrittlement and cracking.

O-ring and sealant manufacturers have internal research programs to evaluate material–fuel compatibility, and manufacturers such as Parker, Precision Polymer Engineering, O-rings Incorporated, and Dichtomatik all provide compatibility charts to assist with polymer selection for use with a particular solvent.[20, 22–24] Rankings are based primarily on pure solvents (not blends), but they do typically include a relative comparison of their products with ethanol and pure gasoline components such as isooctane and toluene with their products. The recommendations listed in the manufacturer's charts are based on experimental data, and the rankings are based on comparisons with similar materials. These charts are intended to serve as general guidelines only.

Important properties for assessing seal performance include primary properties such as volume change (swell and shrinkage), storage modulus, hardness, and the low-temperature operating limit. Since hardness is related to the modulus, it is often reported instead of the modulus. Other important properties that are less frequently reported are tear and abrasion resistance. The storage modulus is often considered to be the best indicator of toughness and is one of the key parameters for predicting seal performance. The storage modulus and lower temperature limit are both determined using DMA measurement, while the volume change is determined from the change in measured volume. Because of the cost and time necessary for DMA measurement, volume change and hardness are the two most frequently employed methods for assessing elastomer performance.

In 1999, Paul Westbrook of Shell Oil Company published a technical assessment of literature pertaining to the compatibility and permeability of oxygenated fuels to materials in underground storage and dispensing equipment.[21] Westbrook's review covered studies that were published from 1975 to 1997. Although the survey focused on MTBE added to gasoline, his team was also able to gather information pertaining to ethanol-blended gasoline as well. Table 3 shows the key properties that pertain to compatibility for isooctane, toluene, and ethanol.

Because the focus of this study was on intermediate levels of ethanol (10–25 vol %) and relevant dispenser materials, this review was limited to ethanol and gasoline blends and elastomers used in fuel dispenser components. Dispenser components are herein defined as those systems pertaining to fuel handing from the fuel truck to the underground storage tank (UST) and from the UST to the dispenser. Vapor recovery systems are included, but the UST is not. Several studies dealt with vehicle fuel system

Table 3. Key properties of isooctane, toluene, and ethanol associated with fluid-elastomer compatibility

Chemical	Formula	Mole wt.	Vapor pressure at 38°C (psi)	Density [at 20°C (g/cc)]	Boiling point (°C)	ΔH_{vap} (BTU/lb)
Isooctane	C_8CH_{18}	114.2	1.7	0.6919	99.2	271
Toluene	C_7H_8	92.1	1.0	0.8660	110.6	363
Ethanol	C_2H_6O	46.0	2.3	0.7890	78.3	920

component evaluations and, as a result, do not provide information pertaining to volume swell and hardness. These studies usually report a pass/fail result for the component tested.

Studies providing swell and/or hardness data are summarized in Table 4 along with the test fluids and elastomers studied. The majority of the reported efforts were directed towards fluorocarbons and NBRs. This emphasis is not surprising since fluorocarbons are known to have excellent fuel resistance and NBR is the most common elastomer used in seals and those applications. However, as shown in the table, several studies did include fluorosilicone and polyurethane, and one included neoprene. The other feature that stands out in the table is that the test fuels are either based on gasoline or Fuel C. Fuel C is a Society of Automotive Engineers (SAE) standard test fuel composed of a 50/50 volume blend of toluene and isooctane.[1] All of the studies listed in Table 4 provide results for swelling, and some include other

Table 4. Test fuel and elastomer type listing for key references

Reference	Test fuel(s)	Elastomer type
P. Touchet, B. Zanadis, M. Fischer, and P. E. Gatza, *Materials Compatibility Studies with Fuel/Alcohol Mixtures*, Technical Report 2366, U.S. Army Mobility Equipment Research and Development Command, Fort Belvoir, VA, July 1982	Fuel C Unleaded gasoline (UG) Leaded gasoline (LG) UG10 LG10 UG20 LG20	Fluorosilicone Fluorocarbon NBR Polyurethane
R. F. Karg, C. L. Hill, K. Dosch, and B. Johnson, "Ultra-high CAN Polymer In Fuel System Application," SAE 900196	Fuel C	NBR
I. A. Abu-Isa, "Effects of Mixtures of Gasoline with Methanol and with Ethanol on Automotive Elastomers," SAE Paper No. 800786	Indolene E10 E15 E20 E25 E50 E75	Fluorosilicone Fluorocarbon NBR Polyurethane
G. Micallef and A Weimann, "Elastomer Selection for Bio-fuel Requires a Systems Approach," *Sealing Technology*, January 2009	CE22 CE85	Fluorocarbon
A. Ertekin and N. Sridhar, "Performance of Elastomeric Materials in Gasoline-Ethanol Blends-A Review," Paper no. 09533, CORROSION 2009 Annual Conference and Exhibition, NACE International, Atlanta R. D. Stephens, "Fuel and Permeation Resistance of Fluoroelastomers to Ethanol Blends," ACS Technical Meeting of the Rubber Division, Cincinnati, OH, October 2006	Fuel C CE10 CE20 CE50 CE85 E100	Fluorocarbon
A. Nersasian, "The Use of Toluene/Isooctane/Alcohol Blends to Simulate the Swelling Behavior of Rubbers in Gasoline/Alcohol Fuels," SAE Paper No. 800790	Gasoline Isooctane/toluene/ ethanol blends	Fluorocarbon Fluorosilicone NBR
L. Nihalani, R. D. A. Paulmer, and Y. P. Rao, "Compatibility of Elastomeric Materials with Gasohol," SAE Paper No. 2004-28-0062	Gasoline E10 E20	Fluorocarbon NBR
B. Jones, G. Mead, P. Steevens, and C. Connors, The Effects of E20 on Elastomers used in Automotive Fuel System Components, Minnesota Center for Automotive Research, Minnesota State University, Mankato, February 22, 2008	Fuel C CE10a CE20a	Fluorocarbon NBR Neoprene

measurements such as hardness and tensile properties. We were unable to find relevant DMA data on polymers exposed to ethanol–gasoline fuel blends in the literature. As a result, there are no comparisons on the effect of ethanol on the lower temperature limit or the storage modulus relationship to temperature, which is, of course, important in an actual sealing application.

The most comprehensive study we found was performed by Touchet et al.[25] on evaluating the corrosion and degradation of various elastomers, plastics, and metals in a variety of test fuels. The elastomer types included in this investigation were fluorocarbons, fluorosilicone, polyurethane, and NBRs. The test fuels included Fuel C, unleaded (32.8% aromatics) and leaded gasoline (aromatic content of 29.7%), E10, and E20. This study is the only one so far identified that provided a direct comparison of elastomer performance of Fuel C with pump-grade gasoline; in this case the pump fuels were unleaded gas (UG) and leaded gasoline (LG). Selected elastomer results for volume swell and hardness are shown in Figs. 4 and 5, respectively.

As expected, the fluorocarbons showed the best fuel and ethanol resistance. The fluorosilicone exhibited 20% volume swell, which is consistent with other studies, but the level of softening was much higher than the NBRs. The results for the NBRs and polyurethanes were mixed and depended on the grade for each material. These results were consistent with other studies showing that low acrylonitrile (ACN) content leads to higher swell and loss of hardness.[13] The Touchet et al. study was one of the few to include polyurethane, and the results show that the polyurethane samples were highly susceptible to degradation for gasoline containing 10 and 20% ethanol by volume.

Another important aspect of this study was the comparison of the base fuels (Fuel C, UG, and LG) for each material type. For each elastomer tested, UG produced a small, but significantly higher level of swell than LG. For fluorosilicone, both fluorocarbons, low nitrile NBR, and one polyurethane material, Fuel C caused much higher levels of swell and softening than the pump-grade gasolines. The higher aromatic content of Fuel C (50% aromatic toluene) compared to the LG (29.7% aromatic) and UG (32.8% aromatic) is likely responsible for this effect. Nersasian[26] also examined at the swelling behavior of fluorocarbon, fluorosilicone, and NBR in fluids composed of toluene and isooctane. For each material, the volume swell increased with toluene (or aromatic) content.

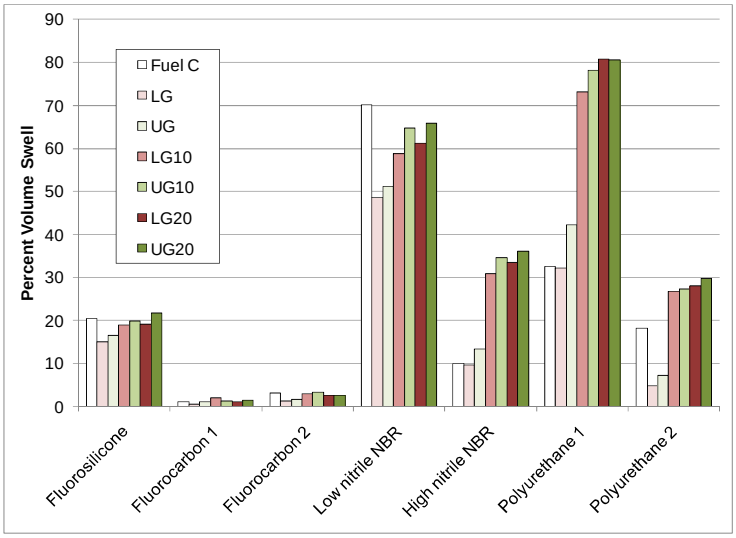

Fig. 4. Volume swell results for selected elastomers for different test fuels. Data obtained from Touchet et al., *Materials Compatibility Studies with Fuel/Alcohol Mixtures*, Technical Report 2366, U.S. Army Mobility Equipment Research and Development Command, Fort Belvoir, VA, July 1982.

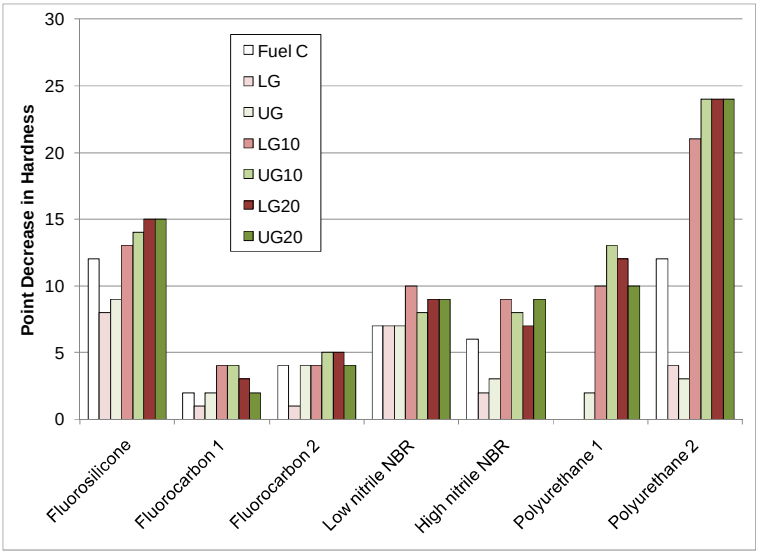

Fig. 5. Decline in hardness for selected elastomers for different test fuels. Data obtained from Touchet et al., *Materials Compatibility Studies with Fuel/Alcohol Mixtures*, Technical Report 2366, U.S. Army Mobility Equipment Research and Development Command, Fort Belvoir, VA, July 1982.

A study by I. Abu-Isa[27] considered the effects of ethanol-blended gasoline on fluorocarbon, fluorosilicone, NBR, and polyurethane. The measured properties were tensile strength, hardness, and volume change on wetted specimens. The elastomer samples were exposed to the test fuels containing 0, 10, 15, 20, 25, 50, and 75% ethanol by volume at room temperature for 72 hr. A federal certification gasoline known as indolene was the base fuel. In this study, the fluoroelastomeric materials (fluorocarbon and fluorosilicone) were the most fuel resistant. E15 produced the highest swell for the fluoroelastomers, which was 7% and 20% for fluorocarbon and fluorosilicone, respectively. These results are consistent with those obtained from Touchet et al.[25] for these materials. Polyurethane and NBR reached a maximum swelling of 56% and 99%, respectively. For polyurethane the highest volume expansion occurred for E20, while NBR had its highest value for E25. Interestingly, neoprene exhibited a maximum swell of 96% for the E0 exposure. The two fluoroelastomers, polyurethane and NBR, exhibited their highest swelling at relatively low blends of ethanol (15–25%). As a result, intermediate levels of ethanol added to gasoline are of greatest concern for degradation of these materials. Neoprene, on the other hand, was most affected by the gasoline, and swelling actually decreased with the addition of ethanol.

Micallef et al.[28] also examined the volume change (and hardness) of fluorocarbons. In contrast to I. Abu-Isa[24] and Touchet et al. (21), Micallef used Fuel C as the control and base fluid for the ethanol blends. The two fuel chemistries were CE22 and CE85. His results showed that CE22 increased the volume by 32%, while the CE85 test fuel had a much smaller effect (16%). Once again the lower level of ethanol was found to be more soluble than high ethanol concentrations. The wet hardness was also observed to drop 14 and 18 points for exposures to CE22 and CE85, respectively. Normally hardness correlates with degree of swell. However, this result may indicate that although CE85 did not permeate to the level of CE22, the increased presence of oxygen (and probably water, salts, and acids) associated with the higher ethanol was able to react with and affect the surface properties of the fluorocarbons. More research on the effects of high levels of ethanol on fluorocarbons is needed to better understand the reaction chemistry that is taking place on the surface of the fluorocarbons. The level of swell observed in the fluorocarbons (in this study) was greater than the values obtained by Abu-Isa. This result is expected since Fuel C has a much higher aromatic content than the indolene-based experiments performed by Abu-

Isa. Unfortunately, Micallef et al. did not report the swell associated with Fuel C exposure, and therefore was unable to assess the Fuel C contribution to the overall swell.

Another study which used Fuel C as the base test fluid was performed by R. Stephens[29] and summarized by A. Ertekin and N. Sridhar.[30] Stephens exposed six different Viton fluorocarbons to Fuel C, CE10, CE25, CE50, CE85, and ethanol for 672 hr at 40°C. Measureable swell was obtained from exposures to Fuel C and varied from 6%–12%, depending on the fluorocarbon type. The addition of ethanol further increased the swelling. The highest level of swell was reported for exposure to CE25, which varied from 12–26% depending on the fluorocarbon type. In general swelling was observed to decrease as the fluorine content of the elastomer increased.

A study by Jones et al.[13] was performed to determine whether E20 had a greater impact than E10 on the volume and mass change for fluorocarbon, NBR, and neoprene. This study differed from the other investigations in that it used the aggressive ethanol formulation described in SAE J1681. As a result, the test fuels contained a small amount of water containing trace levels of acetic and sulfuric acids and sodium chloride. All of these contaminants are found in dispenser-grade ethanol. Fuel C was used as the control. Another key difference from the other studies was that each sample was immersed in the test fluid for 500 hr at 55°C. In contrast, many of the other studies (mentioned in this review) exposed the specimens to the test fluids for approximately 70 hr at room temperature conditions, and for different exposure times. As a result of the more aggressive test conditions, the levels of swelling were higher than the values obtained from other studies. The wetted and dried volume changes for each elastomer are plotted in Fig. 6. The fluorocarbon swelled around 30% upon exposure to Fuel C and CE10a, while CE20a increased the volume by more than 40%. When dried, the fluorocarbon specimens maintained a slight volume increase, indicating that a low level of residual fuel remained in the polymer structure. This conclusion is supported by the mass measurements, which showed a corresponding increase in the dry mass. The two NBR samples provided mixed results: the medium-ACN NBR exhibited much higher

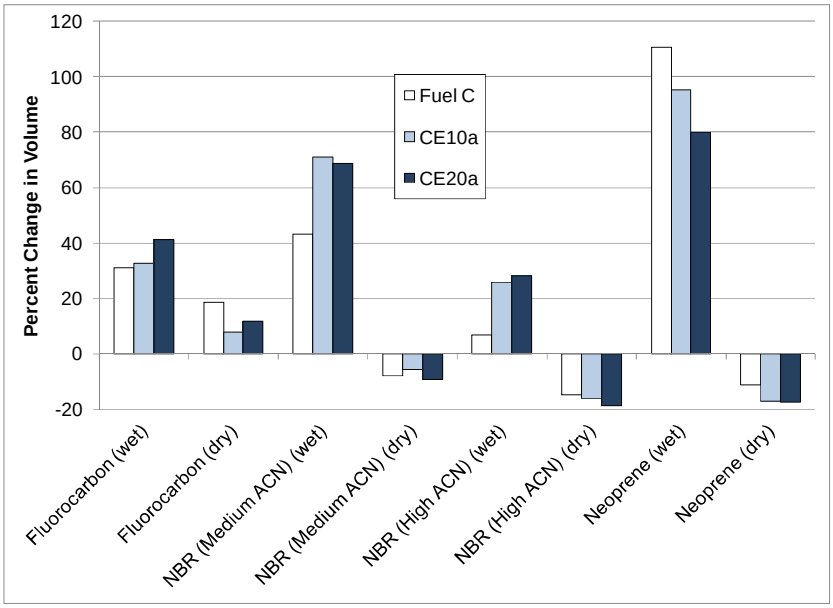

Fig. 6. Percent change in volume for selected elastomers exposed to Fuel C, CE10a, and CE20. Data obtained from B. Jones et al., *The Effect of E20 on Elastomers Used in Automotive Fuel System Components*, Minnesota Center for Automotive Research, Minnesota State University, Mankato, February 22, 2008.

swell but shrank less than the high-ACN NBR after drying. In fact the high-ACN NBR produced the lowest level of swell among the elastomers studied. This observation is noteworthy since fluorocarbons exhibited the lowest level of swell in the other studies. Both NBR samples and neoprene exhibited shrinkage after drying, and the mass loss correlated with the amount of shrinkage observed. This result indicates that material was being extracted from NBR and neoprene by the test fluids. If the extracted material is a plasticizer additive, then the dried specimens would exhibit embrittlement and a loss of durability. In contrast to the other rubbers, neoprene exhibited a decrease in swell with ethanol content. However the resulting shrinkage (during dry-out) was more significant for the samples exposed to CE10a and CE20a.

It is important to note that the volume swell for the fluorocarbon specimens exposed to Fuel C in the Jones study was about 30%, a much higher value than the results shown in the Touchet and Stephens studies. Touchet reported a 20% swell for exposure to Fuel C, while Stephens reported a range of 6%–12%. This discrepancy may be due to compositional difference between the fluorocarbons tested, or due to the higher temperature, which would enable the fluid to more completely permeate the fluorocarbon structure, thereby producing more swell. Unlike the fluorocarbons, NBR has a much higher porosity, and therefore, permeation of fluid would be less sensitive to duration and temperature.

The literature survey shows that maximum volume swell for most elastomers occurs for ethanol concentrations between 10% and 25%. In addition, the volume and hardness can vary considerably according to elastomer type. Within each elastomer class, the swell and hardness change are subject to variability as well. This was especially true for NBRs, which have a wider variability in formulation and processing than most other elastomer types. Low- and medium-ACN NBRs exhibited very high volume swelling compared to NBRs of high ACN content. However, the addition of ethanol was also shown to significantly increase the volume swell of all NBR specimens.

Although the fluorocarbons typically exhibited less swell and a smaller drop in hardness than the other elastomers studied, they were affected by ethanol, which increased swell and softening. Within each study the fluorocarbon samples typically showed the least amount of variability in volume swell and hardness. However, upon drying the fluorocarbons did not shrink or lose mass. Only one study evaluated fluorosilicone rubber, and the degree of swell increased only slightly with increased ethanol content. The fluorosilicone exhibited a relatively low volume swell of around 20% for the fluids that were studied; however, the level of softening was significant. Polyurethane was found to be highly susceptible to swell by ethanol, although the results showed considerable variability between the two samples tested. The only rubber to have reduced swell when exposed to fuel containing ethanol was neoprene. Neoprene swelled 110% from exposure to Fuel C compared to 80% for exposure to CE20. Unfortunately, both of these values would be considered excessive for most sealing applications.

In summary, a review of pertinent studies has shown that most elastomers exhibit some level of swell upon exposure to gasoline. The addition of ethanol to gasoline will increase the swell of most elastomers (except neoprene), and maximum swell occurs at ethanol concentrations between 10% and 25%. Accompanying the volume increase is a corresponding drop in the hardness, and the combination of high swell and increased softening would reduce the effectiveness of the seal. For the test fuels used, the aromatic content also tends to increase elastomer swelling. Therefore, aromatic content of the fuel needs to be considered when designing seals. Fluorocarbon and NBR were the most studied elastomer types, and fluorocarbon performance was observed to improve with increasing the fluorine concentration, while NBR performance improved with increasing ACN concentration. However, many factors, such as processing, additives, and polymer quality, affect fuel compatibility. As a result it is impossible to state, without field experimentation, which elastomer is best suited for a given application. Interpretation is also complicated by the fact that each investigator used different test conditions and test fluids. Thus it is difficult, if not impossible, to compare results from the different studies. This lack of experimental

standardization between researchers, combined with the limited amount of data available, was a primary motivation for the comprehensive ORNL-led study presented in this report.

2.1 REVIEW OF DOE ETHANOL MATERIAL COMPATIBILITY STUDIES

The DOE Office of the Biomass Program (OBP) and the Office of Vehicles Technologies Program (OVT) have funded multiple studies at different locations examining the impact of ethanol on dispenser and vehicle materials. These studies are similar in scope and complementary. The first study conducted by ORNL evaluated the performance of prototype fuel dispenser components in two recirculating (dynamic) test fluids, one representing E85 and the other E25. This study examined and characterized the changes in fuel chemistry with time of exposure. The other two follow-on studies at ORNL were directed towards assessing material performance with exposure to test fluids. These materials studies necessitated the construction of large stir chambers to enable multiple coupon exposures under tightly controlled conditions of temperature, pressure, and fluid flow rate. The ORNL-led materials studies were performed in conjunction with an effort by UL and NREL to evaluate new and used full-scale dispensers with CE17a. In the UL/NREL study, fuel samples were taken periodically from one new and one used dispenser and analyzed to determine if contaminants can be traced to the dispenser polymer materials exposed to the test fluids. In addition, NREL in collaboration with the Coordinating Research Council (CRC) is evaluating the impact of increased ethanol concentration on vehicle fuel system components.[18]

2.1.1 ORNL Dispenser Study Using CE25a and CE85a

In 2007, ORNL began a study (in collaboration with NREL and UL) to evaluate the compatibility of full-scale dispenser hardware with recirculating test fluids. The E85 dispensers in use at that time were not UL-listed, prompting UL and DOE to initiate a study assessing dispenser hardware compatibility with E85. However, the UL tests were limited to static fluid experiments, and concerns were voiced that the static environment may overlook features (such as erosion and passive film removal) that may actually exist as a result of moving fluid. As a result, the DOE Clean Cities Program supported ORNL in setting up a dynamic-based study, which was more reflective of actual field conditions.

The test fuels studied were CE25a and CE85a. Both of these fuel formulations are standard SAE J1681 aggressive mixtures developed for accelerated compatibility testing with ethanol-blended gasoline. In each case the gasoline portion was Fuel C (a 50/50 mix of isooctane and toluene), while the ethanol portion contained up to 0.9% water plus trace levels of NaCl and acetic and sulfuric acids (aggressive ethanol).

ORNL received two prototype fuel dispensers from UL including two air-driven diaphragm pumps. The dispenser components were set up for dynamic operation in which the test fluids were recirculated during operation. The CE25a and CE85a dispensers recirculated the fluids at a rate of 6.3 and 7.9gal/min, respectively. (The source of flow rate difference between the two units was not determined but was likely due to differences in fuel viscosity.) The dispensers were run for 7–10 hr of continuous operation Monday through Friday for 15 weeks during the heat of the summer in 2008. During the summer test period, the temperature ranged from 10 to 40°C. Fluid samples were taken periodically to characterize and measure the level of contaminants (metals and especially hydrocarbons) present in the fluid in order to identify components and materials at risk to degradation. At the conclusion of the 15 week period, the fluids were replaced and run for a second 15 week period during the winter months. Further experimental details are provided in Appendix B.

2.1.2 ORNL CE20a Compatibility Study of Fluorocarbons and Metals

The full-scale dispenser study was followed by a controlled exposure study to investigate the compatibility of selected metals and elastomers with an aggressive E20 formulation. The purpose of the study was to confirm the utility of a specially-designed and sealed chamber to evaluate the compatibility of fluorocarbons, one NBR sample, and selected metals and alloys with a CE20a test fluid. These materials were evaluated as individual coupons and not as part of a component (such as a valve). The metals selected for the experiment covered those used in standard fuel dispenser hardware and included several grades of carbon and stainless steel, brass, bronze, and copper. A report detailing the test protocol and metal analysis was published in 2010 by Pawel et al. at the conclusion of this effort.[31] The elastomers that were investigated included eight fluorocarbon types provided by DuPont and 3M. The metals were evaluated for mass loss and surface analysis, while the elastomeric materials were evaluated for tensile properties, hardness, and swelling. The specimens were placed inside specially designed chambers known as stir tanks or stir chambers (Fig. 7) that allowed multiple (and simultaneous) specimen exposures to a fluid flow of 0.8 m/s while maintaining a constant elevated temperature of 60°C. The combination of dynamic flow coupled with elevated temperature and aggressive fuel chemistry offers the potential to get meaningful comparative results in a relatively short time frame. The results of this study showed that meaningful results (for elastomers and metals) could be obtained for a 4-week exposure period. The study confirmed the stir chamber approach to screen large numbers of samples rapidly in order to assess compatibility of fuel dispenser materials and guide the identification and incorporation of ethanol-resistant materials. Further experimental details are provided in Appendix C.

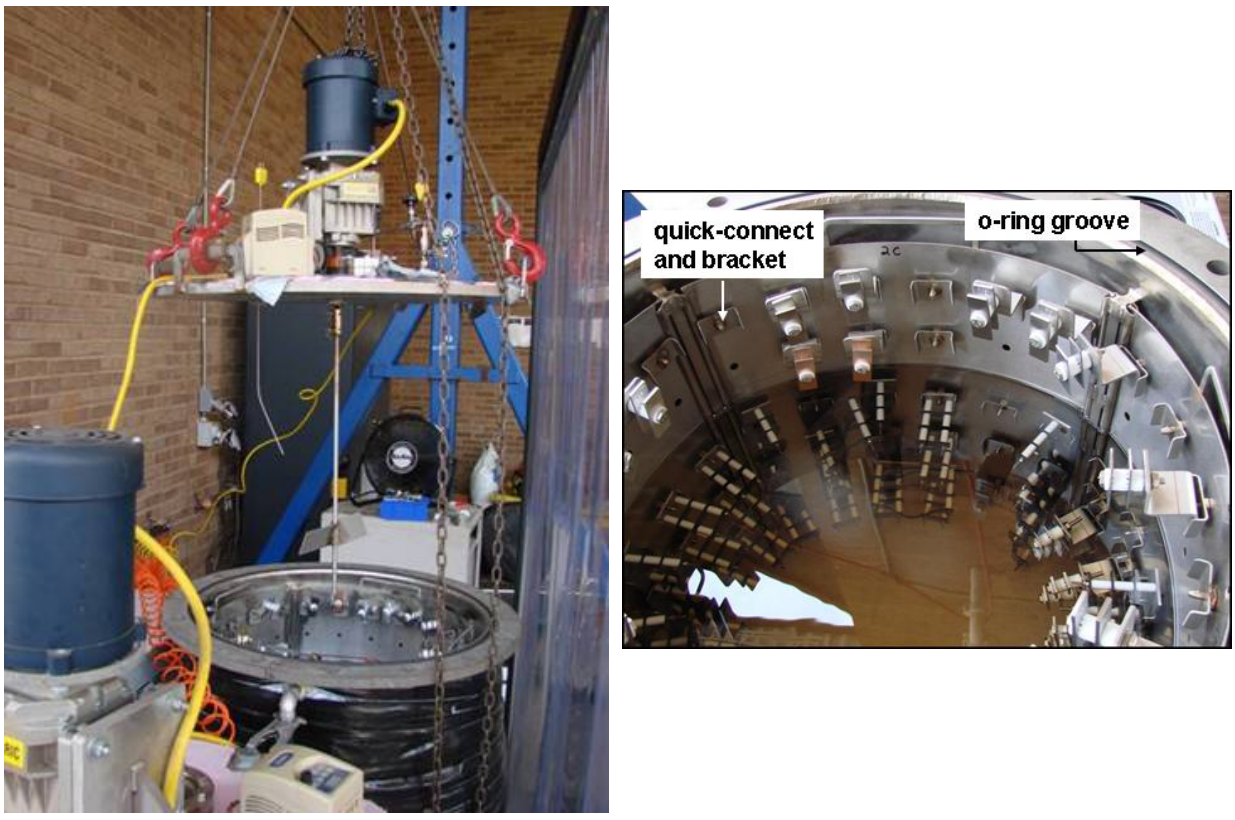

Fig. 7. Experimental stir chamber.

3. ORNL FUEL DISPENSER INFRASTRUCTURE MATERIALS STUDY: METALS, ELASTOMERS, AND SEALANTS

The fluorocarbon and metal coupon study confirmed the operational performance and utility of experimental stir chambers to evaluate large numbers of coupons efficiently. However, the polymers selected for the previous study were limited to eight fluorocarbons and one NBR rubber and did not include many of the polymers typically used in actual dispensers. As a result, ORNL decided to perform a coupon-based screening study to include every material type used in fuel infrastructure system components. These materials included those that are in contact with the fuel from the delivery truck to the UST (Fig. 8) and from the UST to the hanging hardware (Fig. 9). The purpose was to assess the compatibility of representative infrastructure materials with E15 and up to E25 and to assess the rate of change of material properties at these concentrations of ethanol. Sealants were also added to the test matrix since anecdotal evidence suggests that pipe joints present a leak risk. One other limitation noted from the previous study was that the metal specimens did not accurately reflect actual field conditions; that is, metal components are frequently joined or in contact with dissimilar metals. As a result, the follow-on comprehensive study included metal and alloys partially coated with either nickel or chromium to create a galvanic couple to better reflect field conditions.

This study began in 2009. The dynamic stir chambers were used to evaluate the compatibility of the elastomer and metal coupons and sealants. The fuel types that were used in the evaluation were Fuels C, CE10a, CE17a, and CE25a. The specimens were exposed for 4 week periods and then subsequently analyzed for changes in appearance, volume, mass, and hardness. DMA was also used to assess sealing characteristics.

It is important to note that unless a specific material coupon disintegrated or suffered obvious visible damage, it could not stated with certainty how it would perform in the field. Therefore, the purpose of this study was not to set failure criteria associated with material compatibility but rather to screen a large

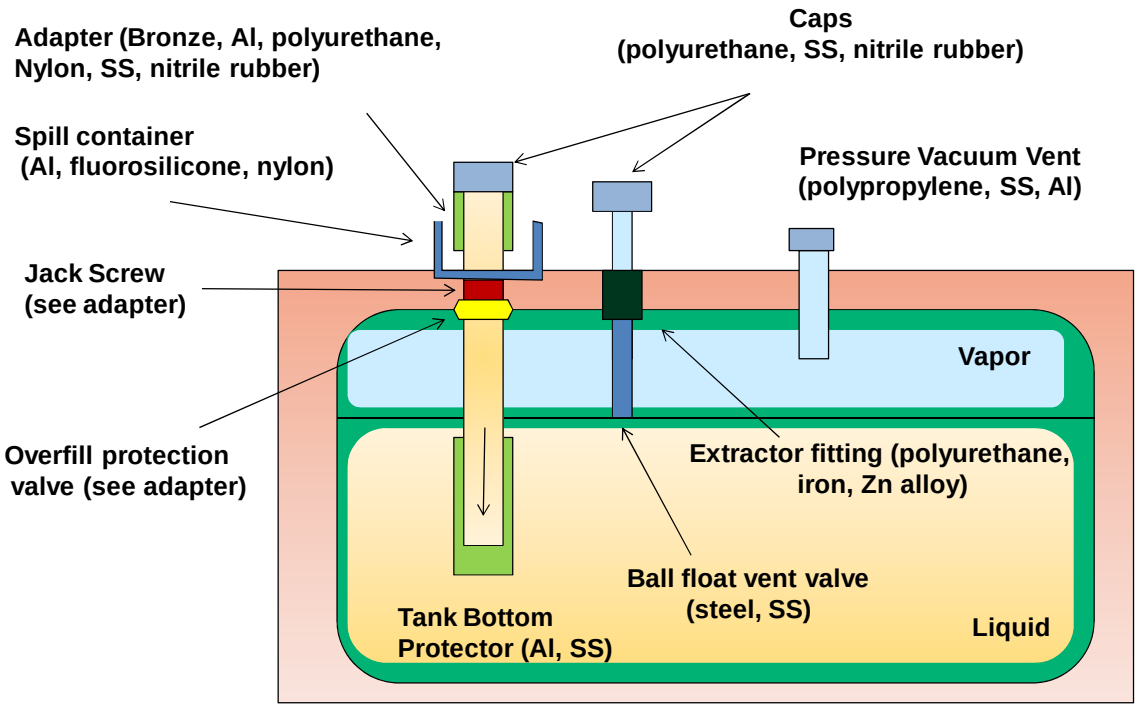

Fig.8. Schematic showing dispenser materials and components from the delivery truck to the UST.

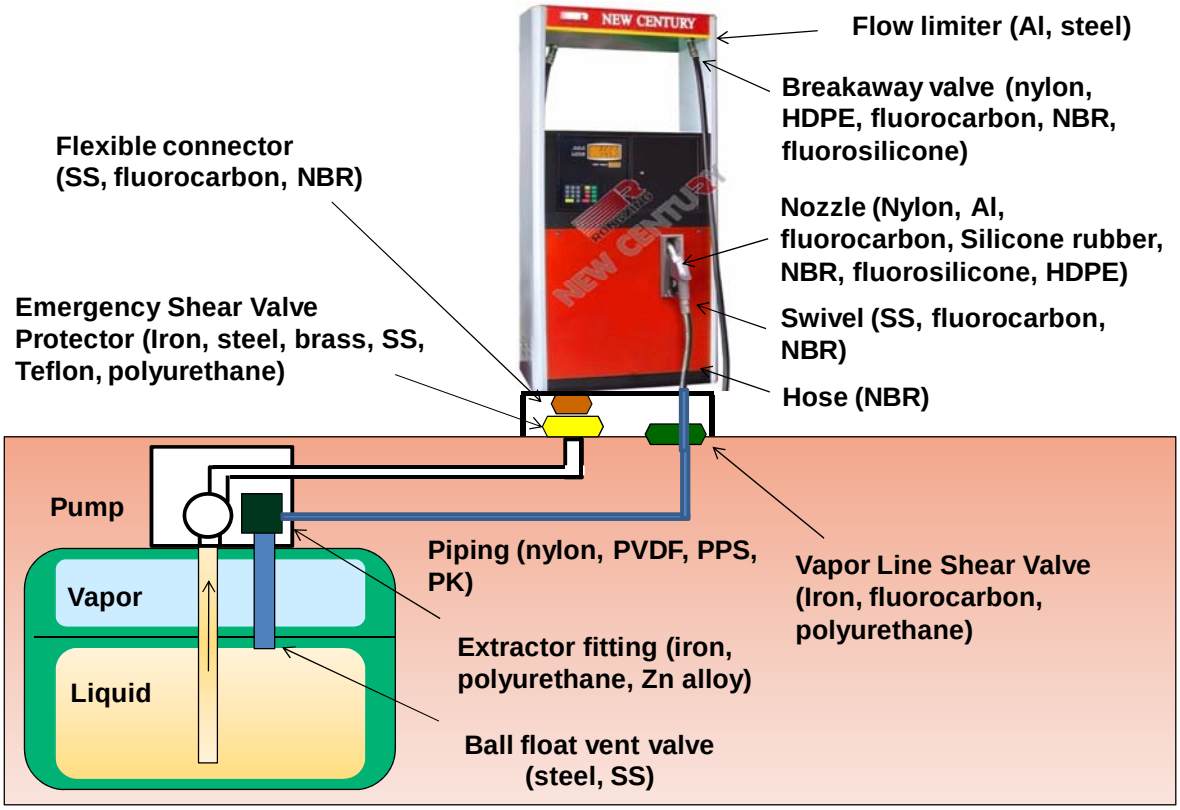

Fig. 9. Schematic showing dispenser materials and components from the UST to the nozzle.

sampling of materials typically used in the infrastructure showing the effect of ethanol concentration on relevant material properties, such as volume swell and hardness. The resulting data will be available to dispenser designers and manufacturers, and it is they who will determine whether the material performance is acceptable or not. The intent of the material selection was to match, to the extent possible, those found in full-scale dispensers and related equipment. The limited availability of this information, however, has created some lack of precision as to which specific formulations to test.

3.1 MATERIALS AND SPECIMEN PREPARATION

The materials examined in this study reflect many of the components used in fuel dispenser components, as shown in Figs. 8 and 9. Guidance on the selection of specific materials (especially polymers) was provided by UL, the API, individual oil companies, and material suppliers. Much information on material selection was provided by the OPW and Dresser-Wayne websites regarding dispenser hardware subsystems and components. Unfortunately, a comprehensive compilation of all legacy materials could not be made since the research team did not have access to the material history and inventory for each dispenser component. In spite of this limitation, a fairly representative matrix of dispenser material types was obtained, although the chosen materials may not be the formulations in actual use. For instance, seals composed of co-polymers such as NBR and SBR may have different amounts of butadiene, depending on the properties desired and the applications used. Additionally, there is a wide range in the type and amount of additives compounded within the base polymer to adjust properties and appearance. Many formulations are proprietary, and the actual composition of the rubber product is unknown. Testing each formulation for each elastomer type was not practical, therefore, testing was limited to samples representative of a specific elastomer class typical of those used in dispenser hardware.

The results from the earlier fluorocarbon-metal coupon study showed that maximum permeability was achieved after 1 week of exposure to either the Fuel C or the CE20a test fuels. Likewise, the corrosion rate of the metal coupons did not change significantly for exposure periods of 1 week or 4 weeks. Although 1week appeared to be sufficient, 4 weeks was selected as the exposure period since it allowed for more accumulation of effects (permeation and leaching or accumulated corrosion) than a 1 week period would allow.

3.1.1 Metals and Alloys

The metals and alloys that were selected for the ORNL CE20a dispenser compatibility study were also used in this investigation. However, to better reflect actual field conditions, a second set of plated specimens had the coating partially removed to form a galvanic couple. The photograph shown in Fig. 10 shows the appearance of two galvanic specimens: nickel-plated aluminum and chromium-plated brass. A complete listing of the metal specimens is shown in Table 5. Brass and aluminum were galvanically coupled with chromium and nickel, respectively, while 1020 carbon steel was galvanically coupled to both metals individually. Chromium and nickel were selected because these combinations of substrate and plating are used in dispensers, and therefore are representative of real possibilities.. If the electrical conductivity of the test fuel is sufficient, measureable corrosion (mass loss) of the test metals should occur. In this study, one specimen per material was evaluated for exposure to the liquid and a second specimen was exposed to the vapor phase. These specimens were weighed before and after exposure to determine the level of mass loss associated with exposure.

Coupons of each material were $5.1 \times 2.0 \times 0.32$ cm ($2.0 \times 0.75 \times 0.125$ in.), with the exception of terne-plated steel and the phosphor bronze specimens, which were only 0.16 cm (0.062 in.) thick. Each specimen included a central mounting hole with a diameter of 0.95 cm (0.375 in.). The total surface area

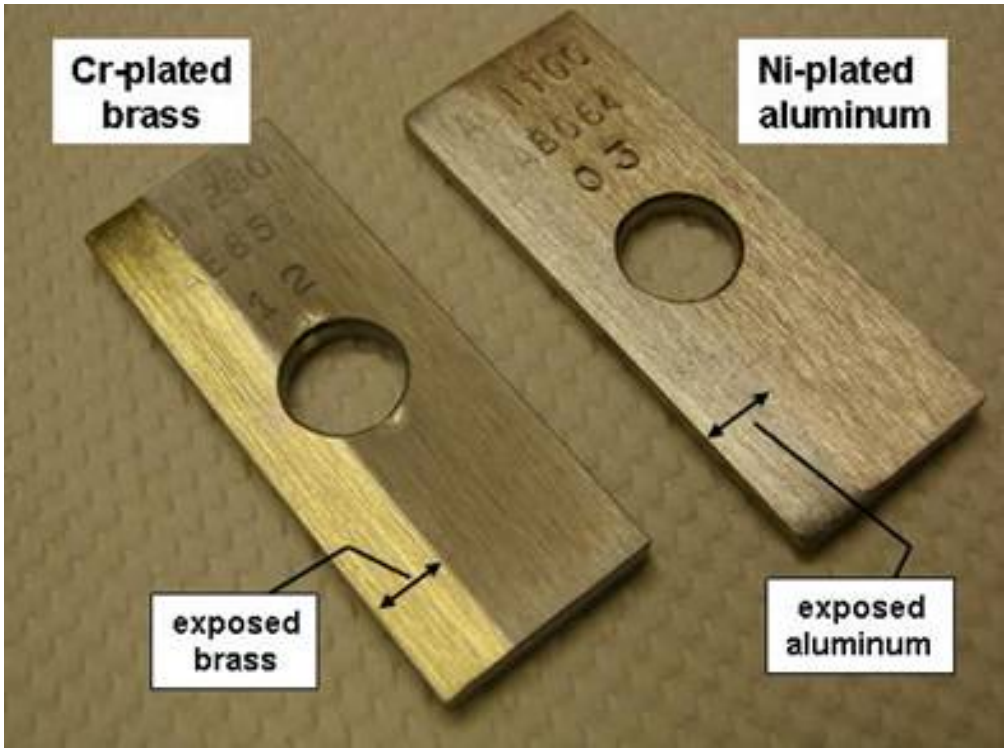

Fig. 10. Representative pre-test appearance of plated coupons after a portion of the plating had been removed to expose the substrate.

Table 5. Metal and alloy specimen listing

Metals having unmodified coupons	Coupons having partial removal of plating to form a galvanic couple
304 stainless steel	Terne-plated steel
1020 carbon steel	Galvanized steel
1100 aluminum	Chromium-plated brass
Cartridge brass	Chromium-plated steel
Phosphor bronze	Nickel-plated aluminum
Nickel 201	Nickel-plated steel
Terne-plated steel	
Galvanized steel	
Chromium-plated brass	
Chromium-plated steel	
Nickel-plated aluminum	
Nickel-plated steel	

was about 24.5 cm^2 for each of the relatively thicker coupons and about 22.2 cm^2 for the relatively thinner coupons. The specimens were handled using lint-free gloves and tweezers. Each specimen was cleaned (ultrasonic treatment in acetone followed by forced air drying) and weighed prior to mounting on assemblies for exposure. The balance used for these experiments was capable of measuring 0.00001 g, but as a practical consideration for coupons of this size, reproducibility of the measurements was ±0.00005 g.

Single specimens of each material were exposed using a stainless steel and Teflon mounting bracket (Fig. 11). Teflon shoulder washers were used to eliminate unwanted metal contact between the metallic specimens and the stainless steel mounting hardware. In addition a Teflon crevice washer was placed on one side of each test specimen to prevent specimen-to-specimen contact. All metallic components of the mounting bracket were type 304 or type 316 stainless steel. The nut and bolt arrangement was tightened until the stainless steel split washer (between the nut and mounting bracket) was completely flattened against the bracket surface. Typically, this caused a slight compression of the Teflon components.

XPS was performed on selected coupon surfaces following testing (to compare with results from unexposed coupons) to assess the corrosion film thickness and composition as a function of ethanol content in the exposure environment.

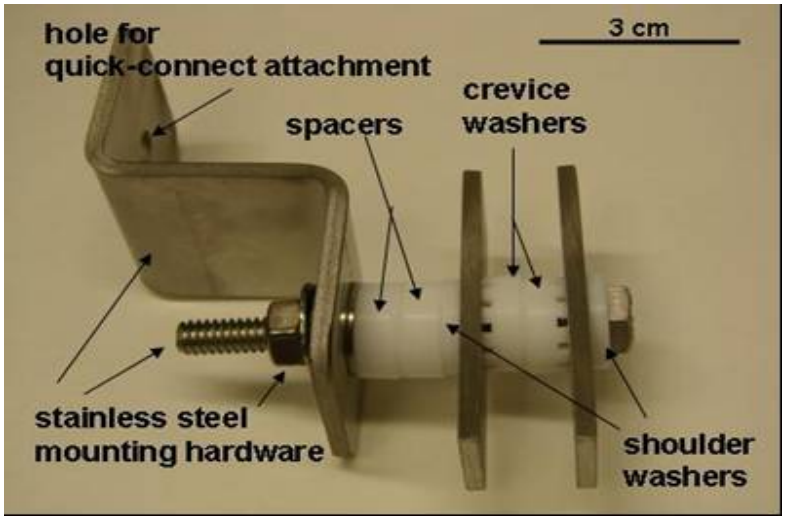

Fig. 11. Mounted specimens and mounting bracket.

3.1.2 Elastomers

As shown previously in Figs. 8 and 9, many dispenser components use the same types of elastomers. Two classes of elastomers (fluorocarbons and NBRs) contained more than one sample type. The eight fluorocarbons used in this investigation are designed for different applications, and therefore differ from each other in fluorine content, additives, and curing process. Several of the NBR samples were developed for use in fuel hoses and also contain different additive packages and formulations. The other material classes, SBR, silicone rubber, fluorosilicone rubber, neoprene, and polyurethane, only contain one sample type. The following is a list of the specimens selected.

1. Fluorocarbon rubbers: A total of eight samples were evaluated—Viton A401C, Viton B601, Viton GF-600S, Viton GFLT-600S, Dyneon FE5620, Dyneon FE5840, Dyneon FPO3741, and Dyneon LFTE6400.
2. NBR: A total of six samples were evaluated. They are identified as NBR#1 through NBR#6.
3. Fluorosilicone rubber
4. Polyurethane
5. Neoprene
6. SBR
7. Silicone rubber

The elastomer specimens used the same mounting bracket as that of the metals. The specimen geometries were rectangular: approximately 1.27 cm wide × 3.81 cm long × 0.25 cm thick (0.5 in. × 1.5 in. × 0.1 in.). There were no tensile specimens used in this study. A total of three specimens were made for each sample and were immersed in the test fluid. In addition, one representative specimen was also placed in the vapor-phase region.

Each specimen selected for fluid compatibility was pre-weighed and measured before exposure to the test fluid. At the conclusion of the exposure runs, the immersed specimens were quickly removed and loaded into a container containing enough fluid to cover the specimens and prevent drying. The wetted specimens were measured for volume swell and mass increase and for hardness (at five random locations on each specimen). The hardness protocol followed the ASTM D2240 type A scale (usually referred to as Shore A hardness) and was used for either wet or dry specimens.[32] These specimens (along with the vapor-exposed samples) were then dried at 60°C for 20 hr and then remeasured (for volume and mass change and hardness) to assess dry cycle property changes. In addition DMA testing was performed on all dried fluid- and vapor-exposed specimens to determine the solvent effects on elastomer performance as a function of temperature.

All DMA testing was carried out using the TA Instruments Q800 on nominal 38 mm long × 13 mm wide × 2 mm thick rectangular samples. The samples were placed in a single cantilever clamp having a fixed length of 17.2 mm and were operated in air under an oscillating amplitude of 40 microns at a fixed frequency of 1 Hz and a heating rate of 3°C/min. The range of temperatures over which the samples were evaluated varied depending on the specific elastomer that was being examined. Measurements were obtained using TA's Universal Analysis software that was provided with the DMA instrument. The DMA instrument used in this study required that the specimens be dried prior to measurement; therefore, DMA measurements were not made for the wetted condition.

3.1.3 Sealants

Pipe thread sealants were identified by ORNL with input from the oil industry and the API as critical materials whose compatibility with the test fuels needed to be determined. Sealant use is ubiquitous in the thread joint assemblies of fuel dispenser systems. Sealants are viscous materials that change state upon drying to become solid. The sealants most often used in gas and diesel fuel systems contain polytetrafluoroethylene (PTFE), better known by its trademark name Teflon. The viscous material containing and surrounding the PTFE particulates varies depending on the application. These sealants are designed to be used alone, but they are often combined with Teflon tape for additional leak protection. The three scenarios evaluated in this study were as follows.

1. RectorSeal brand pipe thread sealant: This PTFE sealant is designed for use with ammonia, refrigerants, and heating oil. It has been widely used in legacy gasoline and diesel fuel systems to seal pipe threads.
2. RectorSeal plus Teflon tape: Discussions with industry have revealed that this combination appears to be widely used in many applications using ethanol–gasoline fuel blends.
3. Gasoila E-Seal: PTFE sealant developed for E10 and E85 use.

Each sealant scenario was applied to three individual stainless steel 3/8th in. pipe plugs and evaluated according to ASTM D 6396 Standard Test Method for Testing of Pipe Thread Sealants on Pipe Tees. The plugs were screwed into a stainless steel cross to a specified torque setting of 27.1 N-m. This torque level was also applied to the RectorSeal/Teflon tape combination. The applied sealant and test fixture are shown in Fig. 12. After curing for 72 hr under ambient conditions, the open end of the cross was attached to a compressed air line and then submerged underwater. Approximately 100 psi of air pressure was applied to each test fixture, and no leaks were observed in each of the three cases. The air line was removed and the open end was left unplugged to allow the test fluids access to the internal as well the external surfaces of the test fixtures.

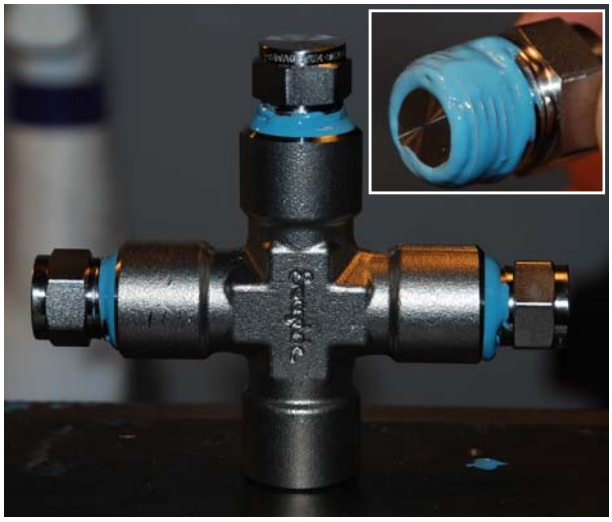

Fig. 12. Thread with applied sealant and the test fixture with three mounted specimens.

3.2 EXPOSURE PROTOCOL

In order to evaluate the material performance at 60°C under dynamic operation, two chambers were designed to allow the coupons to be exposed at a constant flow rate and constant temperature. A

schematic representation is shown in Fig. 13. These stir tanks are equipped with a temperature control system to maintain a constant 60°C fluid temperature regardless of ambient conditions. Each chamber is capable of exposing over 300 individual specimens simultaneously. The chambers were only partially filled to allow a portion of the specimens to be exposed to the fuel vapors (Fig. 13). The test fuels were formulated following the SAE J1681protocol, and these fuels were added after specimens had been loaded onto the inner liner. For each chamber, the fuel was added to a level between the bottom and top sets of samples. The bottom sample set was completely immersed in the liquid, while the top set was left exposed to the vapor phase. After the specimens were loaded and the fuel was added, the lid was attached and the headspace was purged using compressed dry air for 5 min to ensure a consistent starting humidity of 0% for the vapor-exposed specimens. Next the stirring motor was turned on to provide a constant 0.8 m/s flow of the liquid fuel and heat was applied to the tanks via the water jacket. The temperature of the tank fluid reached 60°C approximately 5 hr after start. The tanks were operated continuously for 28 days, after which the tank motor and heat were turned off and the specimens removed. The test fuel liquid level was set to ensure that the vapor phase specimens were not wetted by the rising fluid level at the sides when the paddle was operated.

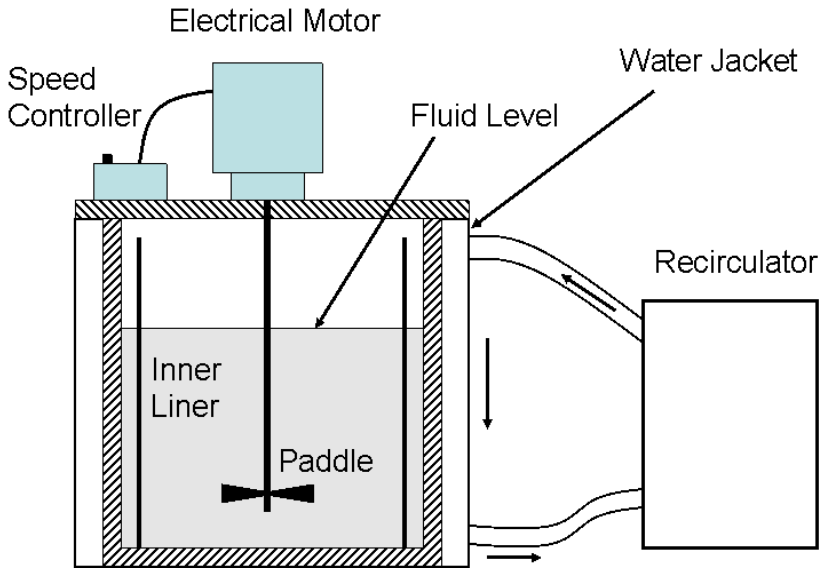

Fig. 13. Schematic representation of dynamic stir chamber.

3.3 ANALYTICAL METHODS

The elastomer samples were measured for mass and volume change, Shore A hardness, and DMA performance. These properties are commonly used to assess the compatibility and performance of materials for use in sealing applications involving exposure to solvent fluids.

The volume increase (or swell) associated with the wetted specimens is an important parameter used to gauge the performance of a material for use with solvents. The level of swell is a measure of the solubility of the elastomer (solute) with the solvent (fluid). High swelling is a concern for several reasons.

1. Swelling indicates that the test fluid can easily permeate into and out of the elastomer. Therefore the seal does not serve as an effective barrier and the solvent may leak out, either as a fluid or gas.
2. High permeation (or high solubility) means that the elastomer (or a component of the elastomer) is more susceptible to dissolution and removal, otherwise known as leaching.

3. Excessive swelling may force the seal to extrude from the joined interfaces, thereby reducing the seal pressure of the elastomer. The extruded portion of the elastomer is also susceptible to damage via abrasion and tearing.

The volume and mass change after drying indicates the extent to which the test fluid was able to dissolve and remove the elastomer and/or its components. If the dried volume is significantly less than the initial volume, then not only is the sealing pressure reduced but gaps may form between the seal and the interface, resulting in an open path to leakage. A reduction in the mass also means that material is lost, and if one or more components are leached out, the physical properties, such as hardness, may change as well.

The durometer hardness test measures the depth of an indentation (in a material) that is created by a given force. As such it is used to evaluate a material's resistance to permanent indentation. There are several different scales used with the durometer depending on the material type. For soft materials, like the rubbers used in this study, the A scale is used and the protocol is outlined in ASTM D2240 type A scale. The Shore A hardness measurement can be used with either wet or dry specimens. In this study, the specimens were measured for hardness in the wetted state and after being dried for 20 hr at 60°C. For each test, the hardness was measured at five locations on each specimen and averaged for a final value. The change in wetted hardness was recorded to determine the hardness decrease (softening) that had occurred when the elastomers were completely soaked with the test fuel. Softening results in a decrease in the sealing pressure caused by relaxation of the elastomer and may subsequently lead to leakage. Also when a substantial drop in hardness is accompanied by a large swell in volume, the elastomer will extrude more easily past the contact surfaces, thereby further increasing the risk of leaking. If, after drying, the hardness is increased from the original condition, then embrittlement has occurred. Embrittlement will increase the chance of fracture, which can cause the seal to fragment and fail under the sealing load, thereby creating a leak.

The third set of tests performed on the elastomers were DMA measurements, which are used to assess damping and stiffness of materials over a range of temperatures.[33] The storage modulus (E′) is measured as a function of temperature. Storage modulus is a measure of material elasticity. It can be described as the ability of a deformed material to recover to its original state after being deformed. The storage modulus is highly dependent on the molecular state of the elastomer and can be used to determine the temperature at which an elastomer transitions from a stiff glassy state to a more pliable rubber state, as shown in Fig. 14. At low temperatures the polymer has a low free volume, which restricts molecular stretching, twisting, and bending, thereby making the elastomer glass-like, hard, and very stiff. When the temperature is slowly increased, the elastomer will expand until the free volume is such that relaxation (stretching, twisting, and bending) occurs and the resulting storage modulus drops by several orders of magnitude. In this state the elastomer is rubbery and viscous. The temperature at which the storage modulus drops suddenly is known as the glass-to-rubber transition temperature (T_g) and is usually referred to as the glass transition temperature. The glass transition temperature is associated with the critical free volume needed for molecular relaxation, above which the material is useful as a seal. Both E′ and T_g are highly dependent on the molecular structure, and changes in these two parameters indicate that important structural changes within the elastomer have occurred.

3.3.1 Sealants

For the first experiment, RectorSeal was evaluated in Fuel C and CE25a. Subsequently, Gasoila E-Seal and RectorSeal plus Teflon tape were added to the stir chambers containing the CE25a and CE10a test fluids. The test methodology followed the ASTM D 6396 Standard Test Method for Testing of Pipe Thread Sealants on Pipe Tees, shown in the flow diagram (Fig. 15) depicting the entire specimen

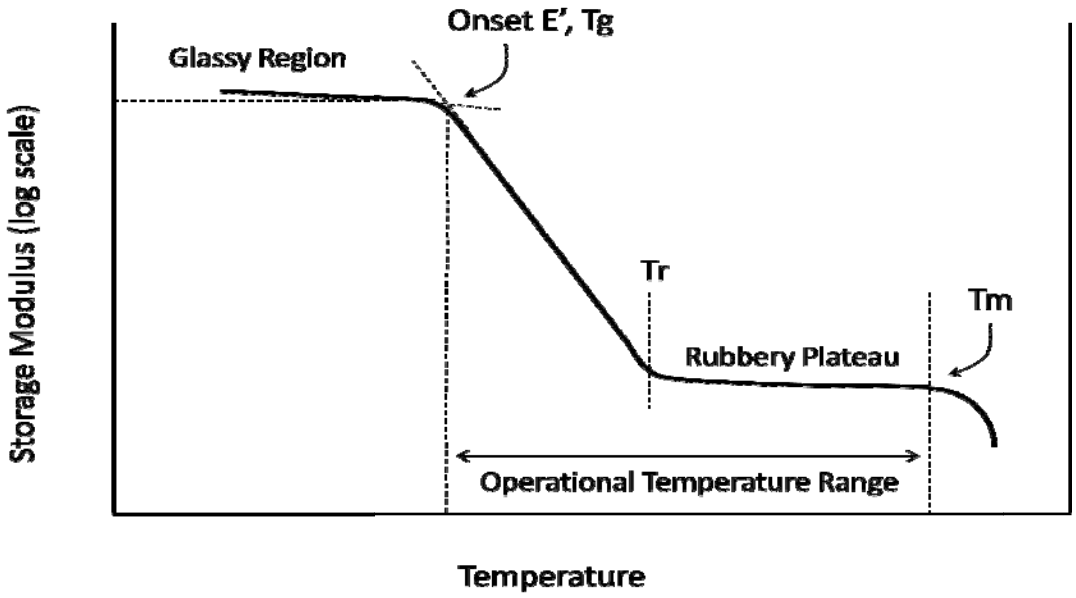

Fig.14. Typical DMA plot of storage modulus with temperature.

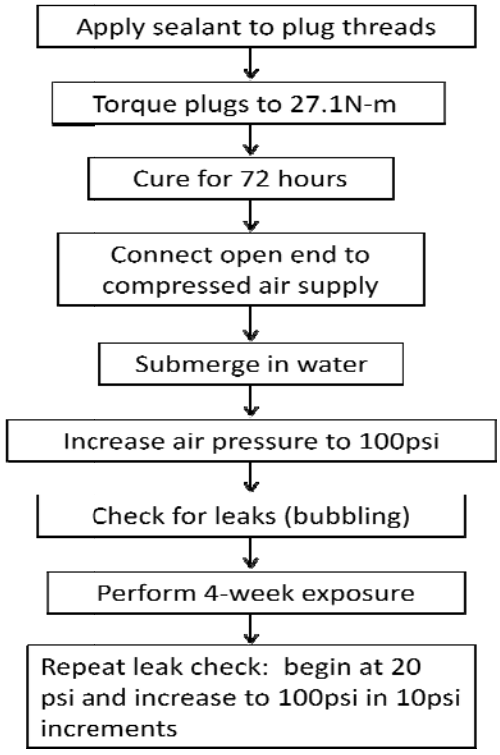

Fig. 15. Schematic of sealant test protocol.

preparation and test procedure. The test fixtures were submerged in the test fluid for the 4 week test period, after which the test fixtures were removed, drained, and allowed to dry for 24 hr before leak testing. The sealants were evaluated by attaching the compressed air line to the open end and submerging each fixture in a beaker of water. The air pressure was initially set at 20 psi and then increased in 10 psi increments (with a 2 min hold time) until either bubbling was visible or 100 psi pressure was reached.

3.3.2 Test Fuels

The fluids used in this study were aggressive formulations based on standards described in SAE J1681 for use in compatibility studies. The test fluids used in this study were based on Reference Fuel C (or Fuel C), which is a mixture of 50% isooctane and 50% toluene. Fuel C produces swelling in polymers that is indicative of highly aromatic premium grades of automotive gasoline. The reference ethanol used in this study is the aggressive ethanol formulation defined in the SAE standard. Aggressive ethanol contains NaCl, acetic acid, water, and sulfuric acid, and the amounts of these components used to make 1.0 Liter of aggressive ethanol are shown in the Table 6.

Table 6. Aggressive ethanol formulation

Component	Amount needed to make 1.0 Liter (g)
CDA ethanol	816.0
Deionized water	8.103
Sodium chloride	0.004
Sulfuric acid	0.021
Glacial acetic acid	0.061

The aggressive formulation is conservative by design but is representative of field conditions since organic acids such as formic and acetic acid are present in certain fuels, including ethanol. These acids can be formed in the production process of ethanol or created via oxidation during handling, transfer, and storage. Sulfuric acid is formed by the reaction of fuel-borne sulfur with ethanol and can be particularly corrosive to metals and polymers. Commercial gasolines contain varying amounts of sulfur, which is usually present as disulfides. Disulfides are converted to sulfonic and sulfuric acids in the presence of atmospheric oxygen and water. Since ethanol is miscible with water, ethanol fuel blends will also contain contaminants previously dissolved in the hydrous ethanol. Any soluble contaminants, such as sodium chloride, residing in the fuel delivery or tank infrastructure will be present in the ethanol blended fuel.

Test fuels containing “C” in the nomenclature will have Fuel C as the base component, while the “a” refers to the “aggressive” ethanol formulation mentioned previously. Therefore a test fuel designated as CE10a will contain 90 vol % Fuel C plus 10 vol % aggressive ethanol. These test fuels are designed to simulate severe, real-world conditions. They are also intended to minimize the length of exposure necessary to rigorously evaluate materials while providing a standard method of testing fuel system materials.

The test fluids selected for this investigation were Fuel C, CE10a, CE17a, and CE25a. Fuel C was selected as the control since it is representative of premium gasoline and is a standard test fluid widely used for studying material compatibility to gasoline. CE10a represents an aggressive formulation of E10, and as such, it can be viewed as a baseline test fuel since E10 is currently available in many, if not most, fuel dispensers.

A major focus of this study was to assess the compatibility of dispenser materials with gasoline blends containing ethanol in excess of 10% by volume. Of immediate concern is the impact associated with the potential of E15 usage, and the further possibility of allowances to E25. Quality surveys on E10 have

shown that the actual ethanol content can vary up to 2% from pump to pump.[34] Therefore, instead of using a CE15a blend, we formulated to CE17a in order to conservatively represent E15 in the field. This composition also matches the test fluid used in the NREL/UL dispenser study. CE25a was selected due to the existing potential for even higher future ethanol concentrations.

4. RESULTS

4.1 PERFORMANCE OF STIR CHAMBERS

The dynamic stir chambers were successfully operated continuously near 60°C for each 28 day exposure period. Daily measurement of the fluid temperature showed that the fluid temperature was maintained at 59 ±1°C. The temperature of the vapor region was less consistent and varied ±5°C for each case. The average daily headspace temperature for each test fluid was as follows.

1. Fuel C: 48.9°C
2. CE10a: 43.2°C
3. CE17a: 48.7°C
4. CE25a: 52.6°C

The stir chambers developed small vapor leaks near the lid bearing; however, at the end of the first set of exposure runs, very little actual fluid was lost, so the following exposure runs were maintained at ambient to maintain consistency.

4.2 SPECIMEN ANALYSIS OVERVIEW

For the metals, the primary concern is corrosion. Therefore, the metals were evaluated according to their mass loss and change in appearance (to determine whether pitting or surface passivation had occurred). On the other hand, elastomers are used to provide stable and durable leak-tight seals. Issues such as elasticity, volume swell, shrinkage, and dissolution determine whether an elastomer will adequately provide a stable and durable seal. The elasticity is assessed through hardness and DMA measurements, while shrinkage is due to volume and mass loss as a result of dissolution of the base polymer or additive. The selected DMA results are tabulated in Appendix D, and the complete curves are available upon request. Volume swell is of primary importance since it indicates the level of mutual solubility between the polymer and test fluid, which ultimately relates to the potential for dissolution and extraction. Increased hardness is also a measure of embrittlement, which leads not only to a loss of elasticity but also to cracking of the elastomer itself. The most straightforward compatibility assessment was sealant performance, which was determined solely by visual detection of leaking of air. Sealants are deemed to meet the standard if no bubbling is detected at pressures less than 80 psi.

4.3 METAL COMPATIBILITY PERFORMANCE

Consistent with the results observed from the initial testing, very little corrosion of any of the metallic coupons was observed in Fuel C, CE10a, CE17a, or CE25a. Coupons exposed to the vapor phase above each solution exhibited slight discoloration in some cases—particularly the brass and bronze coupons—but no measurable weight loss above the routine scatter of the measurement was detected for any materials.

Among the coupons immersed in the different test solutions, 1020 mild steel, 1100 aluminum, 201 nickel, and 304 stainless steel were found to be essentially immune to corrosion for the exposure conditions evaluated. This result is consistent with that of the initial assessment —that is, essentially no weight loss,

no discoloration, and no tendency toward localized corrosion under/near the crevice washers—and suggests that these materials are suitable for extended service in intermediate fuel blends of this type and are not strongly impacted by the concentrations of ethanol in gasoline at these intermediate levels.

Also consistent with previous results,[31] immersed coupons of cartridge brass, phosphor bronze, zinc-plated (galvanized) steel, and lead-plated (Terne) steel exhibited variable degrees of discoloration and minor corrosion product film formation. The highest corrosion rate observed was about 30 µm/year for the cartridge brass immersed in CE10a, and only one other material (bronze exposed to CE25a) exhibited a corrosion rate above 10 µm/year. These rates were calculated assuming uniform weight loss. In most cases, the absolute value of the corrosion rate based on weight loss calculations is slightly comprised of minor amounts of adherent corrosion product, which tend to introduce a small underestimation error in the corrosion rate calculation. But it should be noted that none of the coupons suffered a measureable change in thickness and the original machining marks or plating grain structure remained visible on the coupon surface following testing. Further, based on earlier testing,[31] it is suspected that the corrosion rate of the copper-based materials decreases with extended exposure time.

Besides the fact that only negligible corrosion was observed for the Fuel C immersions (<0.3 µm/year), there was no apparent trend associated with corrosion rate of any materials as a function of ethanol fraction in the fuel. For example, Table 7 shows the corrosion rates calculated from weight change for phosphor bronze coupons as a function of ethanol fraction in the test fuel. These results can be interpreted to mean that, for such low corrosion rates, there are subtleties associated with each exposure condition that influence the amount of corrosion preceding film formation, but that these values are uniformly low and near the limit of detection.

Table 7. Annualized corrosion rates of phosphor bronze

	Reference Fuel C	**CE10a**	**CE17a**	**CE20a**	**CE25a**
Corrosion rate of bronze (µm/year)	0.2	6	4	3	13

Figures 16–18 represent the post-exposure appearance of coupons of cartridge brass, phosphor bronze, and galvanized steel, respectively, resulting from the expanded testing. These images indicate the degree of discoloration and film formation associated with each exposure (other materials indicated far less, or even no, discoloration and film formation). As indicated by the planned interval test results,[31] particularly for the copper-based alloys, these corrosion films form quickly upon exposure to fuel at elevated temperature and tend to be adherent to and protective of the substrate.

X-ray photoelectron spectroscopy (XPS) was performed on representative coupon surfaces following testing (to compare with results from unexposed coupons) to assess the corrosion film thickness and composition as a function of ethanol content in the exposure environment. The corrosion film composition and thickness were not found to be substantially functions of the percent of ethanol in the fuel blends (~ 10, 17, 20, and 25%). In other words, the XPS results for a given material were indistinguishable and independent of ethanol concentration. Representative XPS results, shown in Fig. 19, were measured for cartridge brass exposed to CE25a. The plot reveals the composition of the corrosion product film as a function of depth from the surface (the film is incrementally sputtered from the surface, and the identity of released materials is distinguished by relative energy). As stated, the sputter profiles for cartridge brass exposed to CE10a, CE17a, and CE20a were indistinct from that shown in Fig. 19 for exposure to CE25a.

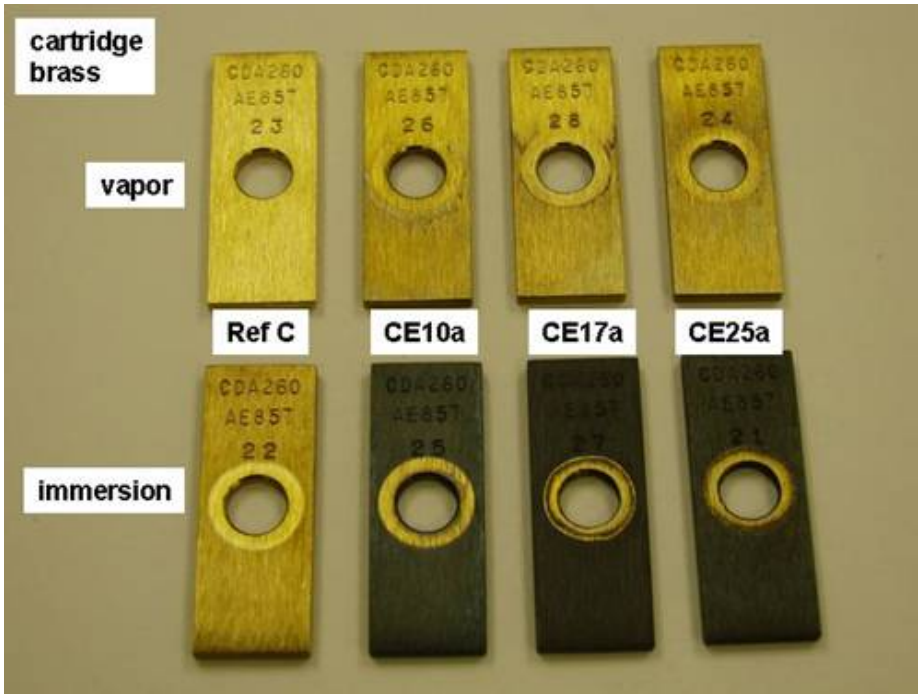

Fig. 16. Post-exposure appearance of the cartridge brass specimens following 28 days of exposure to vapor (~55°C) and liquid (60°C) in the indicated environments.

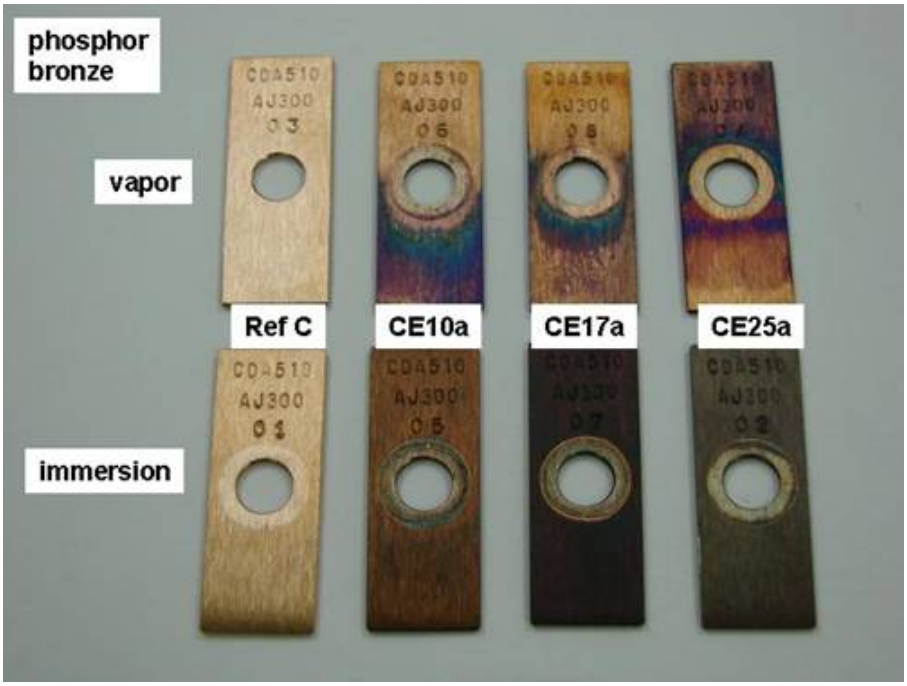

Fig. 17. Post-exposure appearance of the phosphor bronze specimens following 28 days of exposure to vapor (~55°C) and liquid (60°C) in the indicated environments.

Fig. 18. Post-exposure appearance of the galvanized steel specimens following 28 days of exposure to vapor (~55°C) and liquid (60°C) in the indicated environments.

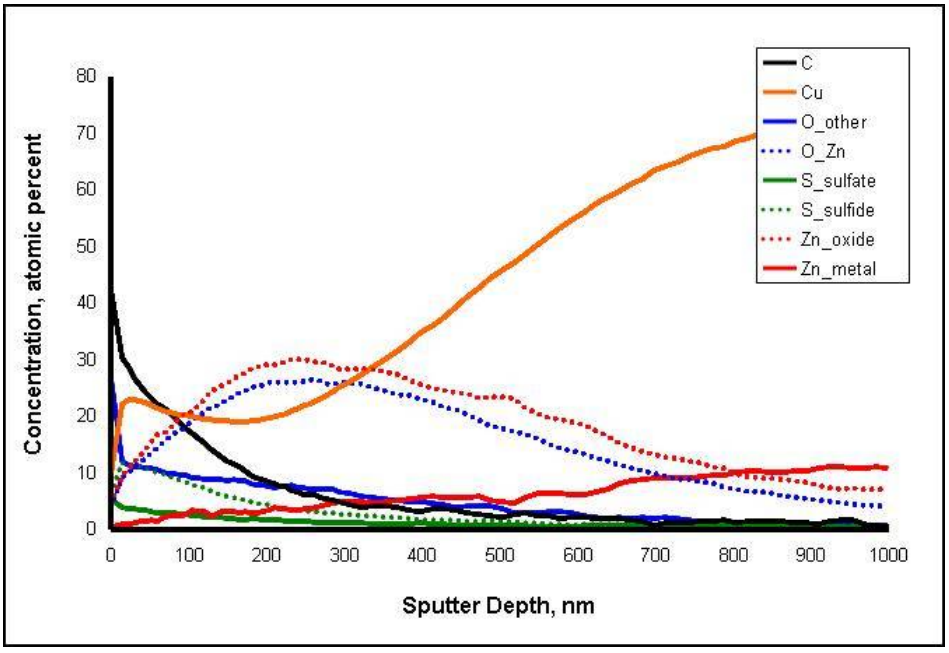

Fig. 19. XPS results for cartridge brass following immersion in CE25a for 28 days at 60°C.

While detailed analysis is quite complicated, a summary analysis of the information in Fig. 19 can be highlighted by a few key points. For example, the copper profile comprises two components—relative predominance of Cu^0/Cu^{+1} near the specimen surface that occurs in concert with relatively elevated sulfur present as a sulfide and a distinct component (Cu^0) representing primarily the bulk copper of the substrate. Taken together, this information suggests the outermost portion of the corrosion product film—on the order of 100 nm—is predominantly copper sulfide (Cu_2S). The source of the sulfur is not certain, but it seems likely to be from the modest addition of sulfuric acid to the aggressive fuel formulations. Deeper into the film (partially mixed with and mostly beneath the outermost surface layer), zinc and oxygen predominate concurrently, presumably as the oxide (ZnO). Approximately 800 nm into the surface film, the relative amount of copper has returned to the value expected within the base metal, but the relative amount of zinc at this location is less than that expected in the base metal by a factor of nearly two, suggesting preferential leaching of zinc to a depth somewhat greater than the corrosion film thickness. (Similar selective leaching of tin and formation of a near-surface sulfide were detected for the bronze specimens.)

Note also that carbon is a ubiquitous contaminant on the extreme surface of all specimens that have been handled in air, but the relatively slow dilution of carbon from the film to a depth of perhaps 300 nm suggests some carbon incorporation into the film during its formation. The source of the carbon could be from degradation of the elastomers exposed with the metal coupons in the same solution environment during testing. In fact, small amounts of ZnO were detected on all metallic specimens following exposure, suggesting at least modest interaction of corrosion products from specimens containing zinc with those that do not results from interaction of dissolved species in the common test fluid. In any case, while there is no doubt some complicated solution chemistry and reactions occur on the surface of metallic specimens exposed to these fuel blends, these reactions appear limited to the extreme surface (on the order of 1000 nm) and no functionally significant degradation was observed.

None of the plated coupons—Cr-, Ni-, Pb-, or Zn-plated steels, Cr-plated brass, or Ni-plated aluminum—revealed any readily observable discoloration/change or measurable corrosion (no weight loss, no pit/crevice initiation). Further, none of the plated coupons with substrates partially exposed revealed accelerated corrosion due to galvanic coupling between the plating material and substrate. Weight changes for each of the partially exposed coupons were found to be directly related to the area fraction of the exposed substrate and the substrate identity. For example, the weight loss for a chromium-plated brass specimen with 30% of the chromium plating removed was found to approximate 30% of the mass loss of a completely bare brass coupon (leaving zero mass loss associated with the intact coating). Figure 20 records the post-exposure appearance of the chromium-plated brass coupons with the substrate partially removed, and this result is representative of the pattern observed on all specimens with partially removed coatings.

4.4 ELASTOMER COMPATIBILITY PERFORMANCE

4.4.1 Fluid (Liquid) Exposures

The *Parker O-Ring Handbook* provides a compatibility rating for the elastomers used in this study with the individual test fluid constituents.[20] A summary of the compatibility ratings is listed in Table 8. In the Parker rating system, 1is satisfactory, 2 is fair (generally acceptable for static seal), 3 is doubtful (sometimes acceptable for static seal), and 4 is unsatisfactory.

According to the *Parker O-Ring Handbook*, only fluoroelastomers (fluorocarbon and fluorosilicone) are deemed acceptable for o-ring applications using the test fuels examined in this study. Likewise, neoprene, SBR, and silicone are not considered satisfactory for standard gasoline use. Yet, new and used fuel dispenser systems feature all of these materials for E0 and E10 use. However, because the solvents listed

Fig. 20. Post-exposure appearance of the chromium-plated brass specimens following 28 days of immersion in the indicated environments.

Table 8. Parker elastomer compatibility rating for o-ring applications[a]

Solvent	NBR	Fluorocarbon	Neoprene	SBR	Polyurethane	Fluorosilicone	Silicone
Gasoline	1	1	4	4	2	1	4
Isooctane	1	1	2	4	2	1	4
Toluene	4	1	4	4	4	2	4
Ethanol	3	3	1	4	4	1	2
Acetic acid	2	2	4	2	4	2	1
Sulfuric acid	3	3	1	1	4	1	2

[a]*Parker O-Ring Handbook*, ORD 5700, Parker Hannifin Corporation, Cleveland, Ohio.

in Table 8 were not tested as mixtures, those results cannot be used to precisely assess compatibility of blends of these solvents. In order to accurately assess material compatibility, it is necessary to expose the material specimens to test fluids composed of the appropriate concentrations of the components listed in Table 8.

As discussed previously in the Introduction section of this report, the Parker rating system is solely based on volume swell and does not take into consideration other physical properties (shrinkage, hardness, etc.) affecting seal compatibility and performance. This study intended to measure as completely as possible the physical properties relevant to sealing. The changes in these properties that occur with exposure to the test fluids will augment the existing body of knowledge on the compatibility of ethanol with various infrastructure materials.

All of the elastomer specimens that were exposed to the test fuels exhibited some level of volume swell. Even the Fuel C test fuel produced significant swelling. This fact indicates that some level of solubility existed with the elastomers and the test fluids. In fact, as shown previously in Fig. 3, the total solubility parameter of E0 is not far removed from the range of solubility parameters for most of the elastomer

samples, which were obtained from various solubility studies.[35–40] Also shown in Fig. 3, the solubility matchup becomes more aligned as the ethanol concentration is increased, and for CE25a, the Total Hansen Solubility Parameter closely matches that of many of the elastomers, which indicates an increased potential for degradation via dissolution and extraction. The penetration or dissolution of the fuels into the elastomer enables the solvent to extract or remove the base polymer (in some cases) or remove any additive agents used as plasticizers, antioxidants, etc. Most elastomers (especially NBR and SBR) are compounded with additives to impart plasticity and durability, both of which are important sealing properties.

The results show that the elastomers largely group together by material class as shown Fig. 21 for volume swell and wet hardness. Interestingly, volume swell was observed in all samples for the Fuel C exposures, and with the exception of polyurethane and the NBR rubbers, ethanol had no measureable effect on the drop in hardness. The fluorocarbons and fluorosilicone exhibited the lowest volume swell and drop in hardness; the level of swelling was less than 20%, which is usually considered the upper limit for many dynamic sealing applications for o-ring materials. For static applications, swelling up to 50% is generally considered acceptable.[20]

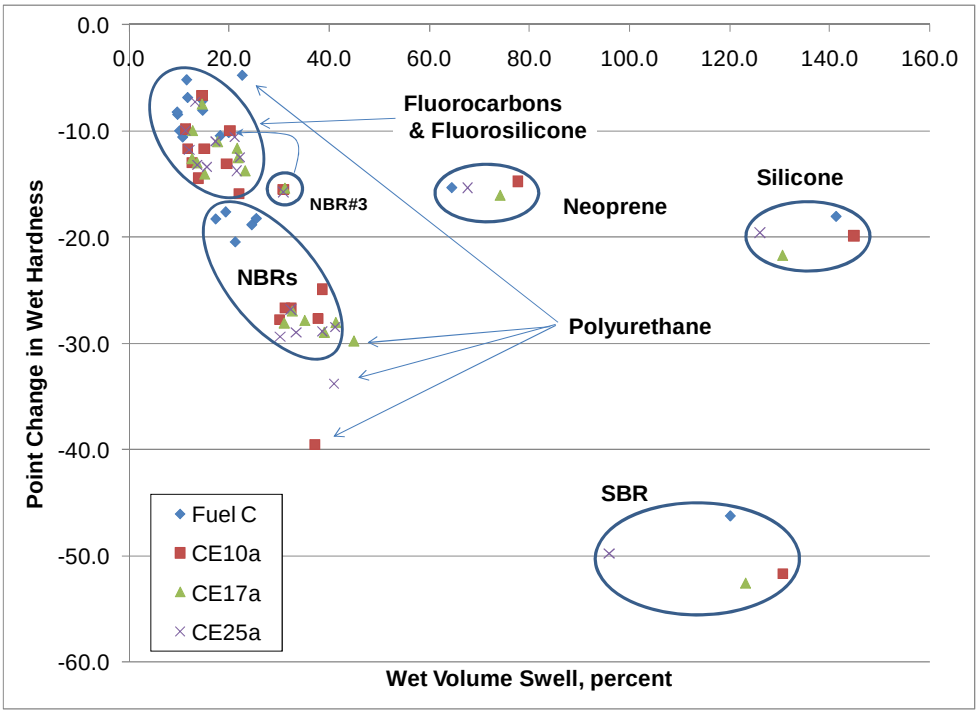

Fig. 21. Decrease in hardness as a function of volume swell and ethanol concentration for each elastomer type evaluated.

When exposed to Fuel C, the NBRs (except for NBR#3) and polyurethane swelled approximately 20% (the upper acceptable limit for many dynamic sealing applications). However, the addition of ethanol subsequently pushed the swell to 30% or higher. The hardness results for the fluorocarbons, fluorosilicone, NBRs, and polyethylene decreased with increased volume swell; the other elastomer types did not show a noticeable trend between wet hardness and swell. Especially noteworthy is the fact that the NBRs and polyurethane exhibited an additional 10 point drop in hardness with exposure to ethanol. This drop is significant and means that these samples will exhibit a greater tendency toward relaxation and reduced sealing pressure for ethanol-bearing fuels. It is important to note that the swell and hardness results for NBR#3 did not group with the other NBRs. In fact NBR#3 did not swell or soften to the same degree as the other NBRs. NBRs have a wide range of properties depending on the additives, copolymer

ratio, degree of crosslinking, and processing. Therefore, it is not prudent (at this point in time) to generalize about the performance of NBRs other than to state that the range of properties is high and is dependent on many factors.

Neoprene swelled between 60% and 80%, while SBR and silicone rubbers expanded by more than 120% (except for SBR exposed to CE25a). This excessive swelling will potentially result in extrusion of neoprene, SBR, and silicon seals through the adjoining surfaces, thereby resulting in a loss of material available for compression against the adjoining faces. For SBR the swelling is also accompanied by a roughly 50 point drop in hardness; the combination of high swell and drop in wet hardness means that SBR is the elastomer most susceptible to extrusion.

Since swelling is a measure of solubility between the test fuel (solvent) and the elastomer (solute), mass loss, and therefore shrinkage will occur (following dry-out) if the test fuels did, in fact, dissolve and leach out elastomer components (either the base polymer or additives). The end result would be a decrease in mass and volume (shrinkage). The results presented in Figs. 22 and 23 show the effects of volume swell on the mass loss and shrinkage after drying for each elastomer for each test fluid. As expected the groupings are similar for mass loss and dried volume when plotted against the wetted volume swell. (In fact Fig. 24 shows an almost linear correlation between mass loss and dried volume change.) Upon drying, each of the eight fluoroelastomers had a slight mass and volume gain compared to their original unexposed condition. This increase is the result of incomplete removal of the test fuel in these specimens after drying and is an indicator that negligible dissolution and leaching occurred for the fluoroelastomers. The fluorosilicone rubbers experience a slight loss of mass and volume, but not enough material leached out to be considered significant. Interestingly, silicone rubber lost around 2% of its original mass and 4% of its original volume, even though the volume swell for this material was the highest measured (more than 120%). The SBR, NBR, polyurethane, and neoprene rubbers exhibited large shrinkages and mass

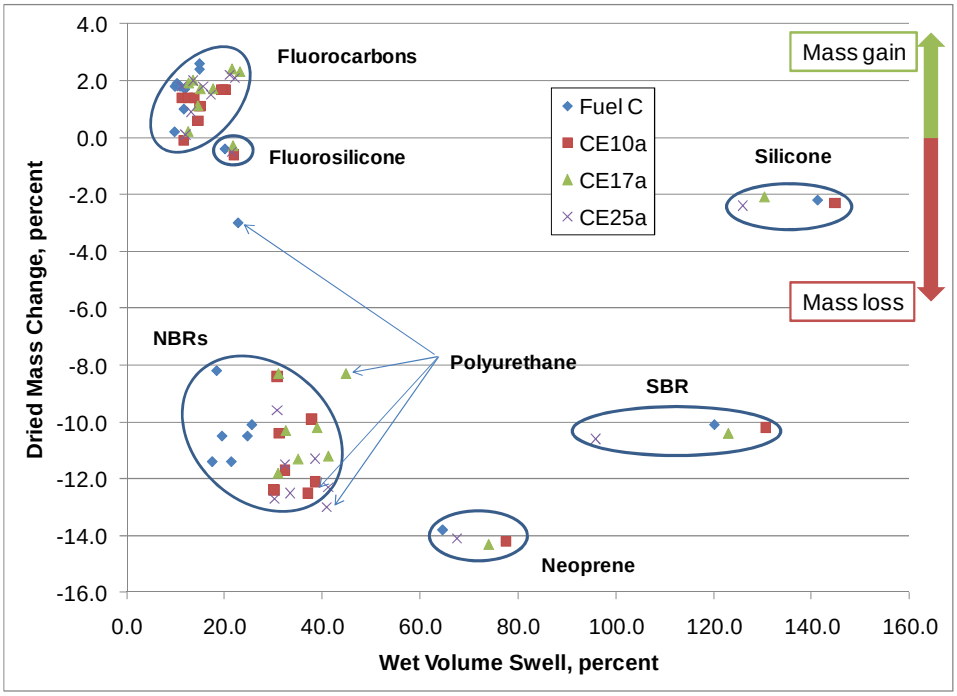

Fig. 22. Mass change of elastomers after drying compared to the initial baseline condition as function of volume swell and test fluid.

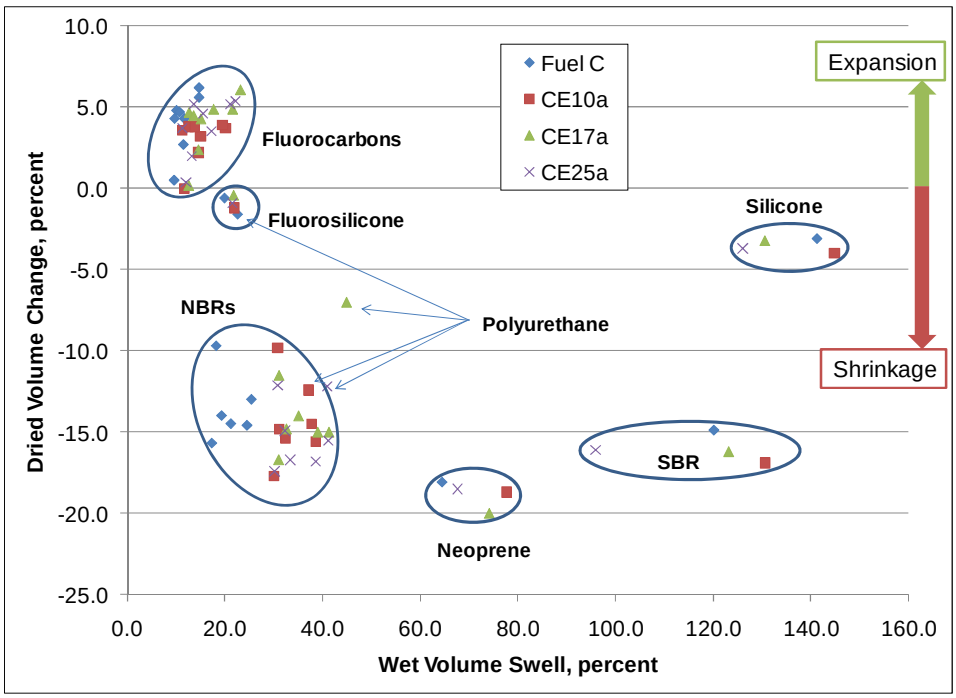

Fig. 23. Dry volume change of elastomers compared to the initial baseline condition as a function of volume swell and fuel type.

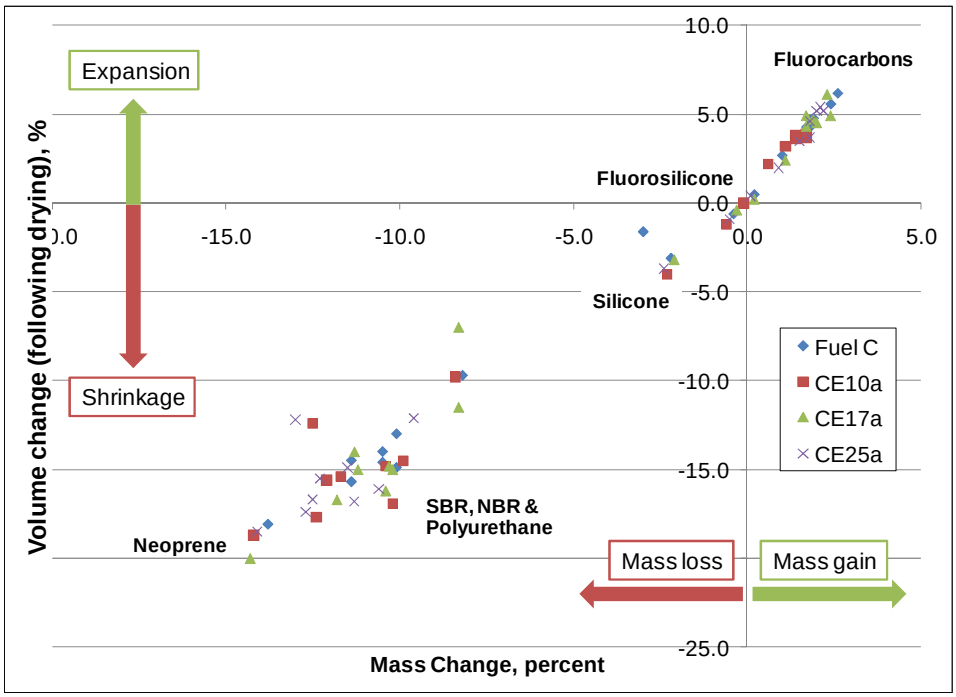

Fig.24. Correlation between dry volume change and dry mass change.

losses. The majority of the samples experienced greater than 10% shrinkage and greater than 7% mass loss. These values are considered high and would not be considered acceptable for most sealing applications. Note that neoprene experienced the highest levels of shrinkage (~17%) and mass loss (~15%).

The change in hardness after drying from the initial state is important because any increase in hardness over the baseline condition represents embrittlement of the material. Dissolution and removal of plasticizers would greatly affect hardness; however, loss of the base polymeric material should not have too much of an effect on the final hardness values since it is not dependent on volume or mass. In fact when point change in dry hardness is plotted against mass change (Fig. 25) and dry volume change (Fig. 26), significant embrittlement is only observed for the NBR samples and neoprene. Interestingly, the dry hardness of polyurethane (specimens exposed to aggressive ethanol) does not group with the NBR samples as it had with earlier property changes. In fact polyurethane (when exposed to aggressive ethanol) is the only elastomer exhibiting a decrease in hardness along with a decrease in mass, an indication that the molecular structure had degraded. Because softening only occurred for the specimens exposed to ethanol, it seems likely that one or more aggressive components were able to react with the polyurethane. In fact Table 8 shows that polyurethane is the least compatible of the rubbers with ethanol, acetic acid, and sulfuric acid. The fluoroelastomers (which includes the eight fluorocarbons and one fluorosilicone sample) also experienced a small decline in hardness, which is likely an artifact of the residual fuel present in the polymer, as demonstrated by the slight increase in dried mass. The final hardness values for the SBR, silicone, and fluorosilicone rubbers were not greatly changed. The embrittlement associated with NBR and neoprene is likely the result of the leaching out of the plasticizers, such as phthalates, resulting in mass loss and shrinkage. NBRs most always contain plasticizers to improve flexibility and durability. The results also indicated that Fuel C was responsible for the embrittlement of these polymers as ethanol did not noticeably add to the increase in hardness.

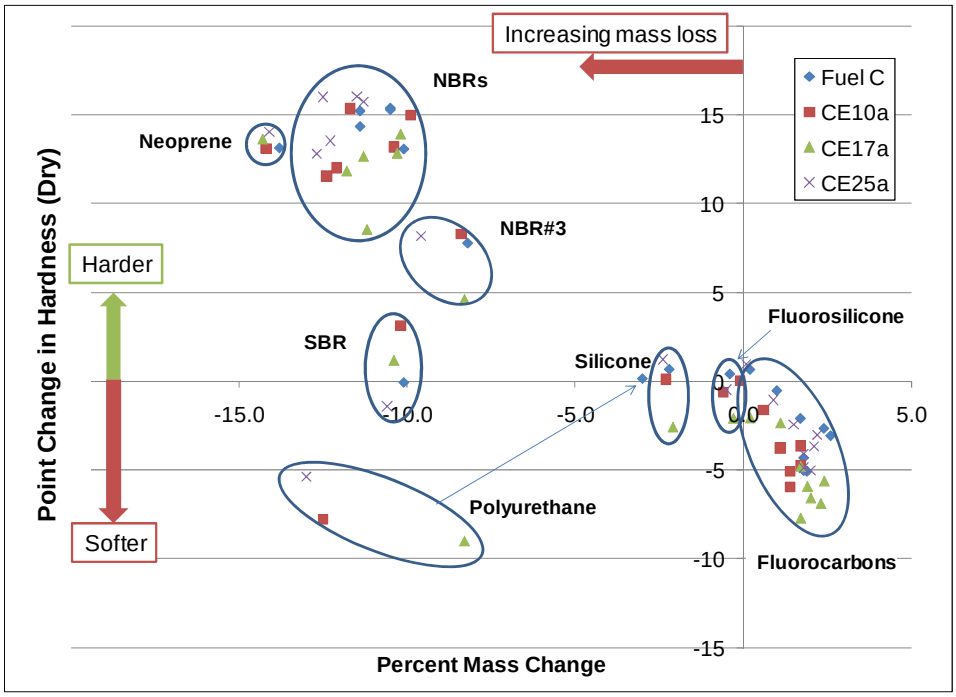

Fig. 25. Change in hardness (after drying at 60°C for 20 hr as a function of the change in dry mass).

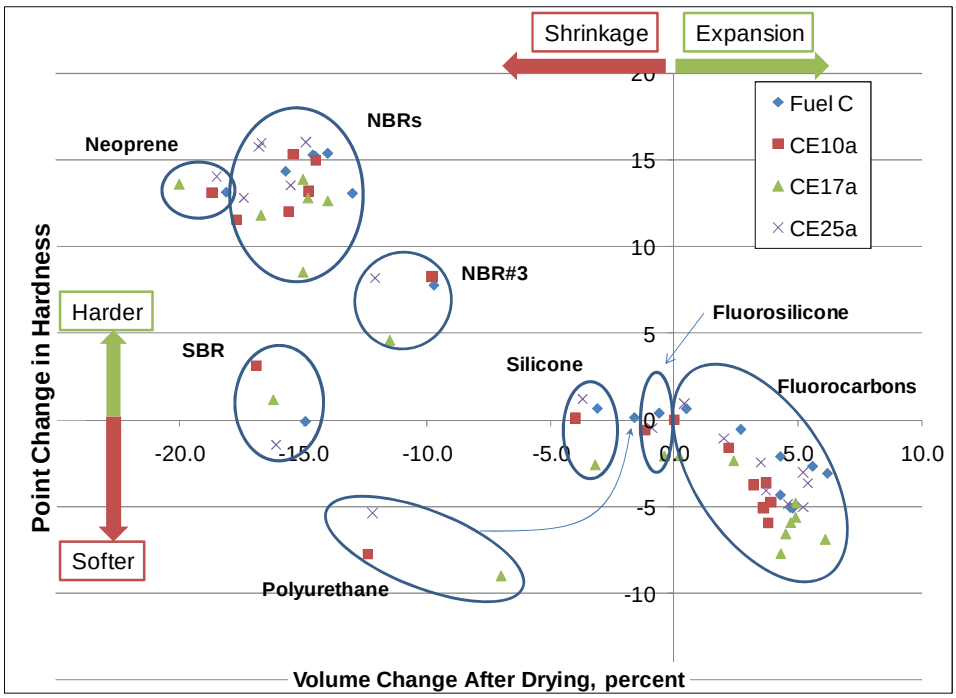

Fig. 26. Change in hardness (after drying at 60°C for 20 hr as a function of the change in dry volume).

The DMA results and curves for each specimen are shown in Appendix B and Appendix C, respectively. DMA results are important since they provide an assessment of the elastomer performance as a function of temperature. DMA measurement is highly sensitive to molecular changes of a polymer and is typically used to assess the degree of cure or crosslinking. Many dispenser elastomer materials undergo a significant change in properties from 0 to 50°C, which is typical of the temperature range of actual use.

Thermal transitions in polymers can be described in terms of free volume, which is defined as the space a molecule has for internal movement and has been shown to be related to penetration of solvent. However, the DMA instrument used in this study was limited to dry operation and solvent penetration effects necessitate wet testing.

The data yielded from the curves (see Appendix B) include the storage modulus (E′), loss modulus (E″), tan delta (ratio of E″/E′), and the temperatures associated with changes and peaks associated with the storage and loss moduli. A typical DMA result is a plot of log scale storage modulus with temperature as depicted in Fig. 14. At low temperatures (usually <0°C for elastomers), the storage modulus is high (1,000 to 10,000 MPa). At these temperatures, the elastomer is very stiff and behaves like a glass. In this glassy region, the free volume is low and the molecule is tightly compressed, which prevents additional molecular motion. At these temperatures, an elastomer may be unsuitable for use as a seal. As the temperature is increased, the expanding volume will reach a critical point, at which large segments of the molecule chains are able to move (via stretch, bending, and rotation), causing the storage modulus to drop to around 10–100 MPa. The temperature at which this begins to occur is the glass transition temperature (T_g). The T_g is normally the most significant transition of a polymer as the physical properties change drastically from a hard glassy to a rubbery state. The onset of the decrease in storage modulus is often referred to as the brittle point, which has been shown to correlate to brittleness, toughness, impact strength, fatigue, aging, strength, and rigidity. The storage modulus (at T_g), along with T_g, provides an ideal means for single temperature quality analysis that is sensitive to molecular polymerization. For rubbers, T_g also represents the lower operating temperature. Changes in T_g are used to monitor changes in

the polymer, including plasticizer removal caused by solvents. Any increase in T_g resulting in exposure to the test fluid would indicate removal of a plasticizer additive and would effectively reduce the operational temperature range of the elastomer. The rubber plateau can also be used to assess plasticizer effects and is important since many of the additives compounded with rubber are designed to function in this region.

The changes in onset storage modulus (onset E′) as a function of the dried mass change are shown in Fig. 27. The onset E′ values can be used to assess elastomer–solvent interactions; however, the results show a wide variation in values for each elastomer type. For most of the fluorocarbons, the storage moduli varied ±10%, and there was little correlation between ethanol content and mass loss. Similar results were obtained for fluorosilicone and silicone rubbers. On the other hand, onset E′ was increased for polyurethane, SBR, and neoprene. An increase in E′ will manifest as an increase in stiffness or hardness, which in turn correlates to embrittlement and loss of durability. For most of the NBR samples, the onset E′ measurements had increased; however, in some cases E′ actually decreased.

The increased dry mass of the fluorocarbon specimens suggests that small amounts of test fluid remained in the molecular channels. However, we would expect any residual fuel to decrease the onset E′ in all cases, which was not observed to be the case. As mentioned previously, several of the NBR specimens showed a decline in the onset E′. The hardness results are shown in Figs. 25 and 26, which indicate embrittlement of the NBR specimens after exposure to the test fluids. Since hardness and storage modulus are both measurements of elasticity, they should correlate with each other; however, the onset E′ did not correlate closely with the dry hardness results. Therefore, the onset E′ may not be a suitable measurement for assessing compatibility effects.

It is important to consider that the hardness values were taken at room temperature, where the material is transitioning to rubber, whereas the onset E′ was measured at much lower temperatures (in the glassy region). The free volume and molecular arrangement of the elastomers in rubber and glassy regions is not the same, and therefore, the correlation may not be valid. A more comparable approach is to measure the storage modulus at a temperature close to where the hardness was measured. When the E′ values were

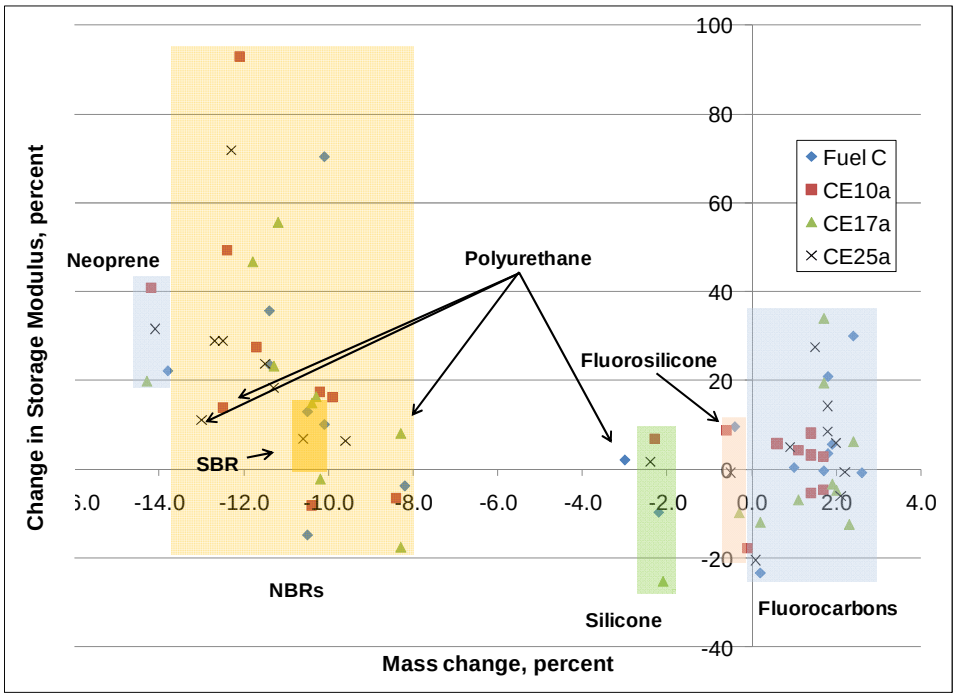

Fig.27. Change in onset storage modulus as a function of dry mass change.

measured at 25°C (E'_{25}), they were found to correlate to the hardness data, as shown in Fig. 28. The correlation between change in hardness and E'_{25} was approximated by the curve shown, although the results for NBR#3 did not follow this relationship. This result is consistent with other data that showed that NBR#3 did not group with the remaining NBRs. The results indicated that the margin of change in E'_{25} was much greater that the corresponding change in hardness, indicating that E'_{25} is more sensitive to solvent effects than dry hardness. The dependency of E'_{25} on the test fluid ethanol content for each elastomer sample is further shown in Fig. 29. The materials exhibiting the largest increase in E'_{25} were the NBRs and neoprene, while the fluorocarbons showed a decrease in E'_{25} for the fluid exposures. Fluorosilicone, SBR and silicone were unaffected. As with hardness, dry-out mass, and shrinkage results for polyurethane, E'_{25} was unaffected by Fuel C but was significantly reduced by the addition of ethanol. In contrast, ethanol had little, if any, effect on the E'_{25} for neoprene. Interestingly, except for SBR and neoprene, the lowest E'_{25} results were observed for the CE17a test fluids. This observation corresponds to the maximum level of swelling that occurred for these materials, which also occurred for the CE17a exposures. For the fluoroelastomers and NBRs, the E'_{25} results for CE25a were nearly the same as those for the Fuel C results.

Similar behavior was observed for the shift in the glass transition temperature as shown in Fig. 30. For the fluorocarbons, Fuel C was observed to reduce the glass transition temperature (between 5 to 10°C). The glass transition temperature was further reduced for the fluorocarbons with the addition of ethanol. The expanded dry volume for the fluorocarbons would be expected to raise the molecular free volume thereby initiating molecular relaxation at a lower temperature than the original condition. In contrast the test fluids increased T_g for the NBRs and SBR, and the Fuel C test fluid caused the highest level of shift for this elastomer type. The probable extraction of plasticizers is one explanation; however, the addition of ethanol actually lowered the T_g from the Fuel C result. If plasticizer extraction alone resulted in the increase in T_g, then it should increase further with the addition of ethanol, especially since the volume swell increased another 30% over the Fuel C exposures. This result suggests that some level of structural change is likely taking place in the NBR and SBR samples, and it appears as though the ethanol exposure may serve to increase the molecular free volume for NBRs and SBR.

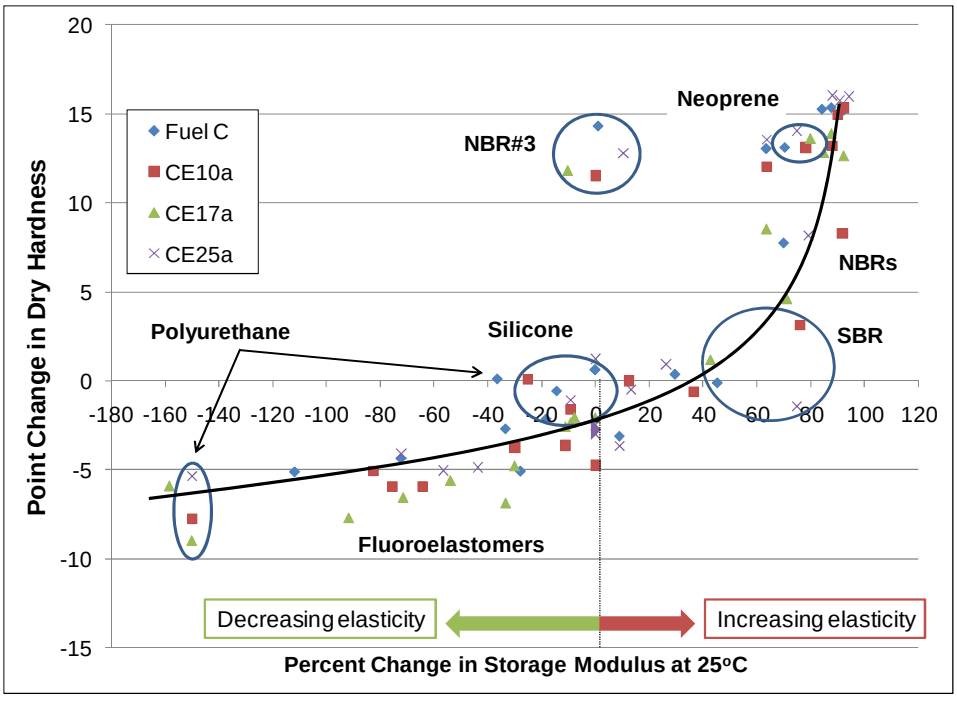

Fig. 28. Correlation of the change in hardness and the storage modulus when measured at 25°C.

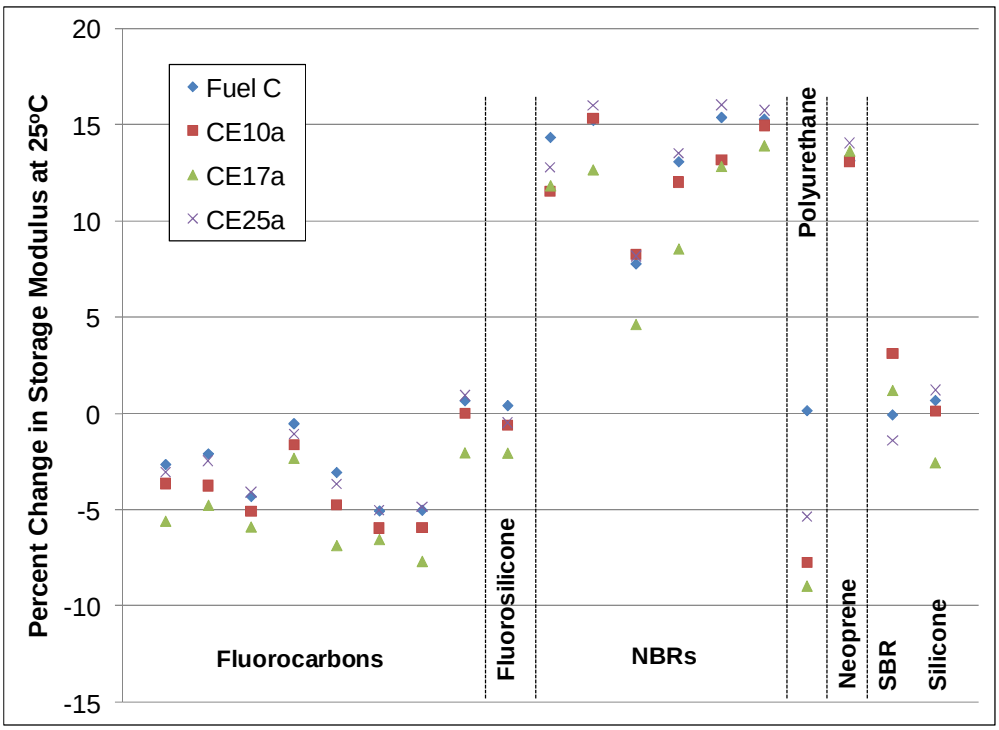

Fig. 29. Percent change in the storage modulus at 25°C for each elastomer sample.

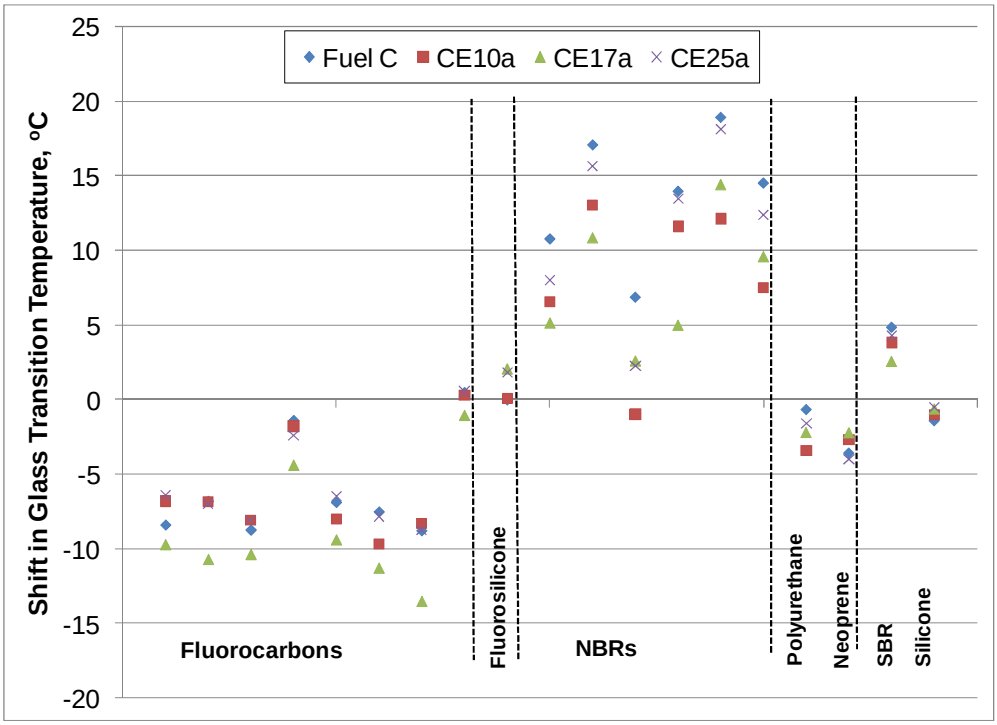

Fig. 30. Shift in the onset glass transition temperature T_g from the initial baseline condition.

4.4.2 Vapor Exposures

The vapor-exposed specimens were measured only for dry hardness and dry DMA properties. The headspace chemistry is expected to affect those properties relevant to sealing since the solvent vapors can also permeate into the elastomers and produce swell. The point change in hardness for the specimens in the vapor region was observed to correlate to the dry hardness changes of the fluid-exposed specimens, as shown in Fig. 31. The results show that the vapor-exposed specimens of NBRs and neoprene experienced significant embrittlement (hardness increase) but not as much as that for the liquid-exposed specimens. One interesting feature is that, in contrast to the liquid exposed-specimens, the vapor-exposed samples showed a significant increase in embrittlement with exposure to CE10a and CE17a. This result suggests that the chemistry of the vapor phase was significantly different from the liquid phase. In field installations, the vapor regions would be expected to have a higher concentration of both isooctane and ethanol relative to the toluene, and subsequently, a higher solubility with the exposed gases may be the case in many instances.

Interestingly the shift in T_g associated with the vapor-exposed specimens correlated well with the fluid-exposed specimens (Fig. 32). Likewise, the storage modulus at 25°C showed a roughly linear relationship between the vapor- and fluid or liquid-exposed specimens for each material and test fluid, in spite of the variability (scatter) of the data (Fig. 33). However, it is interesting to note that E'_{25} results for the fluid-exposed specimens were considerably lower than the results for the vapor-exposed specimens, and thus deviated from the general trend. This observation is important since it shows that NBRs can exhibit a wide range of properties, depending on their particular formulation. The results clearly show that the test fluid vapors impact the performance of the elastomers, albeit to a lower degree. Therefore, it is important to consider the compatibility of the elastomers to the vapors as well as the fluids.

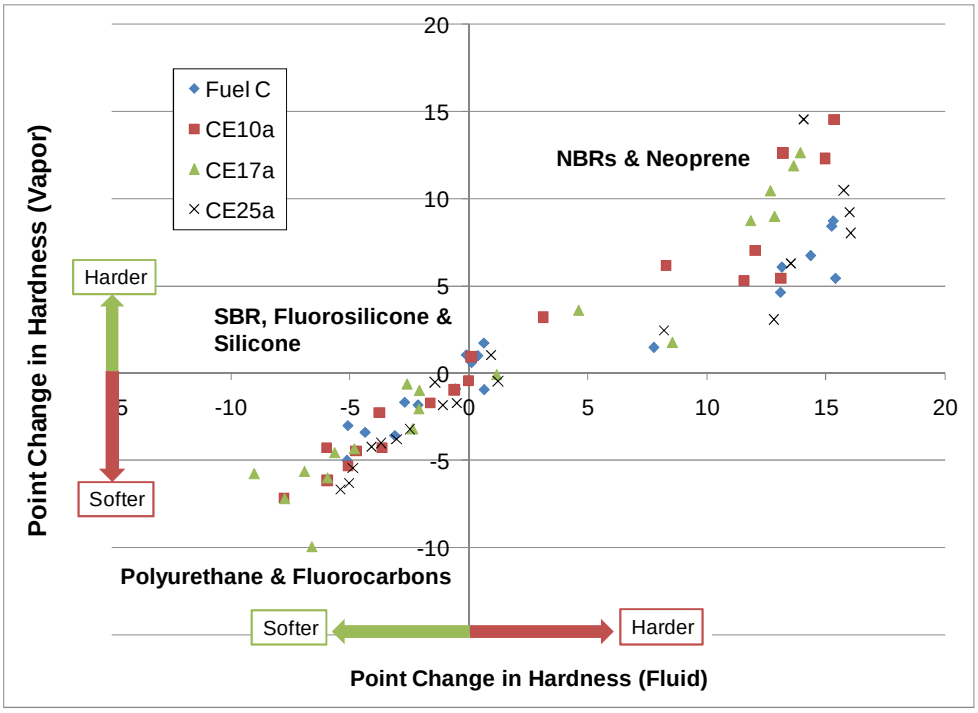

Fig. 31. Point change in hardness comparison between vapor- and fluid-exposed specimens.

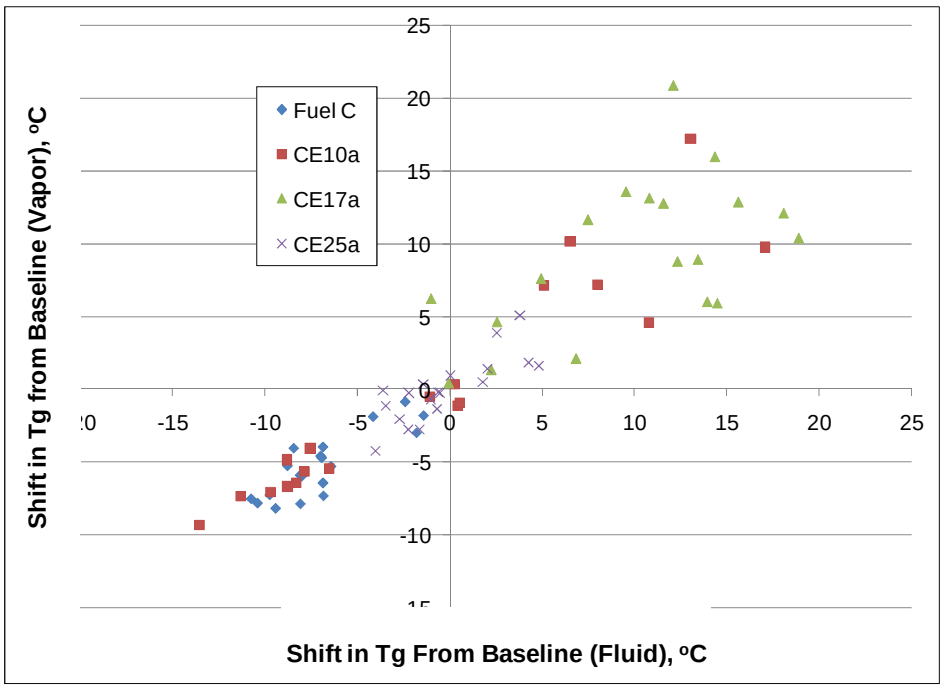

Fig. 32. Shift in T_g comparison between vapor- and fluid-exposed specimens.

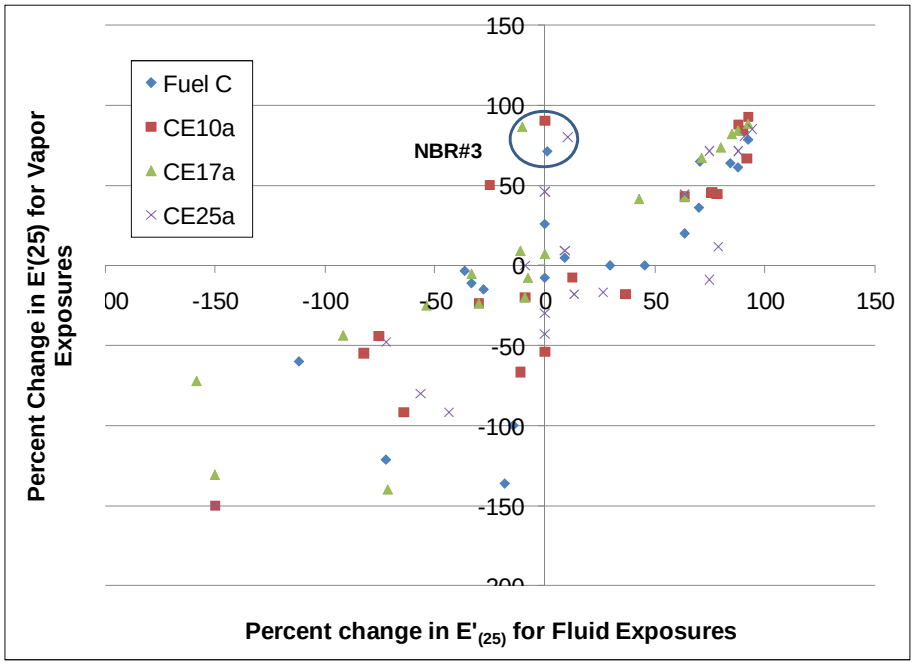

Fig. 33. Shift in storage modulus at 25°C comparison between vapor- and fluid-exposed specimens.

4.5 SEALANT COMPATIBILITY PERFORMANCE

The results in Fig. 34 show that the RectorSeal sealant passed for Fuel C. However, leaking was observed almost immediately at pressures less than 20 psi for the specimens exposed to CE10a and CE25a. These results indicate that the RectorSeal alone may not be compatible with ethanol-blended fuels. However, when Teflon tape is used with the RectorSeal product, leaking did not occur when exposed to CE10a and CE25a. The Gasoila E-Seal product also was observed to successfully pass the leak test by meeting the performance criteria for exposure to CE10a and CE25a.

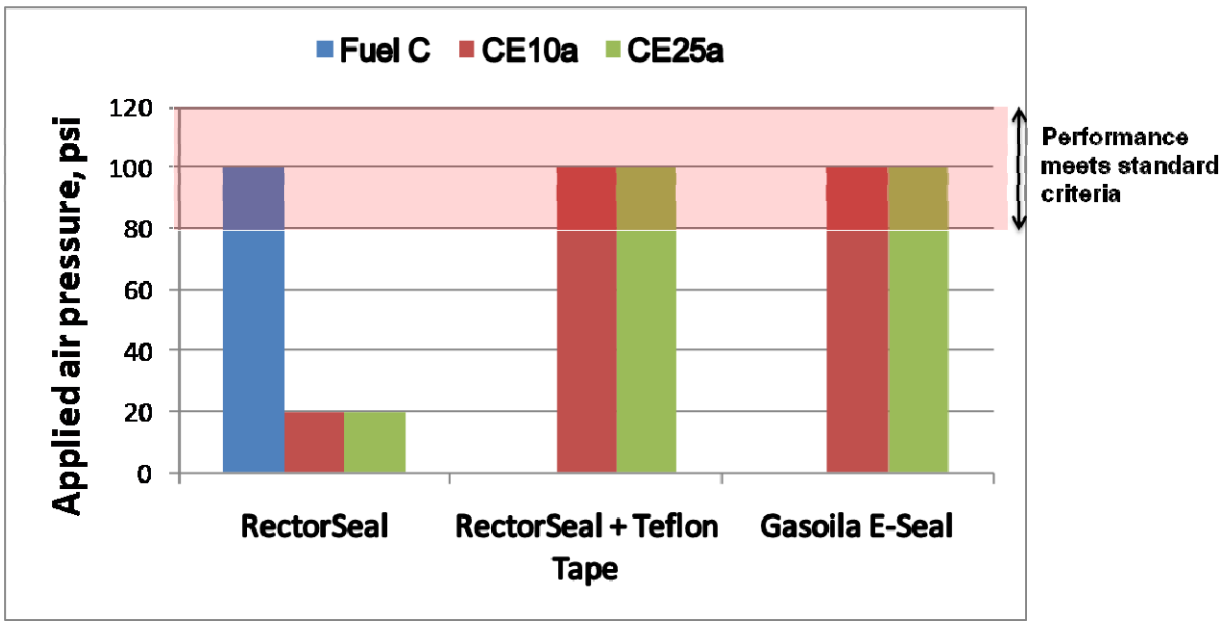

Fig.34. Sealant test results.

5. CONCLUSIONS

5.1 METALS AND ALLOYS

None of the metal or alloy specimens exhibited corrosion rates at noteworthy levels, including those galvanically coupled. This result is consistent with the low electrical conductivities measured for ethanol-gasoline containing less than 25% ethanol. It is important to keep in mind that this study was performed using test fluids that maintained water within the ethanol-fuel phase. Phase separation of the water (from the ethanol) did not occur. However, it is possible that phase separation may occur occasionally in actual use. Another noteworthy consideration is that the test coupons were unstressed, and there is some evidence that stress corrosion cracking may occur, in some instances.[41] However, for unstressed metallic components exposed to single-phase test fluids, corrosion is not likely to occur from exposure to the test fluid alone. However, this may not be the case when the ethanol concentration exceeds 25 vol %.

5.2 ELASTOMERS

O-ring and seal manufacturers use the compatibility rating system mentioned previously to guide material selection for use in a particular fluid. This rating system is based solely on swell and does not consider other properties relevant to seal performance. The seal manufacturers take great pains not to define failure criteria for a particular rubber for the following three reasons.

1. For each elastomer type, there is a wide range of properties, depending on the processing conditions, degree of crosslinking, copolymer levels, additive types, and concentration.
2. There are a wide variety of sealing applications. In fact there are almost as many different applications as there are seal types. O-ring usage is defined as either static or dynamic. The durability is highly dependent on the application, and there are a multitude of dynamic situations such as for pistons, valves, etc., requiring elastomer seals. Even for static face seals, pressure, temperature, lifetime, and even vibration are all factors that must be taken into consideration.
3. The complexity and variety of elastomer formulations and applications mean that any failure criteria would have to be qualified for each of the many formulations, processes, and applications, and are beyond the original scope of this study.

As a result, seal manufacturers will not warrantee their products based on any rating system. In fact the *Parker O-Ring Handbook*[22] clearly states that it is the responsibility of users to field test any seals and o-rings prior to marketing their product. However, because existing elastomer–fluid compatibility data is quite limited, any additional information would be crucial to identifying potential compatibility problems. Additional analysis and correlation of these results to the field are necessary to fully understand and predict the impact of intermediate blends of ethanol on materials.

In this study properties associated with wet and dried conditions were measured. Wetted properties included the volume swell and mass increase and hardness. These properties are important since volume swell (along with mass increase) is a measure of the mutual solubility of the elastomer and test fluid. All elastomers will typically exhibit some level of solubility with fluids. As the fluid or solvent is absorbed into the elastomer, there is a corresponding drop in hardness (softening). Wet hardness is important since it indicates how much softening of the elastomer is taking place during the exposure. Decreasing hardness, especially when combined with significant volume expansion, will also contribute to the ease of extrusion of a material.

Most elastomers exposed to fluids will, at some point, undergo dry-out cycles as well. When the elastomer becomes dry, it will lose mass (and volume) if the solvent dissolves and extracts out one or more components during drying. The loss of mass and volume will increase the potential for leaking since a portion of the original seal is removed, thereby decreasing seal pressure. An elastomer compounded with plasticizers will also be susceptible to embrittlement (or increased hardness) and an overall loss of durability if the solvent is able to extract out the plasticizer components. Embrittlement will lead to decreased durability and increase the potential for cracking during shrinkage and use. Other additive compounds serve to improve durability by providing additional protection against ultraviolet radiation, ozone, and wear. Dissolution and removal of these compounds may not affect the physical properties but will reduce the elastomer durability and useful life. The dried properties (mass/volume change and hardness) provide critical information regarding the ability of the fluid solvent to dissolve and leach out one or more elastomer components.

The physical properties measured for the elastomers (volume/mass change, wet and dry hardness, storage modulus, and T_g) were found to group together according to elastomer type. Even though several NBRs and fluorocarbon samples had different compositions and processing treatments, their physical properties generally fell within certain property groupings, especially for volume swell and hardness. The lone exception was NBR#3, which frequently did not group with the other NBRs.

DMA measurement was useful for assessing solvent effects, especially the storage modulus (at 25°C) and glass transition temperature. The storage modulus is a measure of elasticity and was found to correlate well with the dry hardness. The glass transition temperature is important since it defines the lower

operational temperature limit for an elastomer. Both E'_{25} and T_g showed particular sensitivity to the CE17a test fluid.

5.2.1 Fluorocarbons

Fluorocarbons yielded the lowest decrease in physical properties of the elastomers tested in this study. The addition of ethanol did not drastically affect the measured properties, and the eight fluoroelastomers exhibited only modest swell and softening (wet hardness decrease) upon exposure to the test fuels. The specimens swelled to around 20%, which is considered the upper limit for many sealing applications. Likewise the fluoroelastomers did not experience shrinkage and mass loss at the dried condition, nor did they become embrittled. Interestingly, the specimens exposed to the CE17a test fluid resulted in additional decreases in the glass transition temperature.

5.2.2 Fluorosilicone Rubber

The properties for the fluorosilicone rubber sample were found to be similar to the fluoroelastomer samples. Volume swell was relatively low (<30%). Fluorosilicone did experience a slight decrease in the dried mass and volume compared to the original condition, and the dry hardness was also increased slightly. However, the exceptionally low level of shrinkage and embrittlement that occurred is not considered significant and would indicate that fluorosilicone is acceptable as seal material for ethanol fuel blends. Interestingly, the T_g for fluorosilicone was relatively unaffected by fluid chemistry.

5.2.3 Silicone Rubber

The dried silicone sample lost only 2% of its mass and up to 4% of its original volume. In addition the hardness (after drying) was not altered significantly, indicating that embrittlement had not occurred. However, silicone did undergo the highest level of volume expansion (>120%) when exposed to the test fuels. This excessive swell, especially when combined with a corresponding 20 point drop in hardness, means that seal extrusion is an issue worth consideration, since any reduction of material between the joined interfaces will increase the probability of leaking. Another potential concern associated with the exceptionally high volume swell is the ease of permeation of the fuel through the elastomer. Fuel that can easily penetrate into the elastomer can also be easily released. All elastomers are susceptible to gas permeation, but the level of gas diffusion needs to be kept low. Additional permeability studies need to be performed on silicone prior to use in order to confirm its performance.

5.2.4 SBR

SBR experienced the highest combination of swell and softening. The volume expansion exceeded 90%, and hardness dropped 50 points when wet. The sample use in this study would not be considered compatible with many sealing applications of the test fluids. However, it is important to consider that SBR properties are highly dependent on additives, processing, and copolymer concentrations. This flexibility of design means that there may be appropriate formulations of SBR that will, in fact, meet a given sealing specification.

5.2.5 NBR

The eight NBR samples (and polyurethane) showed a pronounced increase in volume swell and softening when exposed to fuels containing ethanol. Exposures to Fuel C resulted in volume expansion approaching 20%. When exposed to the ethanol-blended test fluids, the NBRs swelled by more than 30%. Likewise, the hardness values dropped an additional 10 points when ethanol was added to the test fluid. When all of the samples (including Fuel C exposures) were dried, 8% to 14% of the mass was lost and the

accompanying shrinkage was between 10% and 18%. The dried hardness was increased 5 to 16 points, indicating that embrittlement had occurred. NBR was one of only two elastomer types (the other being neoprene) that exhibited significant embrittlement in the dried state, indicating that plasticizer components were being removed by the test fuels. The results showed a high degree of variance, which is not surprising since NBR (like SBR) can be designed for a wide variety of applications. NBRs showed a significant increase in Tg with Fuel C exposure, but the addition of ethanol was observed to reduce this shift rather than extend it. Interestingly, the low volume expansion and reduced softening for the samples exposed to Fuel C suggest that these materials may in fact be acceptable for use in some E0 gasoline applications.

5.2.6 Polyurethane

The polyurethane results essentially matched those of the NBRs, with one notable exception: Polyurethane became softer (not harder) when dried from the wetted state, but only for those samples exposed to ethanol; the hardness of the Fuel C exposures was unaffected. This result suggests that the polyurethane sample did not contain plasticizer additives. In fact, according to the *Handbook of Elastomers*,[42] polyurethane does not normally contain large levels of extractable components. However, the reduction in hardness (after drying) upon exposure to ethanol is noteworthy and suggests that the aggressive ethanol may have reacted with the polyurethane, causing permanent weakening. The poor wetted properties combined with the high shrinkage and mass loss indicate that polyurethane may not be an acceptable elastomer in many sealing applications for use with fuels containing up to 25% ethanol. The permanent weakening caused by exposure to ethanol is a potential concern.

5.2.7 Neoprene

The neoprene sample's decrease in wet hardness was relatively low and was comparable to the results obtained for the fluorocarbons; however, the volume swell exceeded 60%, which may limit its use. Particularly disconcerting was the fact that neoprene exhibited the poorest dried properties of the elastomers tested in the study. Upon drying the mass and volume were reduced 15% and 20%, respectively. Neoprene also exhibited a high level of embrittlement, as the hardness was increased by 14 points. The high mass loss and shrinkage, and the accompanying increase in hardness, suggest that neoprene (along with NBR) contained significant levels of plasticizers prior to the exposure runs. These plasticizer additives were removed by the test fuels, leaving the neoprene sample in a less durable condition.

5.3 Vapor-Exposed Specimens

The hardness and T_g results of the vapor-exposed specimens correlated with the results obtained for the wetted specimens of the elastomers tested. Embrittlement was observed for the NBRs and neoprene by vapors alone, which suggests that these materials need to be proven before being employed in vapor-recovery applications. The chemistry of the head space region will have higher concentrations of ethanol and isooctane relative to the toluene due to the volatility of these fuel components. It is reasonable to assume that this scenario will also occur out in the field. The exact concentrations of the fuel components were not measured, but we would expect that the solubility would change.

5.4 Sealants

The results show that although the standard PTFE sealant (RectorSeal) passed the ASTM D6396 criteria in Fuel C, the sealant experienced leaking at low pressures when exposed to either CE10a or CE25a. However, when RectorSeal was combined with Teflon tape, leaking did not occur. The results also show that the Gasoila E-Seal product maintained integrity in both Fuel C and CE25a up to 100 psi. The results

show that the standard PTFE sealants are not compatible without additional sealing brought about by the addition of Teflon tape. The Gasoila E-Seal product was successful at preventing leakage in CE25a according to the ASTM standard.

6. REFERENCES

1. Society of Automotive Engineers, "Gasoline, Alcohol, and Diesel Fuel Surrogates for Materials Testing," SAE J1681, issued September 1993, revised January 2000-01.
2. American Society for Testing and Materials, "Test Method for Testing of Pipe Thread Sealants on Pipe Tees," ASTM D 6396 Standard.
3. *DOE/EIA Annual Energy Review 2008*, DOE/EIA-0384(2008), June 2009, www.eia.doe.gov/aer.
4. Energy Information Administration, *EIA Energy Outlook 2009*, DOE/EIA-0484(2009), May 2009, www.eia.doe.gov.
5. U.S. Energy Information Administration, *EIA Petroleum Supply Monthly*, February 2009.
6. U.S. Energy Information Administration, *EIA Annual Energy Outlook 2010*, December 2009.
7. EPA-HQ-OAR-0211 and FLR-9215-5, October 13, 2010.
8. Brent. D. Yacobucci, *Intermediate-Level Blends of Ethanol in Gasoline, and the Ethanol "Blend Wall"*, Congressional Research Service. October, 18, 2010.
9. K. Boyce and J. T. Chapin, *Dispensing Equipment Testing with Mid-level Ethanol/Gasoline Test Fluid: Summary Report*, November 2010.
10. D. W. Kirk, *Fuel* **62**, 1512–1513 (December 1983).
11. C. M. Hansen, *Hansen Solubility Parameters: A User's Handbook*, 2nd Edition, CRC Press, Taylor & Francis Group, Boca Raton, Florida, 2007.
12. B. H. West et al., Effects *of Intermediate Ethanol Blends on Legacy Vehicles and Small Non-road Engines*, *Report 1*, ORNL/TM-2008/117, October 2008.
13. B. Jones, G.Mead, P. Steevens, and C. Connors, *The Effects of E20 on Elastomers Used in Automotive Fuel System Components*, Minnesota Center for Automotive Research, Minnesota State University, Mankato, February 22, 2008.
14. G. Davis and C. Hoff, "The Effect of Using Ethanol-blended Gasoline on the Performance and Durability of Fuel Delivery Systems in Classic Automobiles," SAE Paper No. 2010-01-2135.
15. H. Jafari et al., Effect of Ethanol as Gasoline Additive on Vehicle Fuel Delivery System Corrosion, *Materials and Corrosion* **61**(5), 432–440 (May 2010).
16. R. F. Karg, C. L. Hill, K. Dosch, and B. Johnson, "Ultra-high CAN Polymer In Fuel System Application," SAE 900196.
17. L. Nihalani, R. D. A. Paulmer, and Y. P. Rao, "Compatibility of Elastomeric Materials with Gasohol," SAE Paper No. 2004-28-0062.
18. D. DiCicco, CRC AVFL-15 Project: E20 Durability Study Fuel System Components, presented to the Mid-level Ethanol Blends Research Coordination Group, May 5, 2010.
19. *Rubber Technology*, 3rd Edition, Maurice Morton, Kluwer Academic Publishers, Norwell, MA, 1999.
20. *Parker O-Ring Handbook*, ORD 5700, Parker Hannifin Corporation, Cleveland, Ohio, 2007.
21. P. A. Westbrook, *Compatibility and Permeability of Oxygenated Fuels to Materials in Underground Storage and Dispensing Equipment, Oxygenate Compatibility and Permeability Report: A Technical Assessment of the Literature circa 1975–1997*, State Water Resources Control Board Advisory Panel, January 1999.
22. *Dichtomatik O-Ring Handbook*, D. Visscher, Editor, Dichtomatik North America, 47690 East Anchor Court, Plymouth, Michigan.
23. O-rings, Inc., http://www.oringsusa.com/html/compatibility.html
24. Precision Polymer Engineering, http://www.prepol.com/

25. P. Touchet, B. Zanadis, M. Fischer, and P. E. Gatza, *Materials Compatibility Studies with Fuel/Alcohol Mixtures*, Technical Report 2366, U. S. Army Mobility Equipment Research and Development Command, Fort Belvoir, Virginia, July 1982.
26. A. Nersasian, "The Use of Toluene/Isooctane/Alcohol Blends to Simulate the Swelling Behavior of Rubbers in Gasoline/Alcohol Fuels," SAE Paper No. 800790.
27. I. A. Abu-Isa, "Effects of Mixtures of Gasoline with Methanol and with Ethanol on Automotive Elastomers," SAE Paper No. 800786.
28. G. Micallef and A. Weimann, "Elastomer Selection for Bio-fuel Requires a Systems Approach," *Sealing Technology*, January 2009.
29. R. D. Stephens, "Fuel and Permeation Resistance of Fluoroelastomers to Ethanol Blends," ACS Technical Meeting of the Rubber Division, Cincinnati, Ohio, October 2006.
30. A. Ertekin and N. Sridhar, "Performance of Elastomeric Materials in Gasoline-Ethanol Blends—A Review," Paper no. 09533, CORROSION 2009 Annual Conference and Exhibition, NACE International, Atlanta, Georgia.
31. S. J. Pawel, M. D. Kass, and C. J. Janke, *Preliminary Compatibility Assessment of Metallic Dispenser Materials for Service in Ethanol Fuel Blends*, ORNL/TM-2009/286.
32. American Society for Testing and Materials, "Test Method for Rubber Property-Durometer Hardness," ASTM D 2240 Standard, 2005.
33. K. P. Menard, *Dynamic Mechanical Analysis: A Practical Introduction*, 2nd Edition, CRC Press, Taylor & Francis Group, Boca Raton, Florida.
34. NREL data sheet provided by Kristi Moriarty on January 13, 2011.
35. A. Huba, L. Molnar, A. Czmerk, and T. Fischl, "Dynamic Analysis of Silicone Elastomers," Budapest University of Technology and Economics.
36. M. Kotal, S. K. Srivastava, and A. K. Bhowmick, "Thermoplastic Polyurethane and Nitrile Butadiene Rubber Blends with Layered Double Hydroxide Nanocomposites by Solution Blending," *Polym Int* **59**, 2–10 (2010).
37. M. Myntti, "Comparing Fuel and Oil Resistance Properties," *Rubber World*, June 1, 2003.
38. N. M. Sammes, S. Vohora, and A. M. Carter, "Swelling Parameter of Polypropylene Used in Household Appliances," *Journal of Materials Science* **29**, 6255–6258 (1994).
39. R. Guo, A. G. Talma, R. N. Datta, W. K. Dierkes, and J. W. M. Noordermeer, "Solubility Study of Curatives in Various Rubbers," *European Polymer Journal* **44**, 3890–3893(2008).
40. R. Mieczkowski, "Solubility Parameter Components of Some Polyurethanes," *European Polymer Journal* **28**(1), 53–55 (January 1992).
41. E. Voegele, "It's not just a pipe dream," *Ethanol Producer Magazine*, January 12, 2009, www.ethanolproducer.com/articles/5270/its-not-just-a-pipe-dream
42. *Handbook of Elastomers*, 2nd Edition, A. K. Bhowmick and H. L. Stephens, editors, Marcel Dekker, Inc., New York, NY, 2001.

APPENDIX A
ORNL/UL POSTMORTEM ANALYSIS OF FACEPLATE RUBBER-CORK GASKETS USED IN NREL/UL DISPENSERS 1, 3, AND 5

APPENDIX A

ORNL/UL POSTMORTEM ANALYSIS OF FACEPLATE RUBBER-CORK GASKETS USED IN NREL/UL DISPENSERS 1, 3, AND 5

ORNL Investigators: Mike Kass, Tim Theiss, Sam Lewis, Chris Janke, Maggie Connatser, and Michelle Kidder

UL Lead Investigator: Tom Chapin

A postmortem study was performed on the rubber-cork faceplate gaskets for Dispensers 1, 3, and 5 from the UL/NREL study. The rationale for selecting gaskets from Dispensers 1 and 5 was that these dispensers were the only ones in which the fuel chemistry was measured periodically throughout the NREL/UL prototype tests. Both of these dispensers exhibited leaking at the faceplate gasket. Comparison of the fuel chemistry results to the postmortem analysis may provide information useful to the interpretation of failure mechanisms. It is important to note that Dispensers 1 and 5 were made by the same manufacturer; Dispenser 1 was a new dispenser, while Dispenser 5 was similar in design to Dispenser 1 and had been used for 5 years. Interestingly, all of the meter seals were cork impregnated with an elastomer. We employed several analytical techniques to characterize and identify the rubber fraction of each gasket. These methods included diffuse reflectance infrared transform (DRIFT) spectroscopic analysis, thermogravimetric analysis (TGA), dynamic mechanical analysis (DMA), and pyrolysis gas chromatography–mass spectrometry (GC-MS).

The design of Dispensers 1 and 5 consisted of four faceplates mounted in a vertical arrangement using four bolts on each faceplate. In contrast, the housing seal for Dispenser 3 was held horizontally in place using six bolts and bore the weight of the top housing section, which was estimated to weigh around 5 kg (~10 lb). Accordingly, the faceplate gaskets for Dispensers1 and 5 had identical designs, but the gasket for Dispenser 3 had an entirely different layout. The gasket material for all three dispensers was rubberized cork.

The appearance of the gaskets is noteworthy. The thicknesses of the gaskets were measured at the compressed region and at the interior edges, which were uncompressed and exposed to the test fuel. The thickness measurements are listed in Table A-1 and show that the Dispenser 3 gasket was much thinner than those of Dispensers 1 and 5. However, without knowing the starting thicknesses, it is impossible to ascertain the degree of compressibility or swelling.

Table A-1. Thickness of the rubber-cork gaskets used as meter seals

Dispenser gasket	Thickness of surface area exposed to fluid (mm)	Thickness of compressed surface area (mm)
Dispenser 1 (new)	1.6	1.14
Dispenser 5 (used)	1.66	1.34
Dispenser 3 (used)	1.42	1.4

Selected gasket sections are shown in Figs. A-1, A-2, and A-3. Visual observation of the three gaskets revealed several interesting features. The most noticeable was the black coloration of the Dispenser 3 gasket elastomer compared to the gray coloration of the elastomer used in Dispensers 1 and 5. The black coloration is indicative of the carbon black, which is commonly added as a pigment and to improve

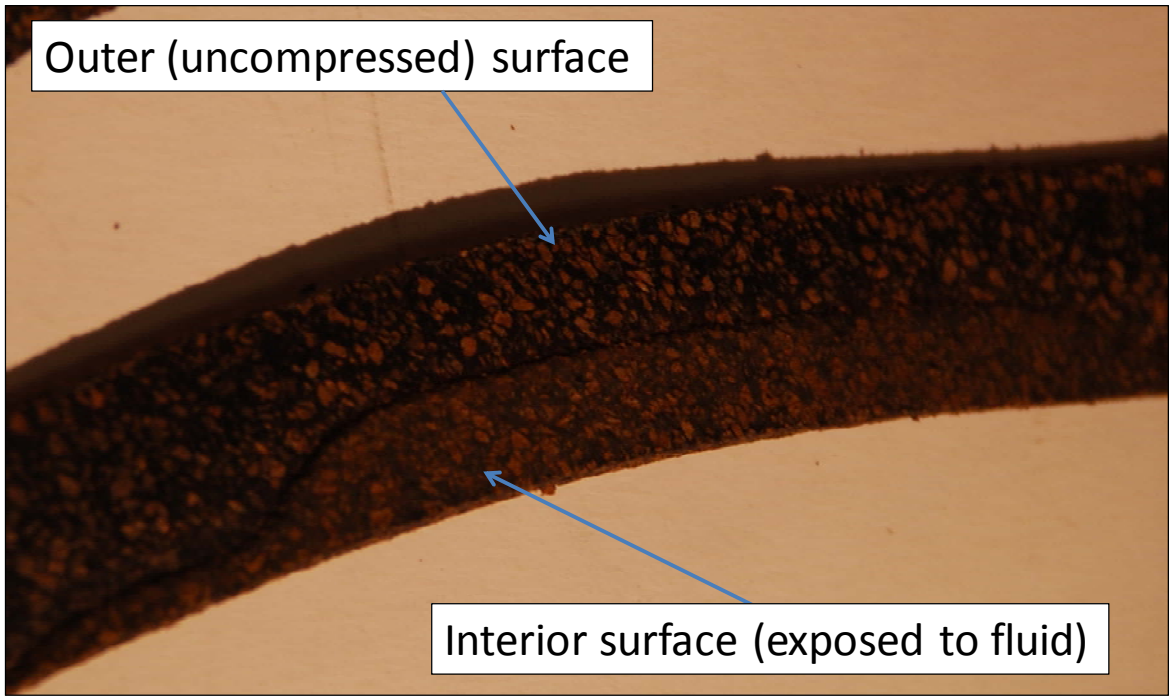

Fig. A-1. Housing gasket for Dispenser 3 (used), which passed the UL 87a tests. Dark regions are the elastomer, and the brown regions are the cork.

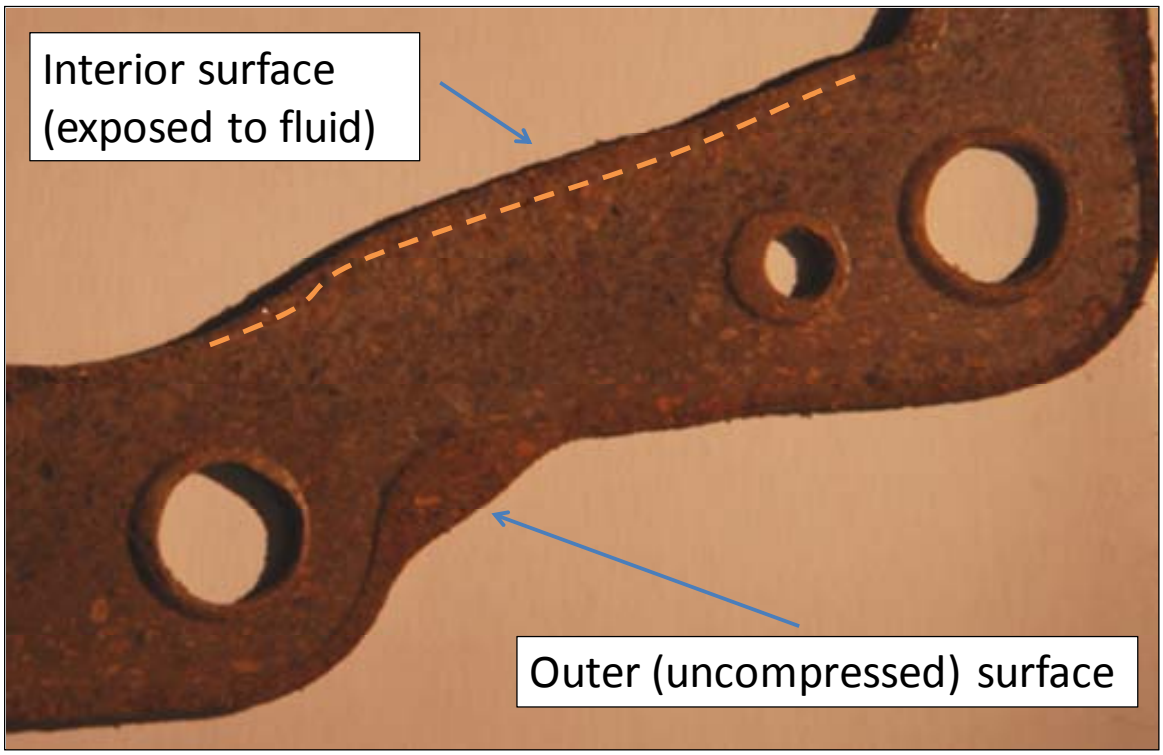

Fig. A-2. Faceplate gasket for Dispenser 1 (new), which failed the UL 87a tests.

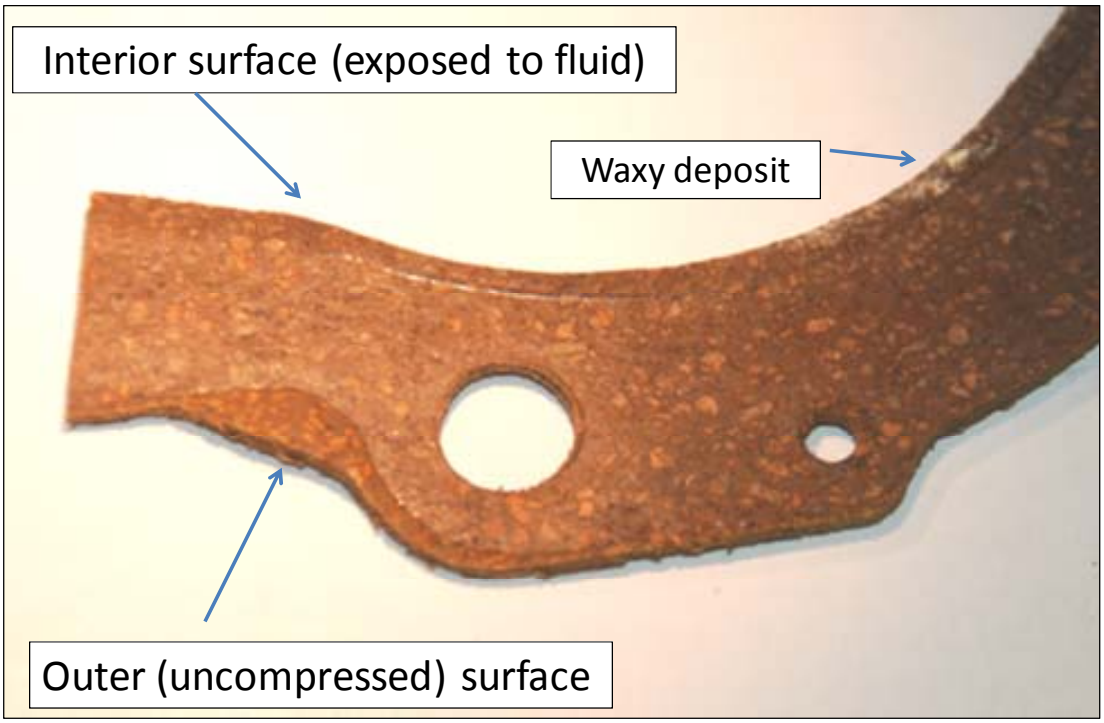

Fig. A-3. Faceplate gasket for Dispenser 5 (used), which failed the UL 87a tests.

elastomer wear and durability. The elastomer bonded to the cork (for Dispensers 1 and 5) either had very low levels or no carbon black additive. Further examination of the Dispenser 3 gasket surface showed very little degradation for the region exposed to the test fluid (Fig. A-1), and the elastomer component of the gasket was intact. In contrast, the region of Dispenser 1 (Fig. A-2) that was exposed to the test fuel was considered very weak, judging by the readiness at which the cork particles could be removed by gentle tugging; in contrast, the compressed section (which was not directly exposed to the test fuel) required much more force to tear. Visual observation indicated that very little elastomer remained in this section. Likewise Dispenser 5 (Fig. A-3) showed some degradation on the exposed gasket surface but not to the degree observed for Dispenser 1. It is important to note that although the gaskets used in Dispensers 1 and 5 appear identical, Dispenser 1 was a new unit, while Dispenser 5 had 5 years of operational use. The absence of the elastomer component of the new dispenser (No. 1) in the fluid contact region is a strong indicator that the polymer was effectively dissolved by the test fuel and most likely caused the observed leakage during the testing procedure.

Sections of each gasket were removed and evaluated for thermogravimetric analysis (TGA). During TGA, a pre-weighed section of the gasket was heated in air and the mass loss as a function of temperature was recorded. The results for the three gaskets are presented in Fig. A-4. Dispensers 1 and 5 gaskets exhibited nearly identical behavior, showing a large drop in mass around 300^{o}C, which is consistent with combustion of the polymer. The hydrocarbon removal for these gaskets was completed at 500^{o}C, and the final mass of the inorganic (noncombustible) portion was almost 35% of the original mass. In contrast, the Dispenser 3 gasket did not finish burning until 600^{o}C, and the final weight was closer to 22%. The results indicate a very high level of inorganic compounds within the gasket rubber portions of Dispensers 1 and 5 that was not present in the rubber fraction of Dispenser 3. Since pure cork typically combusts to a final mass percentage ranging from 5 to 15%, the remainder (which was at least 25%) must have originated in the rubber fraction itself.

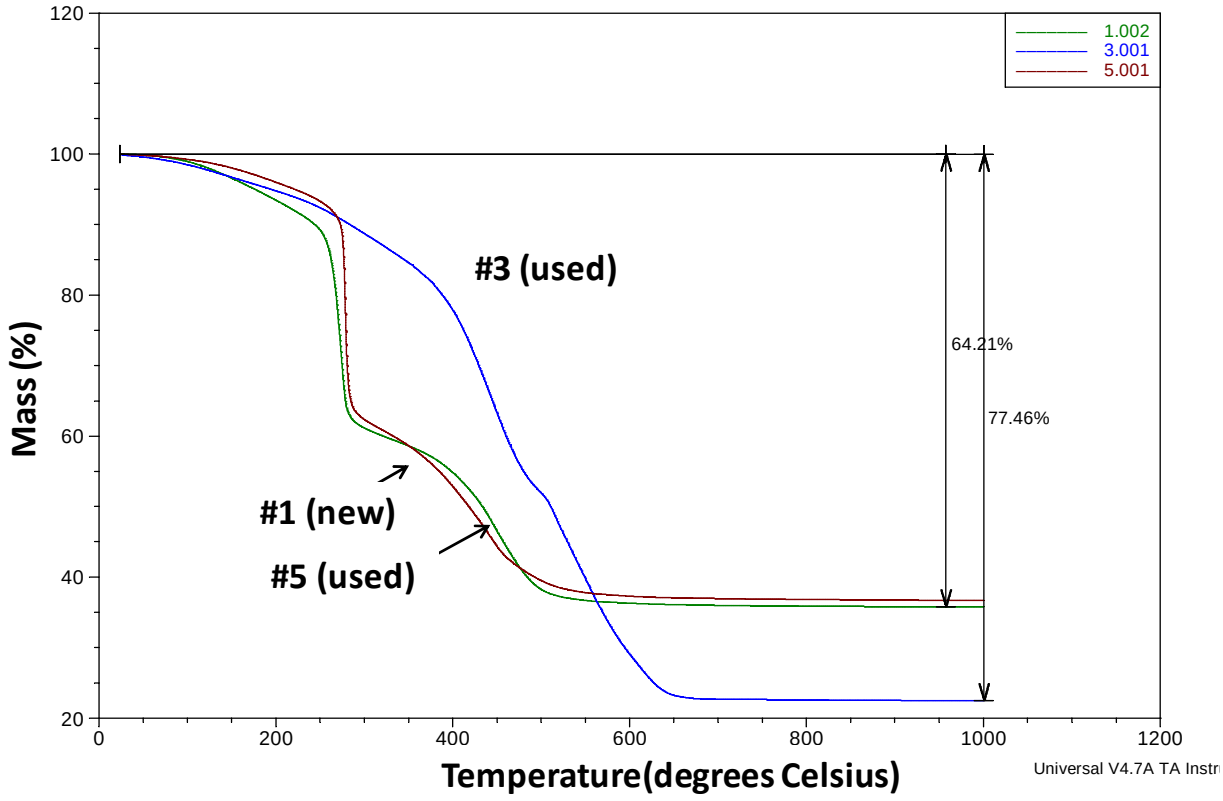

Fig. A-4. TGA (in air) curves for rubber-cork gaskets used in Dispensers 1, 3, and 5.

The inorganic residue from all three gaskets was analyzed for x-ray florescence, and the results showed that the inorganic fraction was predominantly silica. Silica is commonly added to elastomers to impart ultraviolet and heat resistance.

The TGA results show that the rubber-cork gaskets used in Dispensers 1 and 5 were identical and that the gasket used in Dispenser 3 was significantly different. This difference was believed to be primarily limited to the elastomeric portion of the rubberized cork gaskets.

DRIFT and DMA Analysis

Each of the gaskets was sectioned and analyzed using diffuse reflectance infrared Fourier transform (DRIFT) spectroscopy and dynamic mechanical analysis (DMA). The DRIFT technique is useful for identifying functional hydrocarbon groups but cannot be used to identify specific plastic materials. DMA provides a modulus versus temperature curve, and that information provides a better means of identifying a particular polymer compound. The DRIFT analysis showed measurable amounts of isolated hydroxyls (-OH) in the gaskets for the two failed dispensers (1 and 5), while the gasket from Dispenser 3 did not. The presence of the isolated hydroxyls is a strong indicator that the elastomer compound in the cork seal had degraded.

Pyrolysis GC-MS

The rubber fractions of the cork gaskets were evaluated by UL using pyrolysis GC-MS to determine the type of rubber used in the cork. Analysis of gaskets from Dispensers 1 and 5 showed that the rubber

consisted of epichlorohydrin. Epichlorohydrin is an organochlorine compound that is considered soluble with most polar organic solvents. It has excellent resistance with nonpolar hydrocarbons such as gasoline, toluene, and isooctane but would be expected to have solubility with ethanol. Epichlorohydrin rubber (ECO) does not perform well in oxygenated gasoline and will revert towards the uncured product to become soft and devulcanized. This softening is indicative of a reaction of the epichlorohydrin with the test fluid. Because ECO is compatible with gasoline and hydrocarbon fuels, the softening (degradation) is most likely caused by the ethanol component of the test fluid. This assessment is supported by the DRIFT analysis, which showed that the rubber had oxidized.

In contrast, the rubber fraction for the cork gasket used in Dispenser 3 (which did not leak) was found to be NBR. NBR is considered to be more compatible than ECO with ethanol and thus did not leak due to exposure. Based on these results, the incompatibility of ECO with ethanol is likely responsible for the leaking noted at the meter faceplates for Dispensers 1 and 5. The compatibility of the cork fraction was not assessed. The cork fraction was observed to swell upon exposure to the test fluid, but did not appear to physically degrade. Cork, by itself, is too weak to be used without a rubber matrix to impart the necessary strength and elasticity to form an effective seal. The results suggest that the rubber component is the critical component that determines whether the seal is effective or not.

APPENDIX B
ORNL DISPENSER STUDY USING RECIRCULATING CE25A AND CE85A TEST FLUIDS

APPENDIX B

ORNL DISPENSER STUDY USING RECIRCULATING CE25A AND CE85A TEST FLUIDS

ORNL Investigators: Mike Kass, Tim Theiss, Sam Lewis

UL Investigators: Team: Ken Boyce, Tom Chapin, Tom Fabian, Joe Bablo

BACKGROUND

Underwriters Laboratories (UL) was interested in examining the corrosive potential of fuel dispenser components to ethanol-gasoline blends containing 25 and 85 vol % ethanol. UL had an ongoing program to evaluate corrosion in selected dispensers by exposing the components (filter, meter, valve, hose, nozzle, connectors, and tubing) to either CE25a or CE85a fuel compositions under static (noncirculating) conditions. However, it was felt that the data provided from the static experiments may not be applicable to a more realistic environment, whereby materials and components are exposed to moving fluid, rather than static exposure. In recognition of this need, the U.S. Department of Energy supported the National Renewable Energy Laboratory (NREL) and Oak Ridge National Laboratory (ORNL) to undertake a series of prototype dynamic experiments. The objective was to compare the dynamic results measured by ORNL and compare these results with the static results from the earlier UL tests. The results were to be used to assess whether static-based experimentation can adequately reflect the dynamic situation.

DISPENSER COMPONENTS AND EXPERIMENTAL PROCEDURE

Following a series of meetings, UL provided ORNL with two identical fuel dispensers to evaluate for this study. One dispenser was used to evaluate compatibility with E25 fuel (25 vol % ethanol), while the other was used to evaluate the compatibility with E85. The objective was to run a prototype dispenser system for both E25 and E85 fuels to understand the compatibility of these fuels with dispenser materials and components. The dispensers were operated for 15 weeks during the summer months of June, July, and August in order to capture the peak temperatures for 2007. The rate of reaction can frequently be inferred with the rate of corrosion and therefore roughly follows the Arrhenius Equation for the reaction rate with temperature. Therefore corrosion is directly related to temperature, and the peak temperatures associated with summer should provide an upper bound on the rates of corrosion for dispenser materials.

At the conclusion of the 15 week exposure period, it was decided to continue with another 15 week exposure, which would capture the cold ambient conditions associated with the late fall and winter months. The dispensers were refilled with new CE25a and CE85a fuel compositions and operated until a pump failure occurred on January 24, 2007.

The results from the ORNL dynamic experiments will be compared against those obtained from a series of static experiments performed by UL. The dispenser components consisted of a regulator-filter assembly, shutoff valve, hose, and nozzle. These components were assembled and installed in a covered area at the National Transportation Research Center (NTRC) facility by ORNL staff. The dispenser components were connected to a 55 gal 316 stainless steel drum, which served as the fuel storage tank. Each component was thoroughly grounded to prevent static discharge. The drum was also equipped with a flame arrester, and other safety features were added to minimize the potential for fire. Fig. B-1 shows the configuration of both dispenser assemblies, with labels added to one system for component

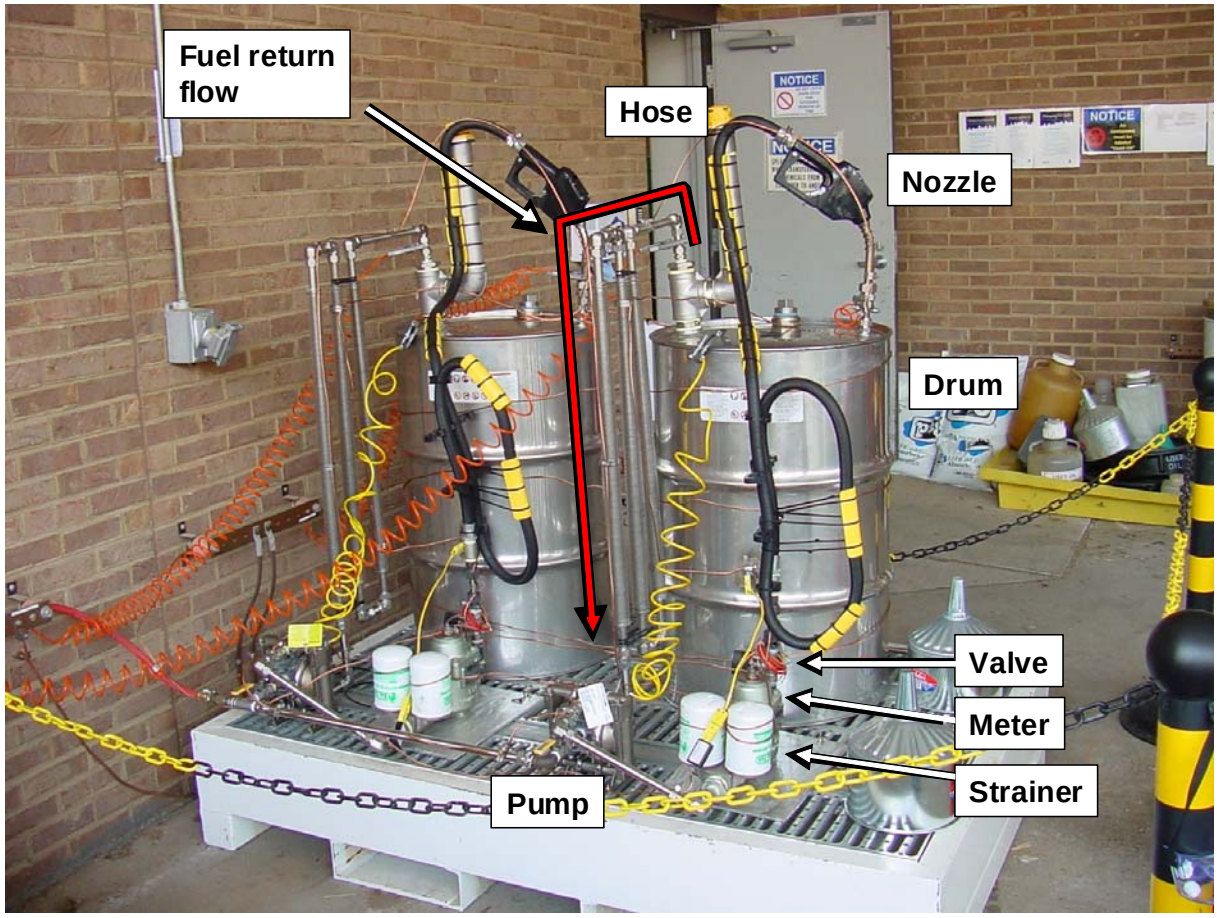

Fig. B-1. Photograph showing assembled and operating dispensers. The left and right units were used for the CE25a and CE85a fuels, respectively.

identification. A block diagram of the dispenser system, including descriptions of key components, is shown in Fig. B-2. To enable continuous flow, the shutoff features of the solenoid valve and the nozzles were disabled. Underwriters Laboratories also provided two air-assisted diaphragm pumps to provide realistic fuel flow (around 8 gal/min). During operation, the fuel was pumped from the bottom of the tank, through the pump, and then through the dispenser assembly. The hose was connected to a stainless steel tube, which returned the fuel to the tank at a level well below the fuel surface (this setup helps to prevent the possible generation of static buildup caused by flow through the gaseous headspace). All of the components not considered in this study were composed of 316 stainless steel to prevent additional contamination.

The two fuel types selected for the dispenser compatibility experiments were CE25a and CE85a. These formulations represent controlled simulations of E25 and E85. Instead of using pump-grade gasoline, the nonethanol component of the fuel consisted of equal parts of isooctane and toluene (Fuel C). A small quantity (0.8 vol %) of a weak acid solution was added to the ethanol portion to simulate impurities that may be present in pump-grade gasoline and accelerate the corrosion process. Approximately 40 gal were prepared for each fuel type. The flow rates for the CE25 and CE85a fuels were measured at 6.3 and 7.9 gal/min, respectively. The reason for this discrepancy is unclear but may be related to viscosity differences in the fuel compositions.

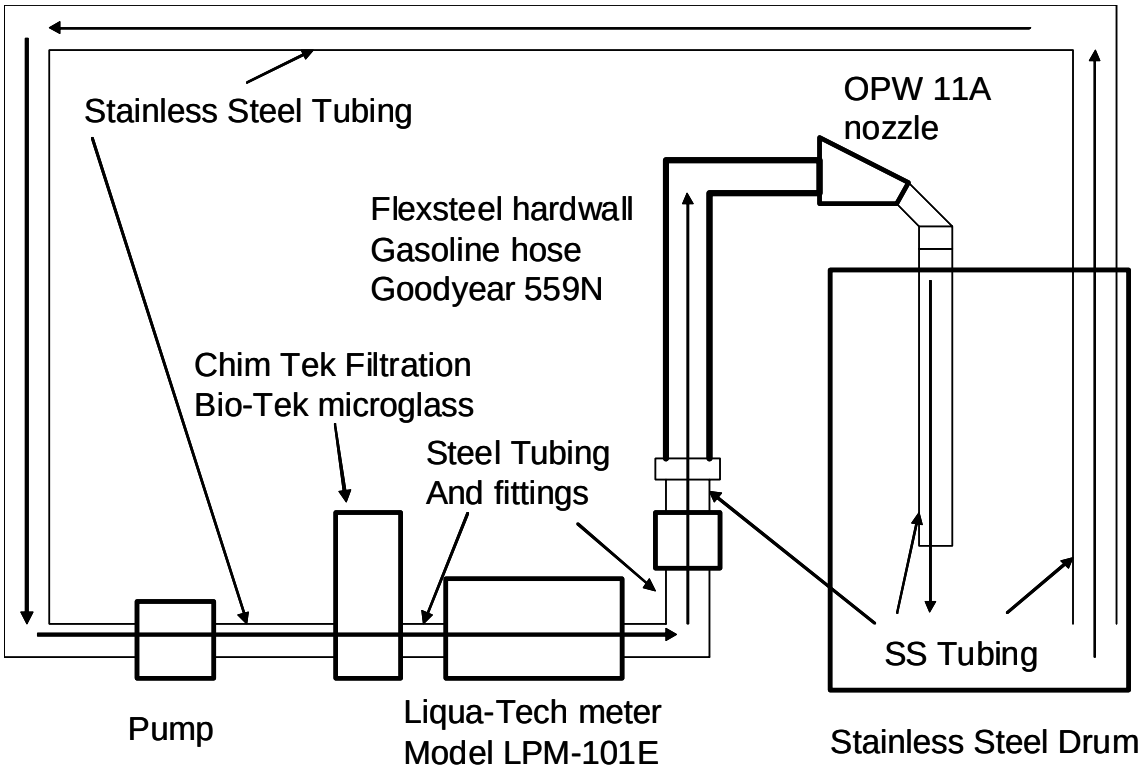

Fig. B-2. Schematic diagram showing the arrangement of the dispenser components. A brief description of the components is included.

The dispensers began operating on June 20, 2007. One-liter fluid samples were extracted once per week for the first two months and then every two weeks thereafter. A timeline showing fluid sample removal is shown in Table B-1. The removed fuel portion was not replaced during the course of this study. For each fluid sample the ambient and fuel temperatures (inside the drum) were measured every 30 min. The pumps were operated roughly 8 hours per day during the 5 day work week.

The temperature profiles for both dispensers were nearly identical. Fig B-3 shows the temperature profile for the CE25a fuel dispenser. The data captures the diurnal cycles associated with ambient temperature changes from the day and night. During the period from June 20 to August 5, the ambient temperature (during the day) approached a maximum of 30^{o}C during the day and dropped to ~23^{o}C during the evening. From August 5 through August 30, the daytime temperature peaked to around 35 to 37^{o}C and dropped to around 25^{o}C during the evening. This period had the hottest temperatures at the test site for 2007. The data also show that (during the evening hours when the pumps were not operated) the fuel did not cool down to ambient temperatures, indicating that the mass of the stagnant fuel was sufficient to prevent rapid heat loss as the temperature dropped. The first 15 week period ended on October 5, 2007. As shown in Fig. B-4, the appearance of the fuels changed considerably over the course of the 15 week evaluation period. Initially, both fuel types were clear with a slight tint of pink coloration. After 6 weeks of pump operation, the CE25a fuel took on an amber color as shown in the photograph. In contrast, the CE85a fuel did turn amber but darkened with prolonged exposure as shown in Fig. B-4. Close-up inspection of the exposed CE85a fuel suggests that the dark tint may be caused by suspended particulates originating from the hose line. No darkening was observed for the CE25a fuel.

Table B-1. Timeline for fuel sample withdrawal

Date	Period	Description
June 20, 2007	First 15 weeks	Began system operation
June 29, 2007	First 15 weeks	Fuel samples withdrawn
July 10, 2007	First 15 weeks	Fuel samples withdrawn
July 17, 2007	First 15 weeks	Fuel samples withdrawn
July 24, 2007	First 15 weeks	Fuel samples withdrawn
July 31, 2007	First 15 weeks	Fuel samples withdrawn
August 7, 2007	First 15 weeks	Fuel samples withdrawn
August 14, 2007	First 15 weeks	Fuel samples withdrawn
September 18, 2007	First 15 weeks	Fuel samples withdrawn
October 2, 2007	First 15 weeks	Fuel samples withdrawn
October 12, 2007	–	Fuel samples withdrawn (control samples)
October 26, 2007	Second 15 weeks	Fuel samples withdrawn
November 9, 2007	Second 15 weeks	Fuel samples withdrawn
November 30, 2007	Second 15 weeks	Fuel samples withdrawn
January 22, 2008	Second 15 weeks	Fuel samples withdrawn (end of study)

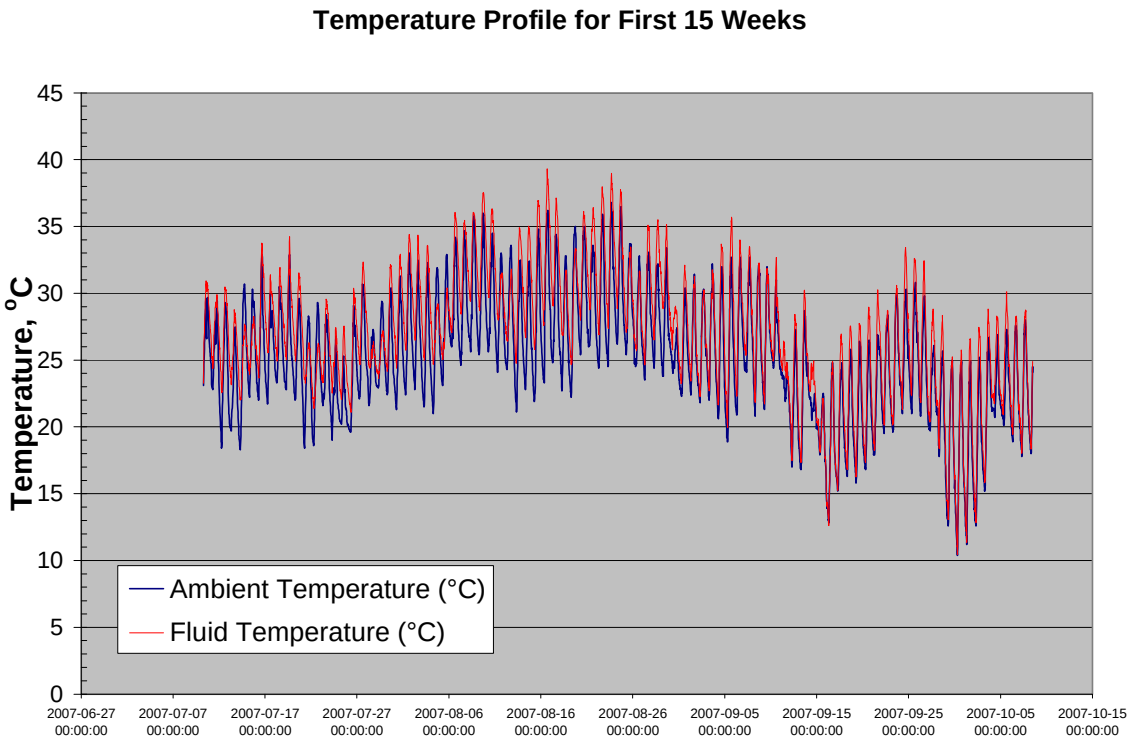

Fig. B-3. Temperature profile for the CE25a dispenser during the first 15 week evaluation period.

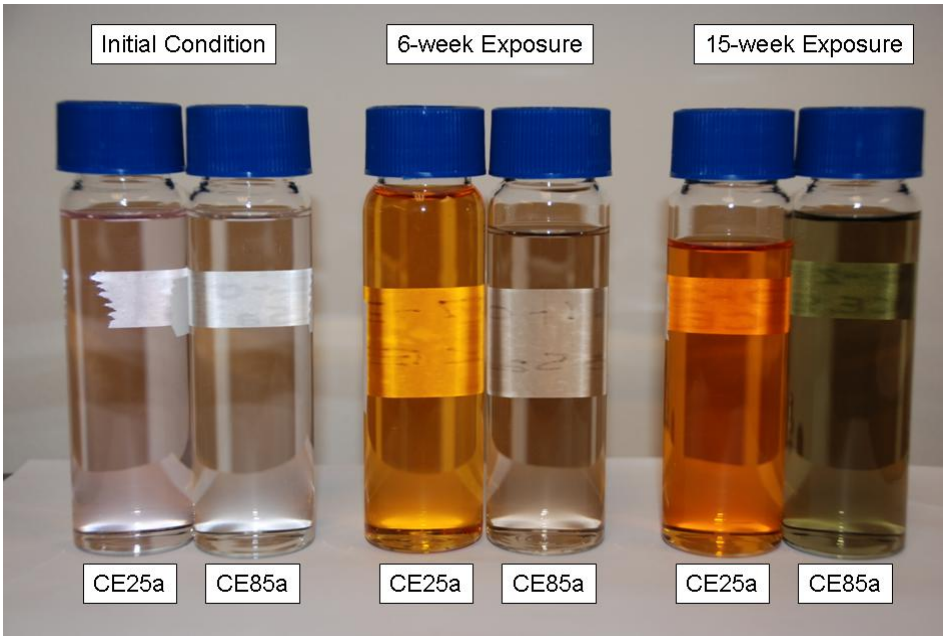

Fig. B-4. Photograph showing the change in appearance (color) of the fuel types during the first (summer) 15 week exposure period.

A second 15 week run was initiated to assess the influence of cooler temperatures and continued exposure of the dispenser components to the two fuel types. New batches of CE25a and CE85a were formulated on October 11, 2007, and on the following day (October 12, 2007) the pumps began operating. Fuel samples were drawn approximately every two weeks, and the dispenser pumps were operated until a pump failure occurred on January 24, 2008. The temperature profiles for the two dispensers during this period were also nearly identical; the profile for the CE25a dispenser is shown in Fig. B-5. The results show that the ambient (and fluid) temperatures steadily dropped over the course of the investigation and, prior to pump failure, the temperature had dropped below freezing for an extended period. The cause of the pump failure was identified as a fractured Teflon diaphragm, which is not a component under evaluation in this study. A discussion with the pump manufacturer revealed that these pumps were not rated for temperatures below 5^{o}C or 40^{o}F. However, as can be seen in Fig. B-5, the pumps, in fact, were operated at temperatures well below the minimum temperature rating. The appearance of the fractured diaphragm indicated that the failure resulted from cold operation and was not influenced by the fuel whatsoever.

The physical appearance of the CE25a and CE85a fuel types at several points during the second 15 week period is shown in Fig. B-6. In contrast to the first 15 week exposure, the color of the fuels did not change as dramatically over the course of the exposure period. The CE25a fuel did change noticeably from a light pink starting color to a light yellow coloration for the 2-week and 14-week sampling intervals. However, for these two sampling periods, the appearance for the CE85a did not change much during this time frame. The less dramatic fuel coloration for the second (winter) 15-week exposure may be due to the fact that relevant mass removal had already occurred during the summer exposure. The lower winter temperature may also be a factor, although the long exposure period means that sufficient permeation and dissolution should have occurred.

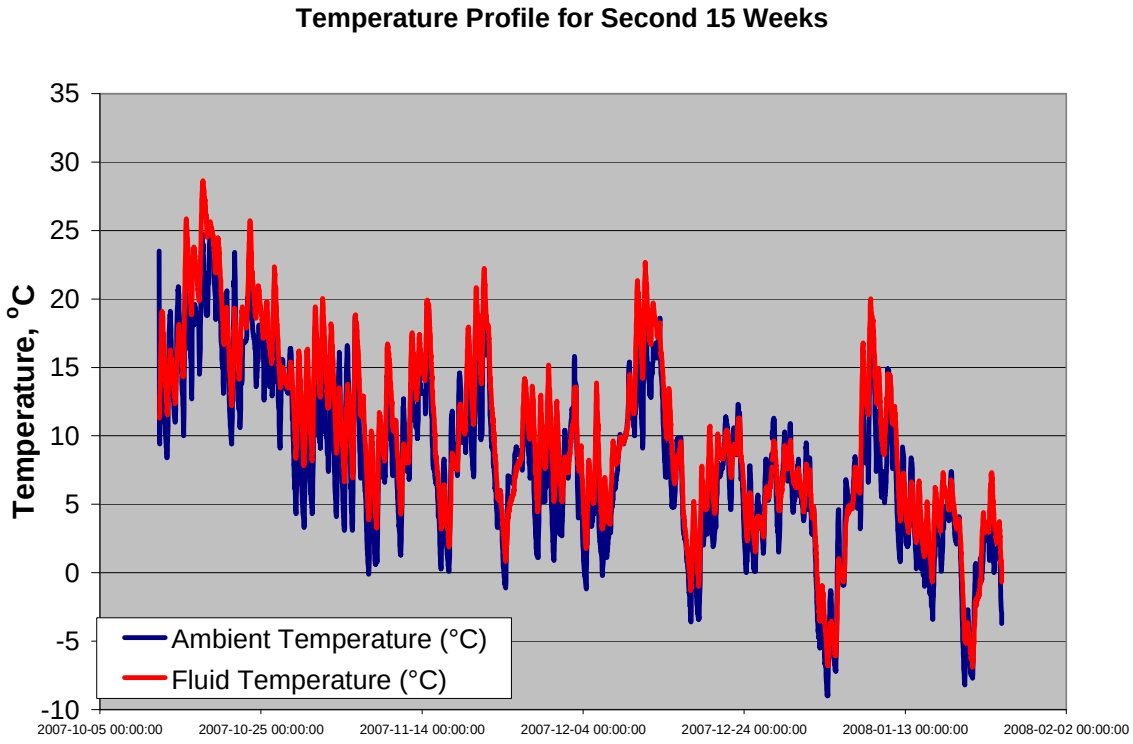

Fig. B-5. Temperature profile for the CE25a dispenser during the second 15 week evaluation period.

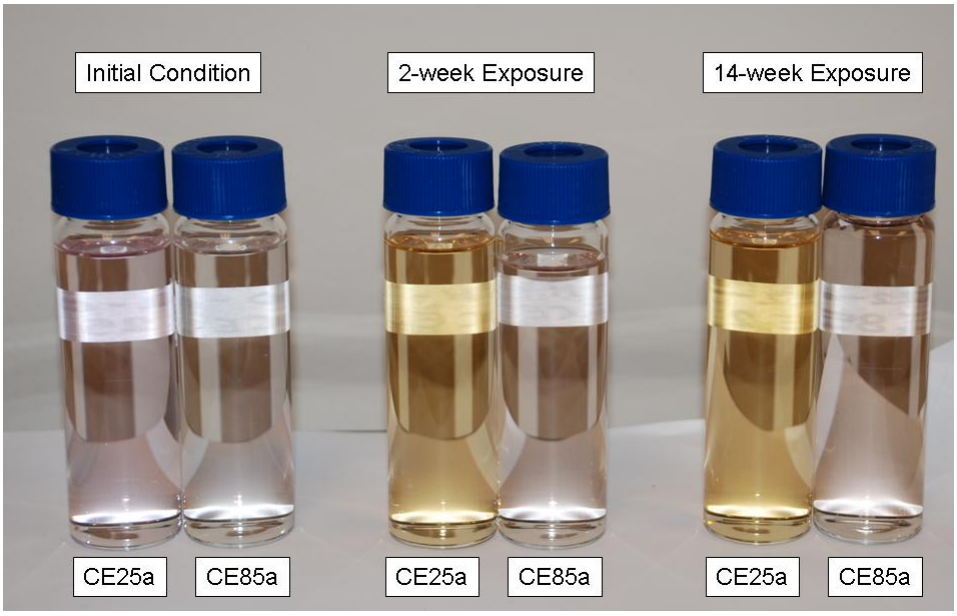

Fig. B-6. Photograph showing the change in appearance (color) of the fuel types during the second 15 week exposure period.

APPENDIX C
COMPATIBILITY ASSESSMENT OF FUEL DISPENSER METALS AND ELASTOMERS IN AN AGGRESSIVE E20 FUEL

APPENDIX C

COMPATIBILITY ASSESSMENT OF FUEL DISPENSER METALS AND ELASTOMERS IN AN AGGRESSIVE E20 FUEL

ORNL Investigators: Michael Kass, Steve Pawel, Chris Janke, Tim Theiss, and Sam Lewis

NREL Investigator: Wendy Clark

UL Investigators: J. Tom Chapin, Ken Boyce, Tom Fabian, and Joe Bablo

INTRODUCTION

In this study the compatibility of selected metals and elastomers with an aggressive E20 fuel formulation was evaluated. The materials were exposed to the test fuel as individual specimens and not as a component or subsystem. The metals selected for the experiment covered those used in standard fuel dispenser hardware and included several grades of carbon and stainless steel, brass, bronze, and copper, while the elastomer study focused on fluorocarbons provided by DuPont and 3M. The metals were evaluated for mass loss and surface analysis, while the elastomeric materials were evaluated for tensile properties, hardness, and swelling. To facilitate compatibility phenomena, the specimens were placed in a specially designed chamber to enable dynamic fluid flow and maintain a constant elevated temperature of 60°C. The combination of dynamic flow coupled with elevated temperature (and aggressive fuel chemistry) offers the potential to get meaningful comparative results in a relative short time. The results of this study are expected to assess the compatibility of fuel dispenser materials and guide incorporation and integration of ethanol-resistant materials.

EXPERIMENTAL METHOD

Materials and Equipment

Dynamic Test Chambers (Stir Tanks). To evaluate the material performance at 60°C and dynamic operation, special tanks were fabricated to allow the coupons to be exposed at a constant flow rate and constant temperature. A schematic representation of one tank is shown in Fig. C-1. The stir tanks were located in an outdoor roofed facility where they were subjected to ambient temperature fluctuations. Therefore, it was necessary to establish a temperature control system to maintain a constant 60°C fluid temperature under diurnal conditions. The chambers were composed of stainless steel and had an overall cylindrical geometry. The inner diameter is 61 cm and the height is 63.5 cm. The wall thicknesses were approximately 2 cm, which would safely withstand 70 kPa (10 psi) of internal pressure associated with heating of the fuels. An inner liner composed of four removable sections (also constructed of stainless steel) was fabricated to enable rapid attachment and removal of the specimens. The specimens were mounted into holders that allowed quick release from the inner liners. The top lid contained a sealed bearing that allowed a motor-driven shaft to turn inside the fluid. To prevent leakage, a Viton™ o-ring was used to seal the top lid to the cylindrical base. A stir paddle was located at the end of the shaft to stir the test fuels. The shaft was operated using a Leeson Hydro-Tech electrical motor designed for continual use, and a Teco controller was used to control the rotational speed of the shaft.

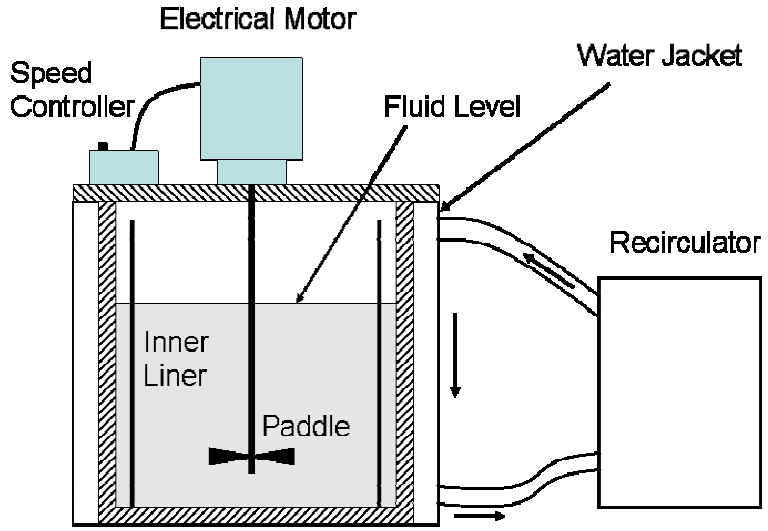

Fig. C-1. Schematic representation of one stir tank assembly including temperature control.

An outer water jacket was used to heat the fluids to the operating temperature. A 50/50 mixture of ethylene glycol and water was circulated through a Cole Parmer Polystat recirculator to control fuel temperature as depicted in Fig. C-1.

The top lid contained ports that provided access for pressure and temperature measurements of the fluid and headspace zones, enabled visual observation of the interior, and allowed for inert gas flow into and out of the sealed tank during specimen removal. Additionally, the outer surfaces of the tanks were insulated to minimize heat losses.

Fuels. The test fuels used in this study were based on standard reference test fuels. The reference fuel used is both an ASTM standard and an SAE standard test fuel to be used in material compatibility experiments. The test fuel formulation used in this study is ASTM Reference Fuel C [1] (also designated as Fuel C by SAE J1681 [2]). Fuel C is composed of 50 vol % isooctane and 50 vol % toluene and has been shown to produce swelling (in vulcanized rubber) representative of highly aromatic premium grades of automotive gasoline [1]. The ethanol fuel blend formulation used in this study contains 80 vol % Fuel C and 20 vol % of aggressive ethanol based on the formulation described in SAE J1681. The designation for this test fuel is CE20a. Table C-1 was extracted from Appendix E of the SAE J1681 protocol and depicts the formulation of aggressive ethanol used in this study to make 1 L of aggressive ethanol. Sulfuric acid is an important constituent of this formulation and is a frequent contaminant in biomass-derived ethanol.

Table C-1. Formulation to make 1.0 liter of aggressive ethanol

Component	Grams in 1.0 L of aggressive ethanol
Ethanol	816.0
Deionized water	8.103
Sodium chloride	0.004
Sulfuric acid	0.021
Glacial acetic acid	0.061

Polymer and Metallic Coupons. Table C-2 lists the metals and elastomeric materials evaluated in this study. The metal-based specimens include several steels, copper, brass, and bronze. The elastomers listed are considered high performance elastomer products. Viton™ and Dyneon™ are products of DuPont and 3M, respectively. Four Viton™ and four Dyneon™ types were evaluated. The main difference between the types of fluorocarbons is the level of fluorine contained within the elastomer structure and the type of curing agent used to crosslink the material. The NBR used in this study is a nitrile rubber and is representative of standard gasoline hoses and contains no fluorine.

Table C-2. List of metal and elastomer coupon materials

Metal and alloy type	Elastomer type
Nickel	Viton A401C
Bronze	Viton B601C
Terne metal (lead-plated steel)	Viton GF-600S
Aluminum	Viton GFLT-S
Stainless steel	Dyneon FE 5620
Brass	Dyneon FE 5840
Mild steel	Dyneon FPO 3741
Galvanized (Zn-plated) steel	Dyneon LFTE 6400
	NBR

The coupon geometry for the metal specimens immersed in the fluids was 2.5 cm by 5 cm and had a thickness of around 0.16 cm. This specimen geometry facilitates both accurate measurement of mass loss and subsequent surface analysis. The elastomer specimens contained several geometries that were specific to the type of testing being performed and were measured and tested at ambient conditions in accordance with ASTM D3767-03 and ASTM D471-06. Dog-bone coupons based on Die C (ASTM D412-06a test method A) were fabricated to obtain tensile strength, elongation at break and moduilus$_{100}$. Shore A hardness properties were also determined on the grip portion of the dog-bone coupons prior to tensile testing in accordance with ASTM D2240-05. In addition, smaller rectangular specimens were evaluated to volume swell (ASTM D471-06). Three coupons were exposed for each material and test condition to obtain some measure of statistics.

Test Protocol. The fuels were prepared by splash bending the isooctane and toluene components inside the stir tanks. For the CE20a fuel the aggressive ethanol component was made first and Fuel C was subsequently added to avoid any possible separation between the water and the Fuel C constituents.

A table showing the test matrix is shown in Table C-3. Four batches of each specimen type were prepared. Each batch contained three samples for each material. However, for each metal to be tested, additional specimens were fabricated for installation into the headspace area to assess compatibility with the vapor phase only. One batch consisted of one set of the metal specimens (listed in Table C-2) and two sets (tensile specimens and hardness/swell specimens) of the nine elastomer types. For each material and coupon geometry, three specimens were evaluated for the fluid exposures. (For the headspace gas exposures the number of specimens per metal was two.) Therefore, the total batch size exposed to each fluid was 24 metal corrosion coupons and 54 elastomer coupons, of which 27 were tensile specimens and 27 were hardness/swell specimens.

Table C-3. Specimen removal and insertion protocol

Batch number	Exposure protocol for specimens per batch		
	Week introduced	Week removed	Total weeks exposed
1	0	4	4
2	0	12	12
3	0	16	16
4	12	16	4

At each specimen removal interval, the elastomer specimens were placed directly from the stir tank into a container filled with the appropriate test fuel and allowed to cool to ambient conditions prior to testing. This was to ensure that the elastomer specimens remained wet in accordance with the standard test protocol. No such requirement was needed for the metal specimens.

EXPERIMENTAL RESULTS

Approximately 140 L of fuel were added to each stir tank. The vertical headspace distance (from the fuel level to the lid) was approximately 43 cm. The specimens were mounted inside the tank prior to adding the fuels.

Stir Tank Performance. The lids were sealed and the stirrer motors were operated at 100 rpm. While the stirrers were running, the temperature control recirculators were set to 60°C and turned on. The motors and recirculators were operated continuously over each exposure period. The flow rate of the fuel past the specimens was estimated at 0.8m/s using a standard flow probe. The temperature of the fuel and headspace area was continuously monitored and showed that 8 h was required to heat the fuel from ambient to 60°C. Since the resulting temperature data for the two tanks were nearly identical, we have elected to use profile for the Fuel C tank shown in Fig. C-2 to assess the temperature performance. The resulting temperature profile clearly shows the three test periods. The results presented in Fig. C-2 show that the fluid temperature was maintained at 60°C during the 4, 12, and 16 week intervals. In contrast, the ambient temperature was much lower and fluctuated dramatically, reaching a low temperature of -10°C to a maximum approaching 25°C. The breaks in the fluid temperature are associated with the end of each period, at which point a portion of the specimens were removed or added per the protocol outlined in Table C-3. A noticeable drop in fluid temperature occurred early in the second (8 week) period between week 4 and week 12. This drop was caused by an unexpected power outage and was immediately corrected. The effect of the power outage on the overall compatibility during this timeframe is considered minimal.

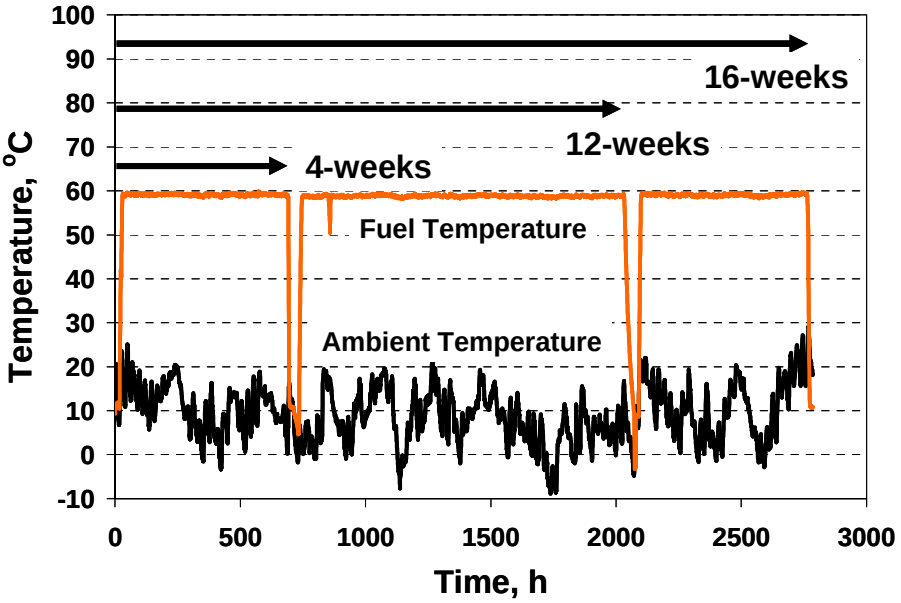

Fig. C-2. Representative temperature profile of the stir tanks during th entire test period. The data were taken for the Fuel C tank; the CE20a results were nearly identical.

The headspace temperature was also recorded for both vessels, and the average values are shown in Table C-4. The temperatures for the Fuel C and CE20a tanks were observed to fluctuate 5°C and 2°C over the course of the study, respectively.

Table C-4. Average headspace gas temperature (°C) for each of the three exposure periods

	Exposure periods		
	0–4 weeks	**4–12 weeks**	**12–16 weeks**
Fuel C	51	46	48
CE20a	56	54	56

During operation the stir tanks became pressurized as the fluids were heated. The maximum pressures reached for the Fuel C and the CE20a fuels were 39 kPa and 67 kPa respectively. These values correspond closely to the theoretical value calculated for these compositions at 60°C. After reaching maximum value, the pressure within the CE20a stir tank was observed to drop steadily over the next 5 weeks to a point just above ambient. This drop in pressure was caused by a leak in the bearing seal and, due to time constraints, was not corrected prior to the end of the 16 week exposure run. The Fuel C tank did not leak, and a pressure of around 35 kPa was maintained throughout the entire test period.

Fluid (Test Fuel) Chemistry. Fluid samples were collected for the initial condition and at the end of each test period (4 weeks, 12 weeks, and 16 weeks). In addition, the headspace gases were collected during the first 4 week exposure period. The compositions of the fluid and gases were evaluated using a gas chromatography and mass spectrometry (GC/MS) analyzer. The compositions of the fluids and headspace gases are shown in Figs. C-3 and C-4 for Fuel C and CE20a, respectively. The baseline data represent the initial condition. For Fuel C (as shown in Fig. C-3) the headspace chemistry consisted of approximately 70% isooctane and roughly 30% toluene. The lower vapor pressure of isooctane results in a much higher concentration relative to toluene in the headspace gas. The relative concentration of the two constituents

in the fluid is unchanged from the baseline values at the end of the 4 and 12 week periods. This test vessel did not leak and was therefore able to maintain fluid chemistry and volume over the entire 16 week test period. Note that the measured fluid chemistry at the end of 16 weeks indicated an increased concentration of isooctane relative to toluene. This result is likely a sampling error since there was no observable leak or loss of fluid in the test vessel and we would expect that the higher volatility of the isooctane to *decrease* the concentration of isooctane relative to the toluene.

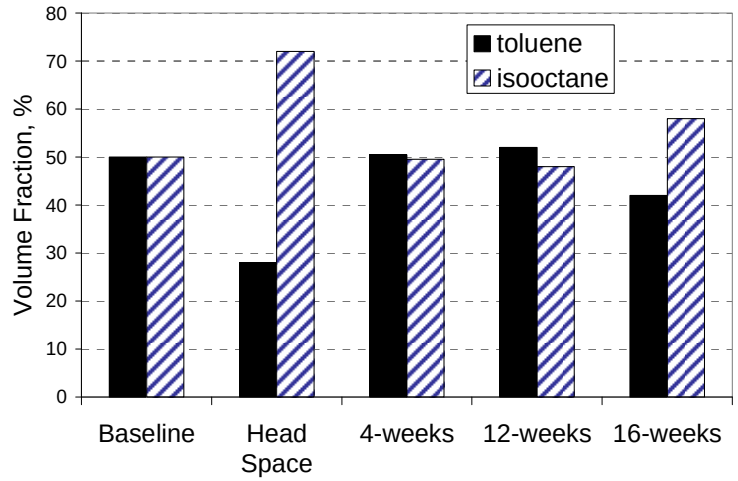

Fig. C-3. Composition of Fuel C in the headspace and in the fluid for each exposure period.

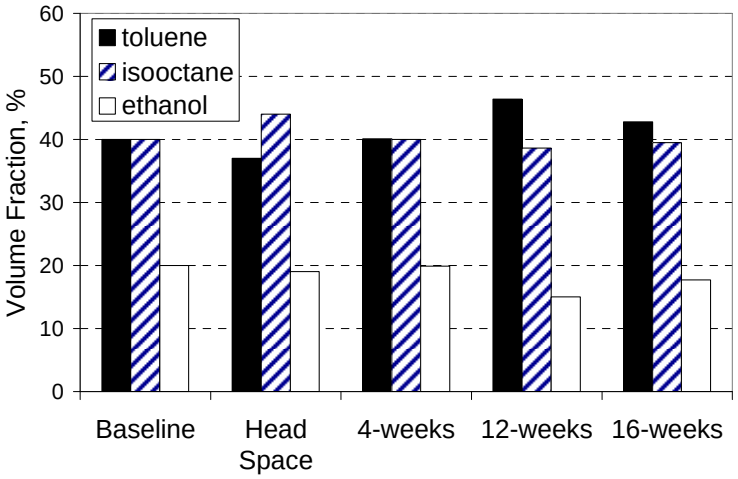

Fig. C-4. Composition of CE20a in the headspace and in the fluid for each exposure period.

Although the tank containing the CE20a fuel had developed a slow leak during the initial 4 week exposure period, the fuel chemistry was relatively unaffected during this period (as shown in Fig. C-4). A sample of the headspace gas showed that the gas concentration consisted of 44 vol % isooctane, 36 vol % toluene, and around 20% ethanol. The higher fraction of isooctane in the gas phase is due to the higher volatility of isooctane relative to toluene. Interestingly, the ethanol concentration was not raised above the fluid level, and this effect may be due to the bound water molecules present in the ethanol. At the end of the 12 week exposure period, the levels of isooctane and ethanol were noticeably reduced. This drop is likely the result of the highly volatile components escaping from the leak. The ethanol concentration had

dropped to around 15% and the isooctane concentration was also less relative to the toluene. After 12 weeks of exposure, the CE20a fluid had dropped around 10 cm from the original level. Approximately 20 L of fresh CE20a was added to raise the fuel back to its original level. The addition of fresh CE20a raised the ethanol concentration in the vessel to around 17 vol %, which was maintained to the end of the final 16 week exposure period.

Metal Coupon Results. A report detailing the metal results can be found in the ORNL/TM-2009/286 Report entitled Preliminary Compatibility Assessment of Metallic Dispenser Materials for Service in Ethanol Fuel Blends by Pawel et al. The metal-based coupons were examined for discoloration and mass loss at the end of each exposure period. The results indicated that none of the metal coupons exposed to Fuel C had noticeable changes in either appearance or mass loss. There was also no significant change in mass loss for each metallic coupon exposed to the vapor space of either fuel type. For the 304 stainless steel, type 1010 carbon steel, 201 nickel, and 1100 aluminum metals, there was also no change in mass and appearance for these materials in the CE20a fluid during the exposure periods. In contrast, the brass, bronze, terne-plated steel, and galvanized steel coupons were found to exhibit a slight mass loss as shown in Table C-5.

Table C-5. Mass loss of brass, bronze, terne-plated steel, and galvanized steel specimens exposed to CE20a fuel

Batch #	Exposure period	Mass loss (mg)		
		Brass	Terne-plated steel	Galvanized steel
1	0–4 weeks	6.14	0.23	0.56
2	0–12 weeks	11.05	1.26	2.08
3	0–16 weeks	11.13	2.47	2.47
4	12–16 weeks	2.49	3.07	5.03

The results observed for the bronze coupons for each of the four batches were very similar to those for the brass specimens and, therefore, were not included into a separate column. The brass (and bronze) coupons were observed to exhibit the highest mass loss of the metal-based specimens. However, the corresponding corrosion rate for these two materials was less than 2 mils/year (which is considered low). The mass loss was observed to be highest during the initial 4 weeks rather than for those specimens introduced to the fluid and during week 12 and exposed for the final 4 week period. Interestingly, the opposite effect is observed for the terne-plated and galvanized steels; both of them lost a much higher mass when exposed to the fuel composition at the end of the test. However, taken in a larger context, these values are not considered significant enough to warrant concerns regarding long-term corrosion. Photographs of the exposed coupons are shown in Figs. C-5 and C-6 for the brass, bronze, terne-plated steel, and galvanized steel. The visual appearances of these specimens were essentially unaffected by exposure to the vapor phase of Fuel C. However, these metals exhibited discoloration when exposed to the CE20a fuels, indicating some degree of surface oxidation and film formation.

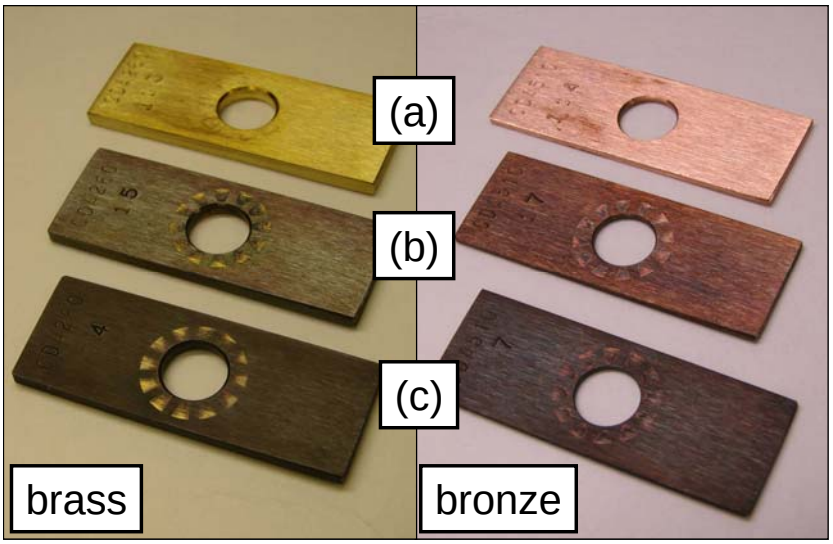

Fig. C-5. Photograph showing discoloration associated with brass and bronze specimens exposed to *(a)* Fuel C headspace, *(b)* between 12 and 16 weeks in CE20a, and *(c)* 0 to 16 weeks in CE20a.

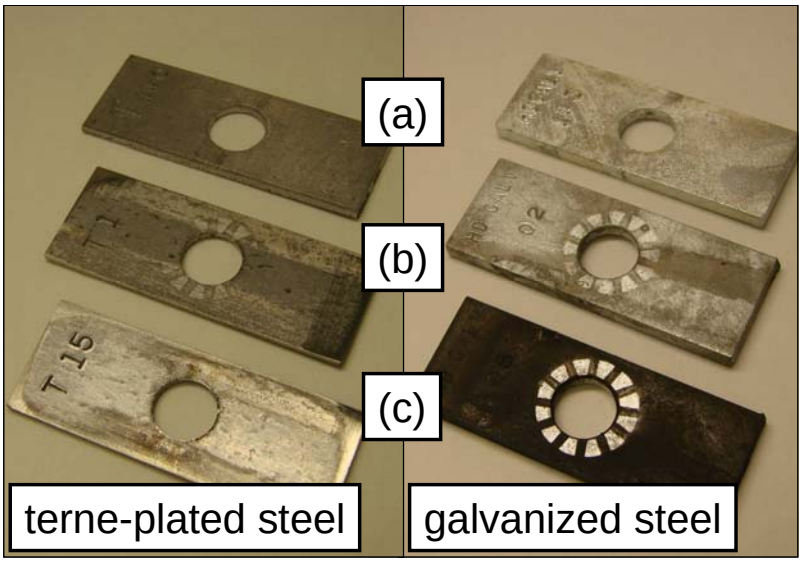

Fig. C-6. Photograph showing discoloration associated with terne-plated and galvanized steels exposed to *(a)* Fuel C headspace, *(b)* between 12 and 16 weeks in CE20a, and *(c)* 0 to 16 weeks in CE20a.

Elastomer Coupon Results. The mechanical properties for the elastomers exposed to Fuel C and CE20a are shown in Figs. C-7 through C-12. Selected mechanical properties include the elastic modulus$_{100}$ (defined as the stress at 100% elongation), tensile strength, elongation at break, and hardness. In each of these figures the exposure times are shown along with the initial condition and against specimens that were thermally aged at 60°C for 4 weeks. Since the mechanical properties of elastomers are highly dependent on temperature, it is important to consider property changes associated with heating to 60°C which are separate from the fluid effects.

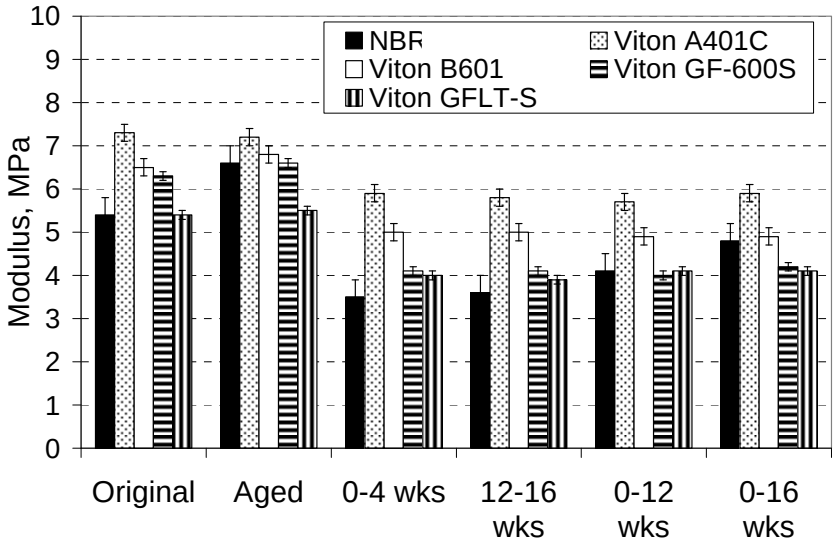

(a)

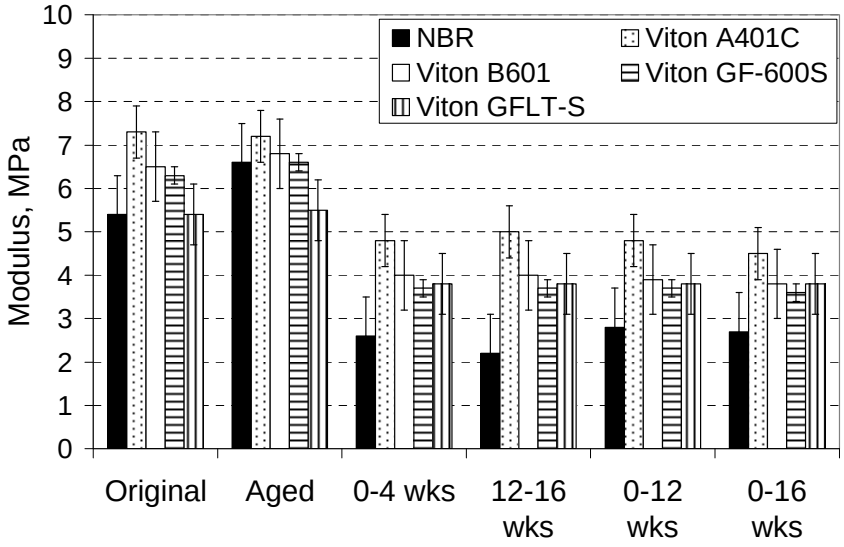

(b)

Fig. C-7. Modulus of Viton™ elastomers measured for the original condition, thermally aged for 4 weeks at 60°C, and selected exposures at 60°C to *(a)* Fuel C and *(b)* CE20a.

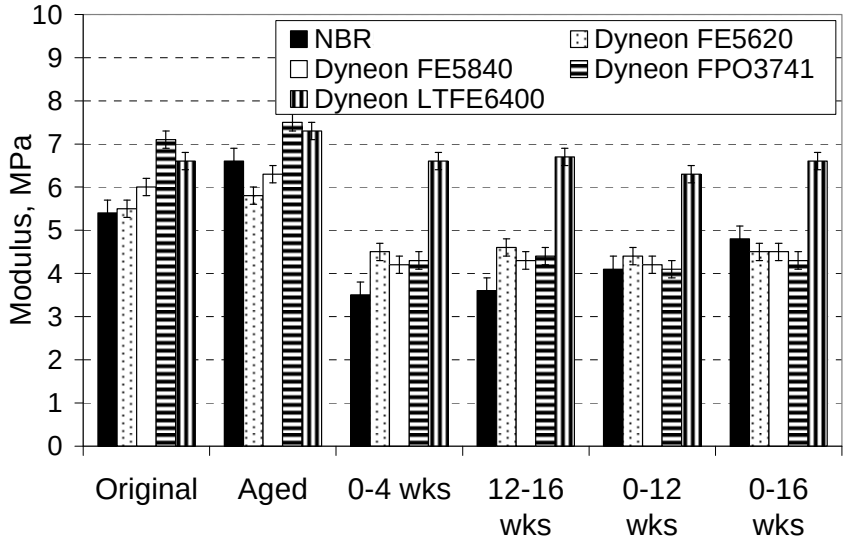

(a)

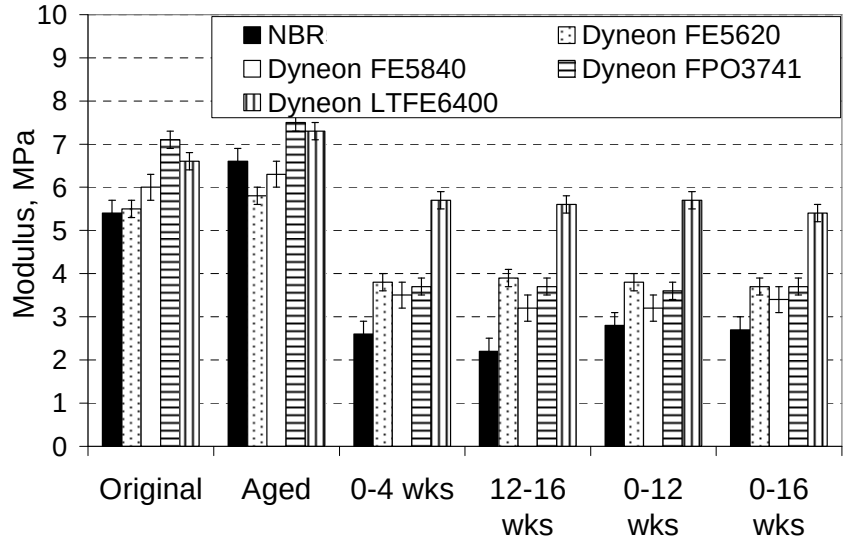

(b)

Fig. C-8. Modulus$_{100}$ of Dyneon™ elastomers measured for the original condition, thermally aged for 4 weeks at 60°C, and selected exposures at 60°C to *(a)* Fuel C and *(b)* CE20a.

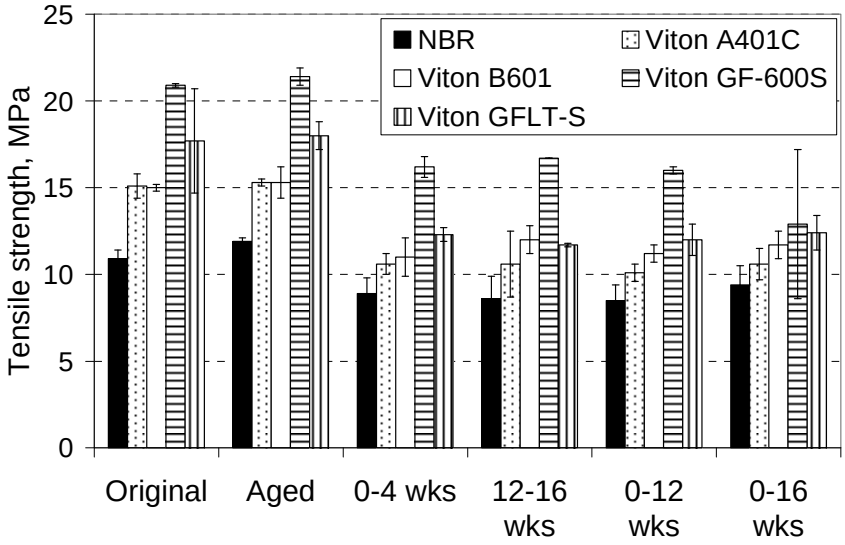

(a)

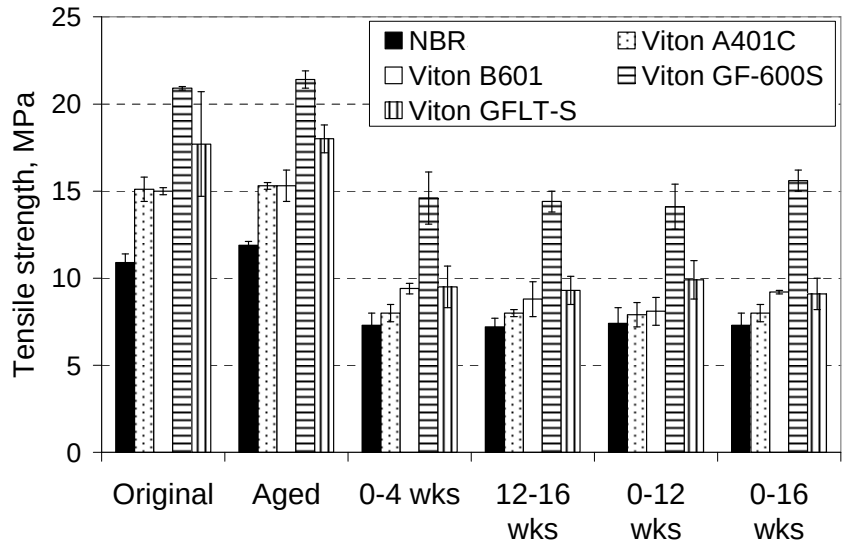

(b)

Fig. C-9. Tensile strength of NBR and Viton elastomers measured for the original condition, thermally aged for 4 weeks at 60°C, and selected exposures at 60°C to *(a)* Fuel C and *(b)* CE20a.

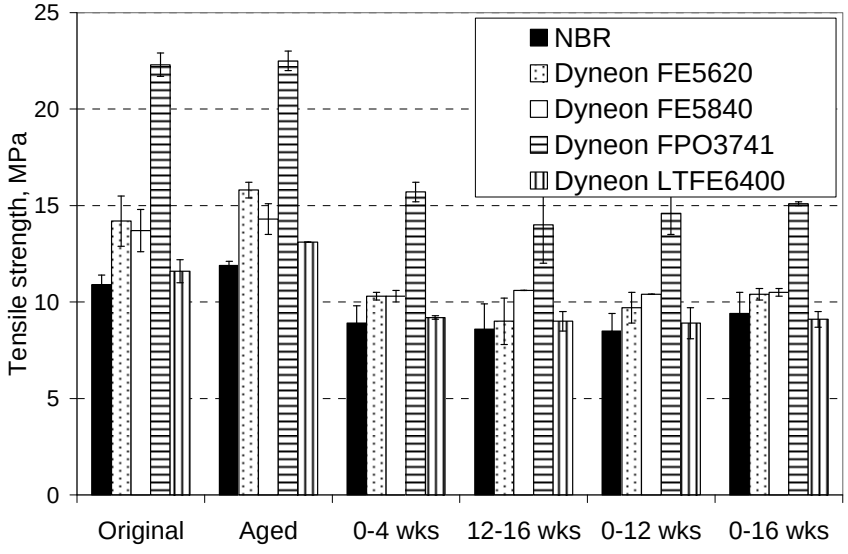

(a)

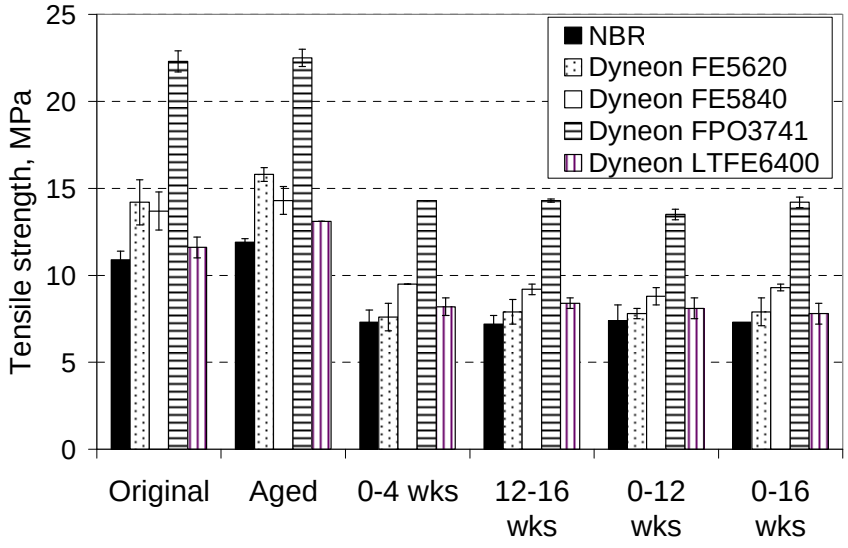

(b)

Fig. C-10. Tensile strength of NBR and Dyneon elastomers measured for the original condition, thermally aged for 4 weeks at 60°C, and selected exposures at 60°C to *(a)* Fuel C and *(b)* CE20a.

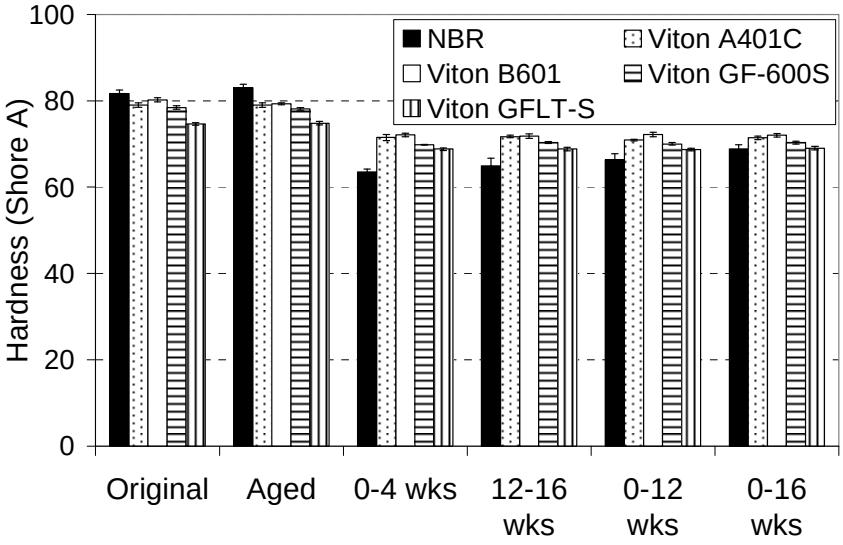

(a)

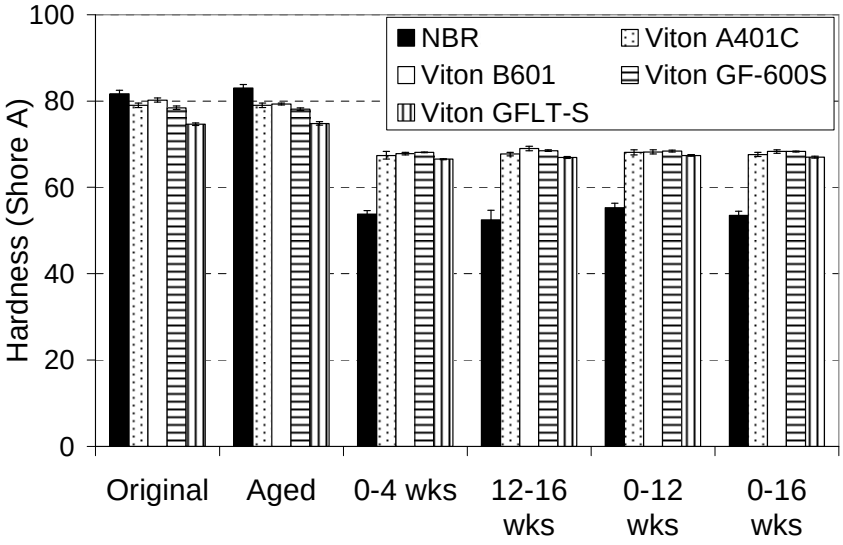

(b)

Fig. C-11. Shore A hardness measurements of NBR and Viton elastomers measured for the original condition, thermally aged for 4 weeks at 60°C, and selected exposures at 60°C to *(a)* Fuel C and *(b)* CE20a.

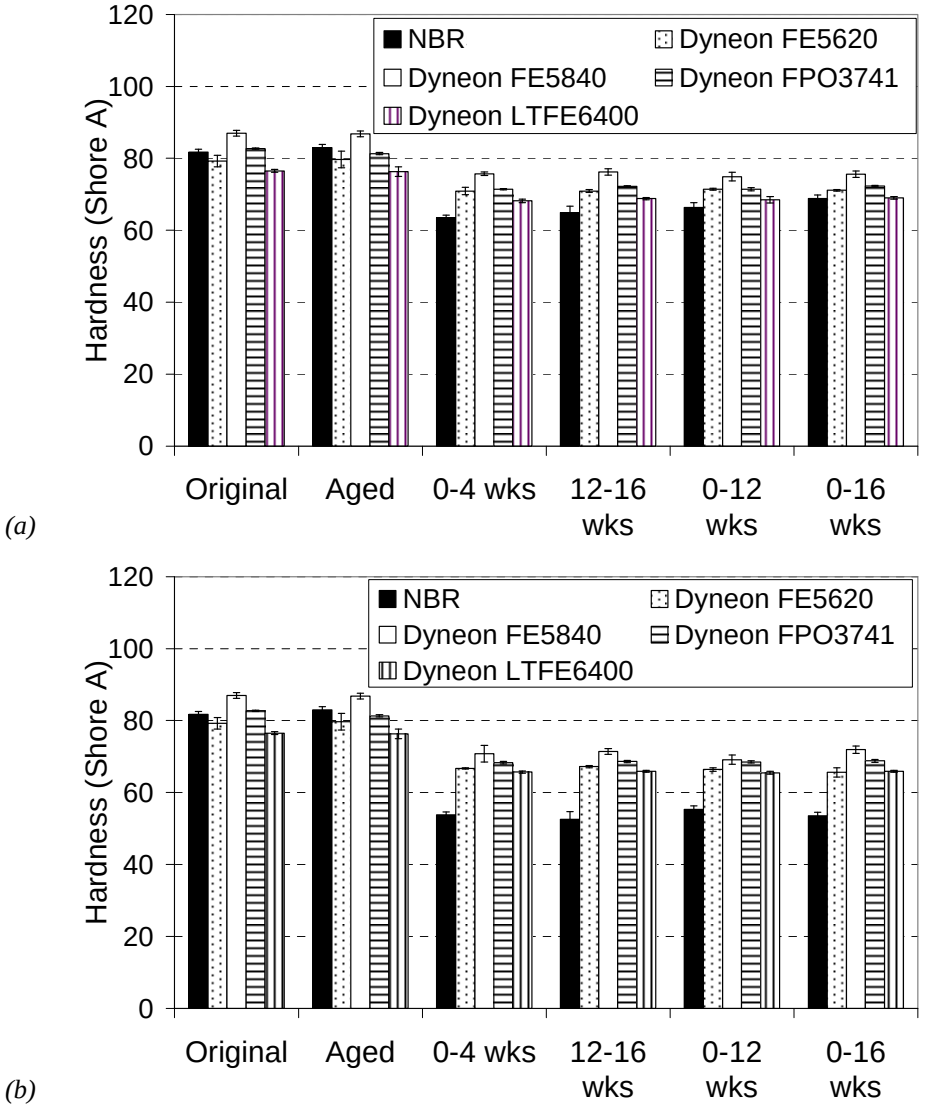

Fig. C-12. Shore A hardness measurements of NBR and Dyneon™ elastomers measured for the original condition, thermally aged for 4 weeks at 60°C, and selected exposures at 60°C to *(a)* Fuel C and *(b)* CE20a.

The elastic modulus results for exposures to Fuel C and CE20a are shown in Figs. C-7 and C-8 for the Viton™ and Dyneon™ specimens, respectively. Thermal aging (for 4 weeks) contributed to a modest increase in the modulus for the Viton™ and Dyneon™ specimens, probably resulting from additional postcuring (crosslinking) of the material. In contrast, the modulus for the NBR specimens increased 20% during 4 weeks of thermal aging. In fact, after aging, the modulus for the NBR was higher than or equal to the moduli of several fluorocarbons; the exceptions were Viton™ A401C, and Dyneon™ FP03741 and LFTE6400. All of the specimens exhibited a decrease in modulus when exposed to Fuel C. The nitrile rubber modulus exhibited the most dramatic drop (~50%) when exposed to Fuel C for 4 weeks and subsequently showed a modest increase in modulus with increased time of exposure. In contrast, the moduli of the elastomers remained relatively constant for each exposure period. At the end of 16 weeks in

Fuel C only Viton™ A401C and Dyneon™ LFTE6400 exhibited significantly higher moduli than NBR, with Dyneon™ LFTE6400 having the best performance (in Fuel C).

When immersed to CE20a the resulting moduli for the elastomers was lower (5 to 20%) than when exposed to Fuel C. The CE20a results also showed that the specimen moduli were not greatly affected by length of exposure time (similar to Fuel C results). However, exposure to CE20a reduced the NBR modulus by approximately 50-60% relative to the original baseline condition. In addition, all of the fluorocarbon moduli were observed to exceed the NBR results. Dyneon™ LFTE6400 and Viton™ A401C produced the highest moduli over the entire test period. Because modulus is a measure of the stiffness of a material, it is an important property reflecting the resilience and elasticity of an elastomer. Elastomers with too low a modulus are more easily deformed, which can result in leakages.

The tensile strength results for the Viton™ and Dyneon™ specimens are shown in Figs. C-9 and C-10. Thermal aging was found to have minimal effect on the tensile strengths of the elastomer specimens, although some samples showed slight increases in strength. Exposures to Fuel C and CE20a dropped the tensile strengths of the Viton™ specimens to around 20–40% and 25–45%, respectively. The Dyneon™ elastomers tensile strengths also dropped similarly. For each specimen (including the standard nitrile rubber sample) the length of exposure time did not have a significant effect on the tensile strength. Note that the Viton GFLT-S specimen exposed to Fuel C showed an average decrease from week 12 to week 16 of exposure but, when taken in context of the large error range, is consistent with the other exposure results. As shown in Figs. C-9 and C-10, Viton GF-600S and Dyneon FPO3741 both exhibited substantially higher strengths than the other elastomer types exposed to CE20a, while the remaining elastomers showed only marginally higher tensile strengths than the standard NBR.

Shore A hardness measurements were taken at five locations for each individual specimen and averaged together with the three coupons representing each material type. The results are shown in Figs. C-11 and C-12 for the Viton™ and Dyneon™ samples, respectively. The hardness values dropped roughly 5-10 points with exposure to Fuel C and 8-12 points when exposed to CE20a. The NBR hardness values declined 13-18 points when exposed to Fuel C versus 26-29 points for exposure to CE20a. The hardness results were not greatly influenced by the length of exposure in either fuel type, and the elastomers all performed about the same. Both fluoroelastomer products (Viton™ and Dyneon™) exhibited hardness increases of at least 13 points compared to NBR when exposed to CE20a.

The degree of volume increase was measured for each elastomer specimen and is expressed as a percentage increase from the original volume in Fig. C-13 for both Fuel C and CE20a exposures. As seen in the figure, the length of exposure time did not significantly affect the volume increase for each sample. NBR exhibited the highest degree of volume swell of the samples tested. All of the specimen volumes did not exceed 20% when exposed to Fuel C, which is representative of standard grade gasoline. More swelling was observed for the specimens when exposed to the more aggressive solution, CE20a. The NBR, Viton™ AC401, and Dyneon™ FE5620 exceeded 20% volume swell, and Viton™ B601 closely approached this value. The lowest volume swell values (<10%) were observed for Dyneon™ LFTE6400 and FE5840 along with Viton™ GF-600S.

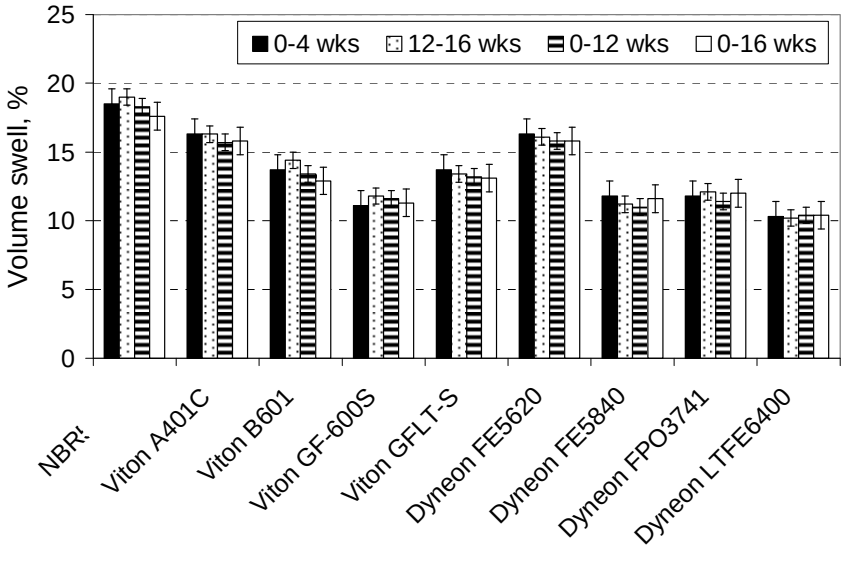

(a)

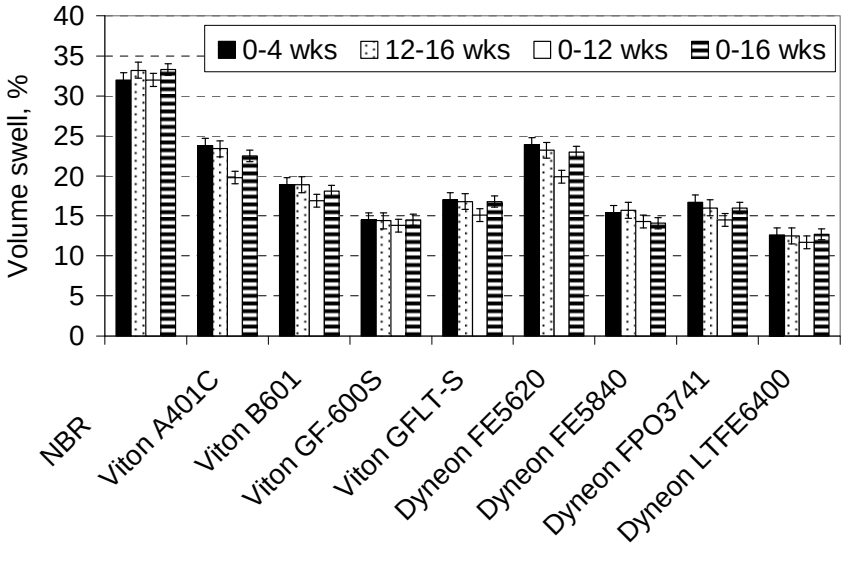

(b)

Fig. C-13. Volume increase of elastomer specimens measured for the original condition, thermally aged for 4 weeks at 60°C, and selected exposures at 60°C to *(a)* Fuel C and *(b)* CE20a.

It is difficult to predict how the elastomers will perform as actual fuel dispenser o-rings and gaskets for a blended fuel consisting of 20 vol % ethanol. CE20a is not a commercial fuel formulation and was developed solely to make compatibility assessment in a relatively short timeframe. The combination of moving fluid, elevated temperature, and aggressive composition serve to accelerate compatibility assessments and provide a guideline for material selection based on performance.

All of the fluorocarbons had similar hardness values and all were higher than NBR. The specimens that exhibited the best combination of mechanical properties and decreased swell in CE20a are Dyneon™ LFTE6400 and Viton™ GF-600S. Interestingly, Dyneon™ LFTE6400 has the highest modulus of the

specimens, while Viton™ GF-600S had the highest tensile strengths. Based on the available information, both of these elastomer types would offer the best compatibility matchups with an E20-type fuel.

Interestingly, the time of exposure had a minimal effect on the mechanical properties or swell associated with the elastomers. Meaningful results were obtained from the initial 4 week exposure period, which indicates that future tests of this type do not need to be extended past this period.

CONCLUSION

Two specialized stir tanks were fabricated to enable a dynamic fluid environment under constant elevated temperature. The tank containing Fuel C maintained temperature and pressure over the study period, but the CE20a tank developed a small leak that caused a small change in fluid composition toward the end of the test. Comparison of the mechanical and physical properties of the elastomers suggests that this change in fuel composition had little effect on their performance.

In general, degradation of mechanical and physical properties of the metal and elastomer specimens occurred during the initial 4 week exposure. Additional exposure did not noticeably enhance property degradation.

Fuel C and the headspace gases did not affect the metal specimens. However, discoloration and mass loss was measured for the brass, bronze, terne-plated steel, and galvanized steel specimens exposed to CE20a. The highest mass losses were measured for the brass and bronze specimens.

The elastomer specimens each suffered property degradation when exposed to both Fuel C and CE20a at 60°C and flowing liquid. However, the decrease in tensile properties and hardness was higher for the specimens subjected to CE20a. In addition, the volume swell was also higher for the CE20a exposures. Interestingly, the modulus for the NBR sample actually improved with the length of exposure to Fuel C so that at the end of the 16 week period, the modulus for the NBR sample was comparable to the moduli of the elastomer samples.

When exposed to CE20a, the elastomer specimens all had higher modulus properties and hardness values than the standard NBR. Viton™ A401C and Dyneon™ LFTE6400 had significantly higher moduli than the other specimens, while Viton™ GF-600S and Dyneon™ FPO 3741 produced the highest tensile strengths when exposed to the aggressive E20 formulation, CE20a. All the elastomer specimens exhibited similar hardness values when exposed to Fuel C and CE20a, and their hardness results were about 20% higher than the NBR sample when exposed to CE20a. The specimens that exhibited the best combination of mechanical/physical properties and low swelling were Dyneon™ LFTE6400 and Viton™ GF-600S.

The results showed that the stir tank approach can successfully evaluate the compatibility of material coupons to a specified test fluid. The temperature and flow rate was held constant over the test periods and degradation of the specimens correlated with the fluid chemistry measured in the prototype experiments using E25a described in Appendix A.

ACKNOWLEDGMENTS

The authors gratefully acknowledge the support of Dennis Smith, Director of the DOE National Clean Cities Program & Vehicle Technology Deployment. Oak Ridge National Laboratory is a multiprogram laboratory operated by UT-Battelle for the U.S. Department of Energy under contract DE-AC0500OR22725. We also would like to acknowledge Eric Nafziger and Norberto Domingo (ORNL) for their support in setting up the stir tanks.

APPENDIX D
TABULATED DMA RESULTS

Table D-1. DMA results for elastomer specimens

			Storage Modulus		Loss Modulus			Tan Delta		
Environment	Elastomer	Fuel Type	Temp/oC	Mpa	Temp/oC	Temp/oC	Temp/oC	Temp/oC	Temp/oC	Temp/oC
	Viton A401C	Baseline	-2.62	2812	-0.10			9.45		
Fluid	Viton A401C	Ref C	-11.05	3654	-8.18			4.72		
Fluid	Viton A401C	CE10A	-9.44	2684	-7.22			4.33		
Fluid	Viton A401C	CE17A	-12.35	2985	-10.04			2.57		
Fluid	Viton A401C	CE25A	-9.04	2794	-6.17			4.69		
Vapor	Viton A401C	Ref C	-6.65	3220	-4.55			5.89		
Vapor	Viton A401C	CE10A	-9.94	3265	-6.90			5.32		
Vapor	Viton A401C	CE17A	-9.86	3673	-7.14			5.25		
Vapor	Viton A401C	CE25A	-7.90	3355	-5.28			6.33		
	Viton B601C	Baseline	0.21	2445	2.30			9.64		
Fluid	Viton B601C	Ref C	-6.64	2436	-4.51			5.66		
Fluid	Viton B601C	CE10A	-6.64	2548	-4.84			5.57		
Fluid	Viton B601C	CE17A	-10.52	2918	-8.10			4.14		
Fluid	Viton B601C	CE25A	-6.77	3119	-4.12			5.54		
Vapor	Viton B601C	Ref C	-3.74	2413	-1.38			8.42		
Vapor	Viton B601C	CE10A	-6.21	3170	-3.62			6.05		
Vapor	Viton B601C	CE17A	-7.31	3170	-5.02			6.01		
Vapor	Viton B601C	CE25A	-4.36	3086	-2.08			7.17		
	Viton GF-600S	Baseline	8.31	2235	10.41			17.34		
Fluid	Viton GF-600S	Ref C	-0.46	2314	1.09			13.38		
Fluid	Viton GF-600S	CE10A	0.24	2308	1.54			13.04		
Fluid	Viton GF-600S	CE17A	-2.08	2159	-0.79			11.36		
Fluid	Viton GF-600S	CE25A	0.22	2425	2.63			13.11		
Vapor	Viton GF-600S	Ref C	3.06	2123	4.97			14.72		
Vapor	Viton GF-600S	CE10A	0.45	2618	2.65			13.07		
Vapor	Viton GF-600S	CE17A	0.50	2588	2.57			13.25		
Vapor	Viton GF-600S	CE25A	2.42	2470	4.30			13.82		
	Viton GFLT-600S	Baseline	-11.17	2150	-9.10			-1.85		
Fluid	Viton GFLT-600S	Ref C	-12.59	2158	-11.78			-3.33		
Fluid	Viton GFLT-600S	CE10A	-12.97	2275	-11.75			-4.21		
Fluid	Viton GFLT-600S	CE17A	-15.31	2000	-13.34			-4.71		
Fluid	Viton GFLT-600S	CE25A	-13.58	2256	-11.17			-3.09		
Vapor	Viton GFLT-600S	Ref C	-12.95	2682	-10.80			-1.67		
Vapor	Viton GFLT-600S	CE10A	-14.15	2875	-11.99			-3.87		
Vapor	Viton GFLT-600S	CE17A	-13.03	2783	-11.76			-3.61		
Vapor	Viton GFLT-600S	CE25A	-12.01	2588	-10.45			-2.88		
	Dyneon FE5620	Baseline	-3.39	3105	-1.00			7.75		
Fluid	Dyneon FE5620	Ref C	-10.31	3080	-8.06			3.26		
Fluid	Dyneon FE5620	CE10A	-11.39	3196	-8.46			3.48		
Fluid	Dyneon FE5620	CE17A	-12.80	2717	-10.18			2.01		
Fluid	Dyneon FE5620	CE25A	-9.90	2917	-7.09			3.67		
Vapor	Dyneon FE5620	Ref C	-8.07	3343	-5.49			4.72		
Vapor	Dyneon FE5620	CE10A	-9.36	3416	-7.49			3.58		
Vapor	Dyneon FE5620	CE17A	-11.56	3715	-8.74			2.76		
Vapor	Dyneon FE5620	CE25A	-8.85	3066	-6.18			3.60		
	Dyneon FE5840	Baseline	7.41	2437	9.74			15.36		
Fluid	Dyneon FE5840	Ref C	-0.14	2573	1.85			11.46		
Fluid	Dyneon FE5840	CE10A	-2.27	2635	0.61			12.27		
Fluid	Dyneon FE5840	CE17A	-3.90	2320	-0.98			10.57		
Fluid	Dyneon FE5840	CE25A	-0.44	2580	2.25			12.35		
Vapor	Dyneon FE5840	Ref C	3.33	2691	5.87			13.14		
Vapor	Dyneon FE5840	CE10A	0.35	2821	3.03			11.90		
Vapor	Dyneon FE5840	CE17A	0.03	2925	1.98			12.46		
Vapor	Dyneon FE5840	CE25A	1.76	2690	4.46			12.64		
	Dyneon FPO3741	Baseline	5.51	2092	7.99			15.54		
Fluid	Dyneon FPO3741	Ref C	-3.31	2528	-1.82			10.92		
Fluid	Dyneon FPO3741	CE10A	-2.78	1979	-1.53			10.54		
Fluid	Dyneon FPO3741	CE17A	-8.02	2802	-5.07			10.09		
Fluid	Dyneon FPO3741	CE25A	-3.26	2390	-1.34			11.23		
Vapor	Dyneon FPO3741	Ref C	0.66	2462	3.15			12.77		
Vapor	Dyneon FPO3741	CE10A	-0.92	2218	-0.19			11.13		
Vapor	Dyneon FPO3741	CE17A	-3.85	2957	-2.15			11.68		
Vapor	Dyneon FPO3741	CE25A	-1.18	2191	0.52			11.25		
	Dyneon LTFE6400	Baseline	-26.33	3701	-24.33			-16.96		
Fluid	LTFE6400	Ref C	-25.88	2837	-23.89			-16.88		
Fluid	LTFE6400	CE10A	-26.05	3044	-24.19			-17.19		
Fluid	LTFE6400	CE17A	-27.40	3256	-25.61			-18.53		
Fluid	LTFE6400	CE25A	-25.79	2943	-23.65			-17.48		
Vapor	LTFE6400	Ref C	-27.47	4482	-24.23			-17.12		
Vapor	LTFE6400	CE10A	-26.01	3208	-24.23			-17.19		
Vapor	LTFE6400	CE17A	-26.84	3455	-24.71			-17.68		
Vapor	LTFE6400	CE25A	-27.28	3271	-25.08			-17.66		

Table D-2. DMA results for NBR specimens

			Storage Modulus		Loss Modulus			Tan Delta		
Environment	Elastomer	Fuel Type	Temp/oC	Mpa	Temp/oC	Temp/oC	Temp/oC	Temp/oC	Temp/oC	Temp/oC
	NBR #1	Baseline	-18.01	4537	-14.12			-4.26		
Fluid	NBR #1	Ref C	-7.24	6153	0.41			7.59		
Fluid	NBR #1	CE10A	-11.48	6776	-2.29			5.74		
Fluid	NBR #1	CE17A	-12.90	6655	-5.26			4.32		
Fluid	NBR #1	CE25A	-10.02	5851	-1.83			6.24		
Vapor	NBR #1	Ref C	-13.43	5280	-7.87			0.10		
Vapor	NBR #1	CE10A	-7.87	7488	-0.54			6.78		
Vapor	NBR #1	CE17A	-10.90	6344	-3.12			4.16		
Vapor	NBR #1	CE25A	-10.80	6332	-5.27			2.21		
	NBR #2	Baseline	-25.02	4847	-22.28			-12.28		
Fluid	NBR #2	Ref C	-7.95	5988	-2.20			5.64		
Fluid	NBR #2	CE10A	-11.98	6180	-6.10			1.50		
Fluid	NBR #2	CE17A	-14.20	5970	-8.35			0.55		
Fluid	NBR #2	CE25A	-9.38	6249	-3.67			4.24		
Vapor	NBR #2	Ref C	-15.24	5866	-10.64			-1.83		
Vapor	NBR #2	CE10A	-7.81	6755	-1.83			6.06		
Vapor	NBR #2	CE17A	-11.89	5626	-5.89			1.94		
Vapor	NBR #2	CE25A	-12.16	6199	-8.25			0.07		
	NBR #3	Baseline	-9.49	4532	-7.76			-0.23		
Fluid	NBR #3	Ref C	-2.64	4362	-0.46			7.15		
Fluid	NBR #3	CE10A	-10.49	4239	-6.18			-2.39	34.75	
Fluid	NBR #3	CE17A	-6.92	3734	-5.19			5.34		
Fluid	NBR #3	CE25A	-7.23	4821	-2.83			17.37		
Vapor	NBR #3	Ref C	-7.39	3927	-5.51			1.65		
Vapor	NBR #3	CE10A	-3.27	4819	-1.31			6.43		
Vapor	NBR #3	CE17A	-4.87	4758	-2.32			5.70		
Vapor	NBR #3	CE25A	-8.16	4212	0.89			-5.77		
	NBR #4	Baseline	-34.94	2914	-26.69	-2.15		-23.15	4.60	
Fluid	NBR #4	Ref C	-20.98	4962	-15.64	5.44		-12.66	10.52	
Fluid	NBR #4	CE10A	-23.35	5622	-17.11	3.62		-13.44	9.42	
Fluid	NBR #4	CE17A	-29.98	4534	-21.63	1.24		-17.48	7.87	
Fluid	NBR #4	CE25A	-21.48	5009	-16.07	5.00		-12.15	10.22	
Vapor	NBR #4	Ref C	-28.94	4239	-22.80	-0.74		-19.43	5.86	
Vapor	NBR #4	CE10A	-22.17	5176	-16.61	2.81		-13.86	8.60	
Vapor	NBR #4	CE17A	-27.34	4908	-22.36	-0.67		-18.66	5.67	
Vapor	NBR #4	CE25A	-26.03	3955	-20.17	0.48		-17.36	5.72	
	NBR #5	Baseline	-27.29	4779	-21.81			-2.92		
Fluid	NBR #5	Ref C	-8.37	5397	-2.71			8.16		
Fluid	NBR #5	CE10A	-15.17	4386	-9.93			4.59		
Fluid	NBR #5	CE17A	-12.91	5558	-8.85			4.94		
Fluid	NBR #5	CE25A	-9.19	5912	-6.10			8.31		
Vapor	NBR #5	Ref C	-16.91	4998	-13.64			1.94		
Vapor	NBR #5	CE10A	-6.41	6415	-2.03			8.50		
Vapor	NBR #5	CE17A	-11.32	5092	-5.69			6.73		
Vapor	NBR #5	CE25A	-15.19	5542	-10.58			3.35		
	NBR #6	Baseline	-25.01	5062	-22.22			-15.21		
Fluid	NBR #6	Ref C	-10.50	4313	-5.38			-1.57		
Fluid	NBR #6	CE10A	-17.51	5883	-12.58			-9.59		
Fluid	NBR #6	CE17A	-15.45	4947	-10.43			-5.60		
Fluid	NBR #6	CE25A	-12.66	5990	-6.84			-1.23		
Vapor	NBR #6	Ref C	-19.10	5537	-15.17			-9.81		
Vapor	NBR #6	CE10A	-13.36	6600	-8.74			-3.88		
Vapor	NBR #6	CE17A	-11.44	4540	-7.72			-3.37		
Vapor	NBR #6	CE25A	-16.24	5857	-12.04			-7.36		

Table D-3. DMA results for non-fluorocarbons and non-NBRs

			Storage Modulus		Loss Modulus			Tan Delta		
Environment	Elastomer	Fuel Type	Temp/oC	Mpa	Temp/oC	Temp/oC	Temp/oC	Temp/oC	Temp/oC	Temp/oC
	Fluorosilicone LM15	Baseline	-53.72	3229	-121.81	-49.79		-119.97	-43.94	
Fluid	uorosilicone LM15	Ref C	-53.76	3538	-50.01			-44.55		
Fluid	uorosilicone LM15	CE10A	-53.67	3509	-49.74			-44.40		
Fluid	uorosilicone LM15	CE17A	-51.68	2910	-49.01			-44.24		
Fluid	uorosilicone LM15	CE25A	-51.92	3204	-48.58			-44.33		
Vapor	uorosilicone LM15	Ref C	-53.30	3920	-50.49			-44.74		
Vapor	uorosilicone LM15	CE10A	-52.79	3699	-49.85			-44.46		
Vapor	uorosilicone LM15	CE17A	-52.33	3710	-49.45			-44.45		
Vapor	uorosilicone LM15	CE25A	-53.25	4097	-50.21			-44.78		
	Polyurethane	Baseline	-15.93	2493	-12.95			-4.67		
Fluid	Polyurethane	Ref C	-16.61	2545	-13.32			-4.52		
Fluid	Polyurethane	CE10A	-19.38	2841	-16.91			-6.05		
Fluid	Polyurethane	CE17A	-18.15	2693	-15.93			-4.82		
Fluid	Polyurethane	CE25A	-17.54	2768	-15.36			-4.90		
Vapor	Polyurethane	Ref C	-17.28	2911	-14.76			-6.49		
Vapor	Polyurethane	CE10A	-17.08	2827	-15.23			-5.15		
Vapor	Polyurethane	CE17A	-16.18	2731	-14.60			-4.83		
Vapor	Polyurethane	CE25A	-18.68	2791	-16.13			-6.34		
	Neoprene Rubber	Baseline	-98.23	4782	-92.32	-22.66		-87.85	-13.23	
Fluid	Neoprene Rubber	Ref C	-101.84	5840	-93.15	-12.30		-91.05	-5.59	
Fluid	Neoprene Rubber	CE10A	-100.95	6740	-92.83	-12.12		-91.63	-5.69	
Fluid	Neoprene Rubber	CE17A	-100.47	5728	-93.06	-12.04		-90.60	-4.72	
Fluid	Neoprene Rubber	CE25A	-102.25	6295	-93.79	-12.48		-91.90	-6.34	
Vapor	Neoprene Rubber	Ref C	-98.32	5989	-91.94	-34.31	-18.63	-91.94	-8.57	
Vapor	Neoprene Rubber	CE10A	-100.30	6426	-93.27	-18.17		-90.57	-9.41	
Vapor	Neoprene Rubber	CE17A	-100.98	5960	-91.62	-12.60		-91.62	-5.50	
Vapor	Neoprene Rubber	CE25A	-102.46	6901	-93.62	-13.10		-92.58	-6.66	
	Styrene Butadiene Rub	Baseline	-37.47	4018	-32.24	-2.15		-29.85	2.05	67.14
Fluid	ene Butadiene Rub	Ref C	-32.63	4422	-27.73	-2.62		-25.81	1.27	80.21
Fluid	ene Butadiene Rub	CE10A	-33.67	4718	-28.62	-3.19		-27.06	0.00	78.44
Fluid	ene Butadiene Rub	CE17A	-34.93	4615	-29.84	-3.68		-27.35	1.01	77.95
Fluid	ene Butadiene Rub	CE25A	-33.19	4291	-27.73	-1.80		-25.98	1.44	79.47
Vapor	ene Butadiene Rub	Ref C	-35.86	4543	-30.09	-1.83		-26.72	2.55	67.47
Vapor	ene Butadiene Rub	CE10A	-32.39	5275	-28.26	-2.79		-25.93	1.37	79.21
Vapor	ene Butadiene Rub	CE17A	-33.61	5239	-28.68	-2.59		-26.66	1.77	75.61
Vapor	ene Butadiene Rub	CE25A	-35.67	4256	-30.76	-2.61		-27.90	2.58	71.27
	Silicone Rubber S06	Baseline	-117.55	7585	-111.31			-107.39	-27.42	51.28
Fluid	icone Rubber S06	Ref C	-118.99	6848	-111.36			-106.76	-26.96	
Fluid	icone Rubber S06	CE10A	-118.58	8101	-111.64			-108.29	-26.31	
Fluid	icone Rubber S06	CE17A	-118.19	5665	-111.59			-106.99	-25.38	
Fluid	icone Rubber S06	CE25A	-118.07	7715	-111.91			-107.91	-27.77	
Vapor	icone Rubber S06	Ref C	-117.23	7342	-111.09			-107.24	-27.31	
Vapor	icone Rubber S06	CE10A	-118.23	7704	-112.06			-107.06	-25.59	
Vapor	icone Rubber S06	CE17A	-117.76	6210	-111.56			-107.77	-26.10	
Vapor	icone Rubber S06	CE25A	-117.82	7323	-111.21			-107.48	-27.16	